6

Prey Capture Behavior and Feeding Mechanics of Elasmobranchs

Philip J. Motta and Daniel R. Huber

CONTENTS

6.1 Introduction

Perhaps the most remarkable thing about the elasmobranch feeding mechanism is its functional diversity despite its morphological simplicity. Compared to the teleost skull, which has approximately 63 bones (excluding the branchiostegal, circumorbital, and branchial bones), the feeding apparatus of a shark is composed of just 10 cartilaginous elements: the chondrocranium, paired palatoquadrate and Meckel's cartilages, hyomandibulae, ceratohyal, and a basihyal. Furthermore, the elasmobranchs lack pharyngeal jaws and the ability to further process food by this secondary set of decoupled jaws as do bony fishes. Despite this, sharks, skates, and rays display a diversity of feeding mechanisms and behaviors that, although they do not match those of the

bony fishes, is truly remarkable, especially considering there are only approximately 1100+ species of elasmobranchs compared to about 24,000 species of teleost fishes (Compagno, 2001; Compagno et al., 2005; Nelson, 1994). The elasmobranchs capture prey by methods as diverse as ram, biting, suction, and filter feeding, and they feed on prey ranging from plankton to marine mammals and giant squid (Cherel and Duhamel, 2004; Frazzetta, 1994; Moss, 1972; Motta and Wilga, 2001; Motta et al., 2010). Understanding the elasmobranch feeding mechanism will shed light on how this functional versatility is achieved and whether or not it parallels that of the bony fishes.

Understanding the feeding mechanism of elasmobranchs is also important to biologists from an evolutionary perspective. The chondrichthyan fishes represent a basal group of jawed fishes that share a common ancestor

with bony fishes (Carroll, 1988; Long, 1995; Schaeffer and Williams, 1977); therefore, they provide insight into the evolution of lower vertebrate feeding mechanisms. Studies on chondrichthyan fishes have provided an understanding of the evolution of the jaw depression mechanism in aquatic vertebrates (Wilga et al., 2000) and the evolution and function of jaw suspension systems in vertebrates (Grogan and Lund, 2000; Grogan et al., 1999; Wilga, 2002). Studies on elasmobranch teeth also provide insight into the evolution of dermal teeth and armor and the patterns of tooth replacement in vertebrates (Reif, 1978, 1980; Reif et al., 1978).

Despite a tremendous increase in the knowledge of bony fish feeding mechanisms in the last three decades (Lauder, 1985; Liem, 1978; Westneat, 2004), there have been fewer studies on elasmobranchs and even fewer on batoids (Bray and Hixon, 1978; Dean and Motta, 2004a,b; Marion, 1905; Summers, 2000) than on sharks (Moss, 1972; Nobiling, 1977; Shirai and Nakaya, 1992; Wilga, 2008). Numerous embryological and anatomical studies on the head of sharks in the previous century or early part of this century (reviewed in Motta and Wilga, 1995, 1999) were influential in our understanding of the evolution and development of the skull and branchial arches; however, following some earlier anatomical studies (Moss, 1972, 1977b; Springer, 1961), there have been relatively fewer studies that incorporate cineradiography, high-speed photography, electromyography, and biomechanical modeling of the feeding apparatus (Ferrara et al., 2011; Ferry-Graham, 1998a,b; Huber et al., 2005; Motta et al., 1997; Wilga and Motta, 1998a,b, 2000; Wilga et al., 2007; Wu, 1994).

The goal of this chapter is to provide a review of the feeding anatomy, behavior, and biomechanics of extant elasmobranchs with an emphasis on the structure and function of the feeding apparatus. To place prey capture and mechanics in a more meaningful framework it is necessary to outline how elasmobranchs approach their prey; consequently, prey approach behavior is briefly discussed. Feeding behavior is considered to be pre-capture behaviors (e.g., stalking, ambushing), whereas prey capture refers to the process beginning with opening of the mouth as the fish approaches the prey and usually ends with the prey grasped between the jaws. Because so little is known of postcapture manipulation or processing, this topic is covered only briefly. During manipulation, the prey is reduced in size by cutting or crushing, often combined with head shaking, and then it is transported from the buccal cavity through the pharyngeal cavity into the esophagus. Similarly, because so little is known of batoid feeding mechanisms, sharks are emphasized more than skates or rays. In some instances, food is used to refer to pieces of whole items offered to an animal under experimental conditions, whereas prey refers to dietary items captured during natural feeding.

The review does not cover feeding ecology and diet (see Cortés, 1999; Wetherbee et al., Chapter 8 of this volume), although diet is occasionally referred to when discussing feeding behaviors and mechanisms.

6.2 Ethology of Predation

6.2.1 Predatory Behaviors

Sharks, skates, and rays must first approach their prey before they can capture it. When the prey is within grasp of the predator, the capture event is usually very rapid as compared to the approach, and at this point either the prey may be held within the grasp of the teeth or it may be transported directly through the mouth to the entrance of the esophagus. If the prey is grasped by the teeth, one or a series of manipulation/processing bites can reduce the prey in size prior to the final transport event. In this manner, we speak of capture bites, manipulation/processing bites, and hydraulic transport, the last of which invariably involves suction of the water with the entrained food (Motta and Wilga, 2001). The mechanics of swallowing—that is, getting the food into and through the esophagus—is still unresolved.

Because of the inherent difficulty of studying elasmobranchs in their natural environment, predatory behavior is generally poorly understood, especially as compared to that of bony fishes. Large or pelagic sharks are perhaps the least understood, but their foraging patterns are being revealed due to the advent of telemetry studies (Domeier and Nasby-Lucas, 2008; Holland et al., 1999; Klimley et al., 2001) and the attachment of small animal-borne video cameras and other biosensors (e.g., accelerometers) to free-swimming sharks (Heithaus et al., 2001, 2002a; Sims, 2010; Heithaus and Vaudo, Chapter 17 of this volume). A great deal of what we know of predatory behavior is from anecdotal or one-of-a-kind observations (Pratt et al., 1982; Strong, 1990), telemetry studies (Klimley et al., 2001), behavioral studies of shallow-water benthic elasmobranchs (Fouts and Nelson, 1999; Strong, 1989), and laboratory studies (Lowry et al., 2007; Sasko et al., 2006) or is inferred from morphology (Compagno, 1990; Myrberg, 1991). Surprisingly, the more accessible batoids are vastly understudied as compared to sharks (Belbenoit and Bauer, 1972; Lowe et al., 1994).

How sharks and rays approach and hunt their prey is perhaps the least understood aspect of their feeding biology. Most elasmobranchs are probably very opportunistic in what they prey on and how they acquire their prey (see Chapter 17 of this volume). When hunting by speculation, the fish searches an area that it expects to have prey or it follows another organism expecting that

animal to flush prey out by its presence (Curio, 1976). *Dasyatis* rays will position themselves at regions of higher tidal water movement, such as near beach promontories, waiting for prey organisms to be swept by. Large aggregations of rays may be found at these locations during periods of swift tidal movement (Motta, pers. obs.). Large tiger sharks, *Galeocerdo cuvier*, occur most frequently in Shark Bay, Western Australia, during the season that dugongs, an important prey item for this size class of sharks, are present (Heithaus, 2001; Wirsing et al., 2007). Tiger sharks aggregate at the northwestern Hawaiian Islands during June and July, coinciding with the summer fledging period of blackfooted and Laysan albatross birds, upon which they prey (Lowe et al., 2003), and white sharks, *Carcharodon carcharias*, aggregate at Seal Island, South Africa, to prey on Cape fur seals (Martin et al., 2005). Each March and April, whale sharks, *Rhincodon typus*, aggregate on the continental shelf of the central western Australian coast, particularly at Ningaloo Reef, in response to coral spawning events that occur each year (Gunn et al., 1999; Taylor and Pearce, 1999). Perhaps the largest aggregation of whale sharks in the world occurs off the Yucatan Peninsula, where they feed on rich plankton blooms in relatively shallow water (Hueter et al., 2008; Motta et al., 2010). White sharks, *C. carcharias*, spend a lot of time patrolling near seal colonies off the South Farallon Islands and Año Nuevo Island, California. Most of the shark's movement is back and forth parallel and near to the shoreline as it intercepts seals and sea lions that are departing from and returning to their shore-based rookeries. In some cases, the sharks pass within 2 m of the shore. Prey capture, however, is infrequent compared to the time spent patrolling (Klimley et al., 2001).

Ambushing involves the predator trying to conceal or advertise (aggressive mimicry) its presence while lying in wait for the prey (Curio, 1976). By partially burying themselves in the soft substrate, Pacific angel sharks, *Squatina californica*, ambush demersal fishes. These sharks appear to actively select ambush sites within localized areas adjacent to reefs (Fouts, 1995; Fouts and Nelson, 1999). Pacific electric rays, *Torpedo californica*, either ambush their prey from the bottom or use a search-and-attack behavior from the water column. During the day, the rays ambush their prey of mostly fishes by burying themselves in sand and jumping over the prey. After swimming over the prey, the rays cup their pectoral fins around the prey while electrically discharging. They then pivot over the stunned prey so as to swallow it head first. At night, the rays are seen swimming or hovering in the water column 1 to 2 m above the substratum. The rays then lunge forward over the prey, cup their pectorals over the prey while discharging, and either pin the prey to the bottom or, using frontal somersaults and peristaltic-like movements of the disk, move

the prey closer to the mouth for swallowing (Bray and Hixon, 1978; Lowe, 1991; Lowe et al., 1994). Similar stereotyped prey capture behavior has also been described for the electric rays *T. marmorata*, *T. ocellata*, and *T. nobiliana* (Belbenoit and Bauer, 1972; Michaelson et al., 1979; Wilson, 1953; reviewed in Belbenoit, 1986).

Ambushing behavior of rays and sharks has been observed at the inshore spawning grounds of chokka squid (*Loligo vulgaris reynaudii*) off South Africa. Diamond rays, *Gymnura natalensis*, camouflage themselves in the substrate and then lunge out toward female squid as they try to spawn on the bottom. Large numbers of sharks and rays aggregate at these spawning grounds. In addition to pyjama catsharks, *Poroderma africanum*, and leopard catsharks, *P. pantherinum*, ambushing the spawning squid from the rocky reef substrate, the rays and sharks also chase down the squid to capture them or simply bite off the attached egg masses from the substrate (Smale et al., 1995, 2001).

In contrast to ambushing, the stalking predator approaches the prey while concealed and then makes a sudden assault (Curio, 1976). White sharks, *Carcharodon carcharias*, will stalk prey downstream in oceanic or tidal currents (Pyle et al., 1996), and they stalk Cape fur seals primarily within 2 hours of sunrise when light levels are low (Martin et al., 2005). Sevengill sharks, *Notorynchus cepedianus*, capture elusive prey using a stealthy underwater approach with very little body movement and only slight undulatory motions of the caudal fin. They move within striking distance and make a quick dash at the prey, which can include fur seals (Ebert, 1991). Using animal-borne video technology, Heithaus et al. (2002a) observed tiger sharks, *Galeocerdo cuvier*, stalking their benthic prey from above, in some cases getting as close as 2 m from large teleost fishes before the shark was detected.

Other elasmobranchs may lure prey to them. Luminescent tissue on the upper jaw of the megamouth shark, *Megachasma pelagios*, might attract euphausid shrimp and other prey into its mouth (Compagno, 1990). The white tips on the pectoral fins of oceanic whitetip sharks, *Carcharhinus longimanus*, might act as visual lures to aid in the capture of its rapid moving prey (Myrberg, 1991), and bioluminescence in the cookie-cutter shark, *Isistius brasiliensis*, might serve to lure pelagic predators from which it gouges chunks of flesh (Jones, 1971; Papastamatiou et al., 2010; Widder, 1998).

Most elasmobranchs will scavenge food when given the opportunity. Sevengill sharks, *Notorynchus cepedianus*, will feed on marine mammals, including whale and dolphin carcasses, bait left on fishing hooks, and even human remains (Ebert, 1991). Tiger sharks, *Galeocerdo cuvier*, are notorious opportunistic feeders; in addition to their regular diet, they will scavenge food ranging from dead dugongs to human refuse (Heithaus,

2001; Lowe et al., 1996; Randall, 1992; Smale and Cliff, 1998). Blue sharks, *Prionace glauca*, will similarly scavenge human refuse and dead or injured birds, although they have been observed to stalk resting birds and perhaps scavenge mesopelagic cephalopods (Henderson et al., 2001; Markaida and Sosa-Nishizaki, 2010; Stevens, 1973, cited in Henderson et al., 2001). Sleeper sharks, *Somniosus microcephalus*, will scavenge fishery offal and carrion, including fur seals (Cherel and Duhamel, 2004). White sharks, *Carcharodon carcharias*, often scavenge whale carcasses (Casey and Pratt, 1985; Curtis et al., 2006; Dicken, 2008; Dudley et al., 2000; Long and Jones, 1996; McCosker, 1985; Pratt et al., 1982). Large gray reef sharks, *Carcharhinus amblyrhynchos*, at Enewetak Island, Marshall Islands, follow carangid jacks as both scavengers and predators (Au, 1991), and velvet belly lantern-sharks, *Etmopterus spinax*, undergo a dietary shift, with larger individuals incorporating scavenging of fish and cephalopods (Neiva et al., 2006).

Although many species of sharks forage solitarily, in some cases aggregations of sharks will come together to feed. Blacktip reef sharks, *Carcharhinus melanopterus*, and lemon sharks, *Negaprion brevirostris*, were observed to apparently herd schools of fish against the shoreline and then feed on them (Eibl-Eibesfeldt and Hass, 1959; Morrissey, 1991), and oceanic whitetip sharks, *Carcharhinus longimanus*, were observed to herd squid at night (Strasburg, 1958). Thresher sharks (*Alopias*) are reported to apparently work in groups to capture fish, using their long caudal fins to herd and stun fish (Aalbers et al., 2010; Budker, 1971; Castro, 1996; Coles, 1915; Compagno, 1984). Sevengill sharks, *Notorynchus cepedianus*, will circle a seal and prevent its escape. The circle is tightened, and eventually one shark initiates the attack that stimulates the others to begin feeding (Ebert, 1991). Although some authors have considered these behaviors cooperative, they could simply reflect aggregations of animals at a prey item and not cooperative foraging (Motta and Wilga, 2001; see Chapter 17 of this volume for a definition of cooperative foraging). So-called feeding frenzies of sharks appear to be nothing more than highly motivated feeding events involving generally many individuals. The sharks have been described as attacking prey or food items indiscriminately, moving at an accelerated speed, and disregarding any injuries they may receive in the attack. Injured or hooked sharks are often attacked and consumed by the other sharks. These feeding bouts, which can involve as few as six sharks to hundreds of sharks, can end as abruptly as they begin (Gilbert, 1962; Hobson, 1963; Nelson, 1969; Springer, 1967; Vorenberg, 1962). The feeding ecology, behavior, and diet of epipelagic, deepwater, and tropical marine elasmobranchs are also reviewed by Kyne and Simpfendorfer (2010), Stevens (2010), and White and Sommerville (2010).

6.2.2 Feeding Location and Prey Capture

Sharks approach their prey on the surface, in midwater, or on the bottom. One of the older misconceptions was that sharks must roll on their side to take prey in front of them because of their subterminal mouth (Budker, 1971). In fact, the mouths of modern sharks do not preclude them from feeding on prey in front of or above them, and sharks will approach surface or underwater food with a direct head-on approach or will roll on their side to bite at the food (Budker, 1971; Motta, pers. obs.). White sharks, *Carcharodon carcharias*, will approach in their normal orientation, roll on their side, or roll completely over so their ventral side is up when they feed on underwater bait or a floating whale carcass (Dicken, 2008; Pratt et al., 1982; Tricas and McCosker, 1984). During surface feeding, *C. carcharias* may bite such prey as elephant seals and then retreat until the prey lapses into shock or bleeds to death. The shark then returns to feed on the prey (McCosker, 1985; Tricas and McCosker, 1984). Tricas and McCosker referred to this as the "bite and spit" strategy. Klimley (1994) and Klimley et al. (1996) proposed, however, that white sharks hold the pinniped prey tightly in their mouth and drag it below the surface, often removing a bite from the prey in the process. The prey may be released underwater, after which it floats or swims to the surface and dies by exsanguination. Meanwhile, the shark follows the prey to the surface to begin feeding after it dies. Martin et al. (2005) also found no support for the "bite and spit" behavior in white shark predation on Cape fur seals off South Africa. The sharks often performed a subsurface carry whereby the shark carried a dead or incapacitated seal underwater before feeding on it. After capturing a seal or decoy in its jaws, the shark often repurchased or repositioned the prey by lifting its snout, removing the upper teeth with the lower teeth remaining in the prey, then quickly protruding the upper jaw and bringing the teeth in contact with the prey again. This would bring the longitudinal axis of the food item in line with the longitudinal axis of the shark. These sharks displayed a variety of surface attacks on seals including subsurface attacks that launched the shark partially or completely out of the water in a vertical to near vertical orientation and inverted breaches with the body in an inverted position.

Blue sharks, *Prionace glauca*, approach schools of squid on the surface with an underwater approach or a surface charge. Small anchovies are captured from a normal swimming posture, but when capturing larger whole mackerel from behind blue sharks may roll on their side (Tricas, 1979). Large schools of oceanic whitetip sharks, *Carcharhinus longimanus*, have been observed swimming erratically in a sinuous course on the surface with their mouths wide open. These sharks made no attempt to snap up the small tuna through which they were swimming,
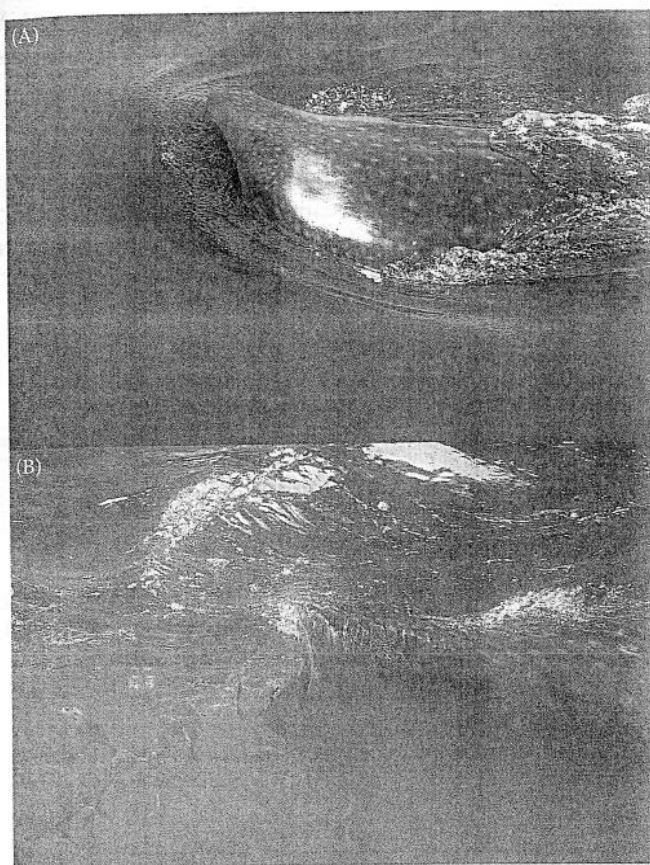
FIGURE 6.1
(A) Surface and (B) subsurface view of two surface ram filter feeding whale sharks, *Rhincodon typus* (size between 5 and 8 m TL). (From Motta, P.J. et al., *Zoology*, 113, 199–212, 2010. With permission.)

rather, they appeared to simply wait for the fish to swim or leap into their mouths (Bullis, 1961). Surface-feeding blacknose sharks (*Carcharhinus acronotus*), oceanic whitetip sharks (*C. longimanus*), white sharks (*C. carcharias*), and Caribbean reef sharks (*Carcharhinus perezi*) may raise the head just prior to prey capture (Bullis, 1961; Frazzetta and Prange, 1987; Motta and Wilga, 2001; Tricas and McCosker, 1984). This might place the open mouth in line with food as the shark approaches (Frazzetta and Prange, 1987). Whale sharks, *Rhincodon typus*, will make regular dives through the water column foraging for food. They will also swim slowly (average 1.1 m/s) at or near the surface with their body at an angle and the top of the head clear of the surface while feeding (Figure 6.1) (Gunn et al., 1999; Motta et al., 2010).

Rays and skates will also feed off the bottom. The ventral mouth of Pacific electric rays, *Torpedo californica*, does not preclude them from foraging in the water column in addition to sitting on the bottom. After stunning the prey, which can result in breaking of the vertebral column, they manipulate the prey toward the mouth with the pectoral fins or force the stunned prey to the

substrate (Bray and Hixon, 1978; Lowe et al., 1994). The thorny skate, *Raja radiata*, is primarily a benthivorous feeder as a juvenile or adolescent, but benthopelagic food items, including fishes, become important to larger individuals (Skjaeraasen and Bergstad, 2000). Dietary items indicate that *Dasyatis say* and *D. centroura* in Delaware Bay frequently feed off the bottom on free-swimming organisms (Hess, 1961). The midwater-swimming cownose ray, *Rhinoptera bonasus*, will descend to the bottom and excavate benthic invertebrates, including bivalves (Sasko et al., 2006). The lesser electric ray, *Narcine bancroftii*, captures buried benthic prey by protruding its jaws up to 100% of its head length beneath the substrate and sucking the prey into its mouth (Dean and Motta, 2004b). Mobulid rays, including *Manta birostris* and *Mobula tarapacana*, filter feed both at the surface and in midwater, extending their cephalic wings to funnel prey and water through the mouth. Upon encountering a patch of prey, they will often swim in a circular formation or somersault while filter feeding to stay within the patch (Notarbartolo di Sciara and Hillyer, 1989; Motta, pers. obs.).

Some sharks will also take prey buried within the substrate or capture prey on the bottom. Leopard sharks, *Triakis semifasciata*, can apparently suck worms out of their burrows in addition to biting pieces off their benthic prey (Compagno, 1984; Talent, 1976). The epaulette shark, *Hemiscyllium ocellatum*, and the whitespotted bamboo shark, *Chiloscyllium plagiosum*, occasionally thrust their heads into the sediment up to the level of the first gill slit, apparently using suction to capture their benthic prey of worms and crabs. They then winnow the prey from the sand in the buccopharyngeal cavity and eject the sand through the first gill slit (Heupel and Bennett, 1998; Wilga, pers. obs.). Skates and rays primarily feed in or on the bottom by biting pieces of sessile invertebrates or excavating buried prey, although they will feed in the water column (Abd El-Aziz, 1986; Ajayi, 1982; Babel, 1967; Ebert et al., 1991; Edwards, 1980; Goitein et al., 1998; Gray et al., 1997; Hess, 1961; Hines et al., 1997; Holden and Tucker, 1974; Howard et al., 1977; Lucifora et al., 2000; Muto et al., 2001; Orth, 1975; Rudloe, 1989; Sasko et al., 2006; Sherman et al., 1983; Skjaeraasen and Bergstad, 2000; Stokes and Holland, 1992; Thrush et al., 1991; Valadez-Gonzalez et al., 2001; VanBlaricom, 1976). Rays dig up prey by pectoral "wing-flapping," or they hydraulically mine the prey by jetting water through the mouth (Gregory et al., 1979; Howard et al., 1977; Muto et al., 2001; Sasko et al., 2006; VanBlaricom, 1976). As discussed above, the cownose ray, *Rhinoptera bonasus*, uses a combination of wing flapping and water jetting to expose prey in the wild (Sasko et al., 2006; Schwartz, 1967, 1989); however, in the laboratory, the rays rest on the substrate on the tips of their pectoral fins and use repeated jaw opening and closing movements at 2.4 to

2.9 cycles per second to generate water flow in and out of the buccal cavity. The ventrally directed jet of water resuspends the sand and bivalve food, resulting in the effective separation of food and sand so the rays can capture the food. The large subrostral lobes are depressed, forming a chamber around the food item that it encloses laterally and partially anteriorly; the two lobes have been observed to move independently and push food toward the mouth (Sasko, 2000; Sasko et al., 2006).

Large-scale destruction of eelgrass, *Zostera marina*, beds in the Chesapeake Bay has been attributed to the excavation behavior of *Rhinoptera bonasus* (Orth, 1975). Excavation of benthic prey by rhythmic flapping of the rostrum and pectoral fins is common in other rays (Babel, 1967; Hines et al., 1997; Howard et al., 1977; Thrush et al., 1991; VanBlaricom, 1976). Southern stingrays, *Dasyatis americana*, excavate lancelets, *Branchiostoma floridae*, from the sandy substrate, and the presence in the gut of only medium- and large-sized prey led Stokes and Holland (1992) to speculate that the rays are winnowing out the sand and smaller lancelets while retaining the larger ones. Winnowing prey from ingested sediment is perhaps common in rays. The lesser electric ray, *Narcine bancroftii*, which specializes in wormlike prey including polychaete worms and anguilliform fishes, uses suction to capture the prey along with some sediment and ejects the latter out of the mouth, spiracle, or gill slits (Dean and Motta, 2004b; Funicelli, 1975; Rudloe, 1989). Similarly, during food processing, *R. bonasus* can separate prey from sand, flushing the sand out of the mouth and gill slits. This ray can also strip unwanted parts of the food item (e.g., mussel shell, skin and vertebral column of fish, shrimp shell) from the edible parts and eject the unwanted pieces. Larger pieces are ejected from the mouth, and smaller particles such as sand exit through the gill slits (Sasko et al., 2006).

Bottom-feeding horn sharks, *Heterodontus francisci*, use suction and biting to remove benthic invertebrates such as anemone tentacles, polychaetes, and urchins. They remove their prey with a "pecking-like" motion, often while they are raised on their pectoral fins (Edmonds et al., 2001; Strong, 1989). Gray reef sharks, *Carcharhinus amblyrhynchos*, in Hawaii primarily feed near the bottom on reef-associated teleosts and supplement their diet with invertebrates (Wetherbee et al., 1997). Rays are often taken by sharks, particularly hammerhead sharks (Budker, 1971; Gudger, 1907). Great hammerhead sharks, *Sphyrna mokarran*, have been observed to use their head to deliver powerful blows and to restrain rays on the substrate prior to biting pieces off the ray (Strong, 1990). They also exhibit a "pin and pivot" behavior during which the shark forcibly presses the ray against the substrate with the ventral surface of the cephalofoil and then, with a twisting motion of the body, pivots its head while remaining atop the ray as it engulfs part or all of

the ray (Chapman and Gruber, 2002). Small bonnethead sharks, *Sphyrna tiburo*, capture their food by depressing the mandible considerably as they swim over the food, catching the food either within the mouth or with the anterior mandibular teeth (Wilga, 1997; Wilga and Motta, 2000). Perhaps the strangest means of prey processing occurs when juvenile lesser spotted dogfish, *Scyliorhinus canicula*, use their dermal denticles on the tail to anchor food items so bite-sized pieces can be torn away by the jaws (Southall and Sims, 2003).

6.3 Feeding Mechanism

6.3.1 Mechanics of Prey Capture

When the shark, skate, or ray is within striking distance of its prey it begins the capture sequence. Prey capture is generally very rapid compared to the approach and typically lasts from about 100 to 400 ms. Capture begins when the mouth starts to open and lasts until the prey is grasped between the teeth or the jaws are closed on the prey (Motta et al., 2002). In some cases, the mouth is briefly closed just prior to opening, and under those circumstances this closing may be said to mark the initiation of capture. Capture may then be divided into three or four phases for heuristic purposes, although they are all continuous and rapid. If the slightly agape mouth is closed prior to mouth opening, this is termed the *preparatory phase* and is more common in suction-feeding bony fishes than elasmobranchs (Ajemian and Sanford, 2007; Lauder, 1985). An expansive phase follows during which there might be cranial (head) elevation accompanied by depression of the lower jaw. The branchial apparatus may also be expanded and the paired labial cartilages that lie at the edges of the mouth extended during this phase. The compressive phase begins at peak gape, and as the lower jaw is elevated the upper jaw (palatoquadrate cartilage) might be protruded toward the lower jaw. Cranial depression also occurs during this phase in many sharks, although surface-feeding *Carcharodon carcharias* can keep the cranium elevated until the recovery phase. At the end of the compressive phase, either the prey is grasped between the teeth or the food is already well within the buccal cavity. The recovery phase is marked by retraction of the upper jaw and the recovery of the other elements (hyomandibula, ceratohyal, basihyal, and branchial arches) back to their original resting positions (Figure 6.2) (Ajemian and Sanford, 2007; Frazzetta, 1994; Frazzetta and Prange, 1987; Matott et al., 2005; Moss, 1972, 1977b; Motta and Wilga, 2001; Motta et al., 1997, 2008; Tricas and McCosker, 1984; Wilga and Sanford, 2008).

Sharks and batoids capture their prey in a variety of ways. Ram feeding is perhaps the most common prey capture method in sharks, especially in carcharhinid and lamnid sharks. During ram capture, the shark swims over the relatively stationary prey and engulfs it whole or seizes it in its jaws. The food is then moved from the mouth through the pharyngeal cavity into the esophagus by hydraulic suction. Bonnethead sharks, *Sphyrna tiburo*, ram feed benthic food by depressing the mandible and scooping the food up as they swim over it (Wilga and Motta, 2000). White sharks, *Carcharodon carcharias*, primarily ram capture their food, sometimes approaching the food at such great speeds that they leave the water when feeding on surface-dwelling prey (Klimley, 1994; Klimley et al., 1996; Martin et al., 2005; Tricas, 1985; Tricas and McCosker, 1984).

Inertial suction feeding, or simply suction feeding, involves a decrease in the pressure of the buccopharyngeal chamber such that the prey or food is pulled into the mouth. There is a functional continuum from pure ram to pure inertial suction, and fishes can, and often do, use a combination of both (Norton and Brainerd, 1993; Wilga and Motta, 1998a). Caribbean reef sharks, *Carcharhinus perezi*, taking pieces of food will primarily over-swim the food item by ram but also employ some suction as witnessed by the food being sucked into the mouth rapidly when it is very close to the approaching shark. Sixgill sharks, *Hexanchus griseus*, will also position themselves close to bait, sitting on the bottom and sucking it into their mouth (Motta, pers. obs.).

Sharks specialized for suction prey capture, such as the nurse shark, *Ginglymostoma cirratum*, and the white-spotted bamboo shark, *Chiloscyllium plagiosum*, exhibit a suite of kinematic and morphological characters, including a relatively small mouth (generally less than one-third head length) as compared to ram-feeding sharks, small teeth, a mouth laterally enclosed by large labial cartilages, hypertrophied abductor muscles, and rapid buccal expansion (Ajemian and Sanford, 2007; Lowry and Motta, 2008; Lowry et al., 2007; Matott et al., 2005; Moss, 1965, 1977b; Motta and Wilga, 1999; Motta et al., 2002, 2008; Nauwelaerts et al., 2008). Suction feeding appears to be the predominant prey capture behavior in some clades, including the orectolobiforms and batoids. Specialization for suction feeding apparently evolved independently in conjunction with a benthic lifestyle, and these suction specialists feed on both elusive and non-elusive prey that live in or on the substrate, are attached to it, or are associated with the bottom (Ajemian and Sanford, 2007; Belbenoit, 1986; Clark and Nelson, 1997; Edmonds et al., 2001; Ferry-Graham, 1998b; Fouts, 1995; Fouts and Nelson, 1999; Heupel and Bennett, 1998; Moss, 1977b; Motta et al., 2002; Robinson and Motta, 2002; Tanaka, 1973; Wilga, 1997; Wilga and Motta, 1998a,b; Wu, 1994). Suction feeding near the
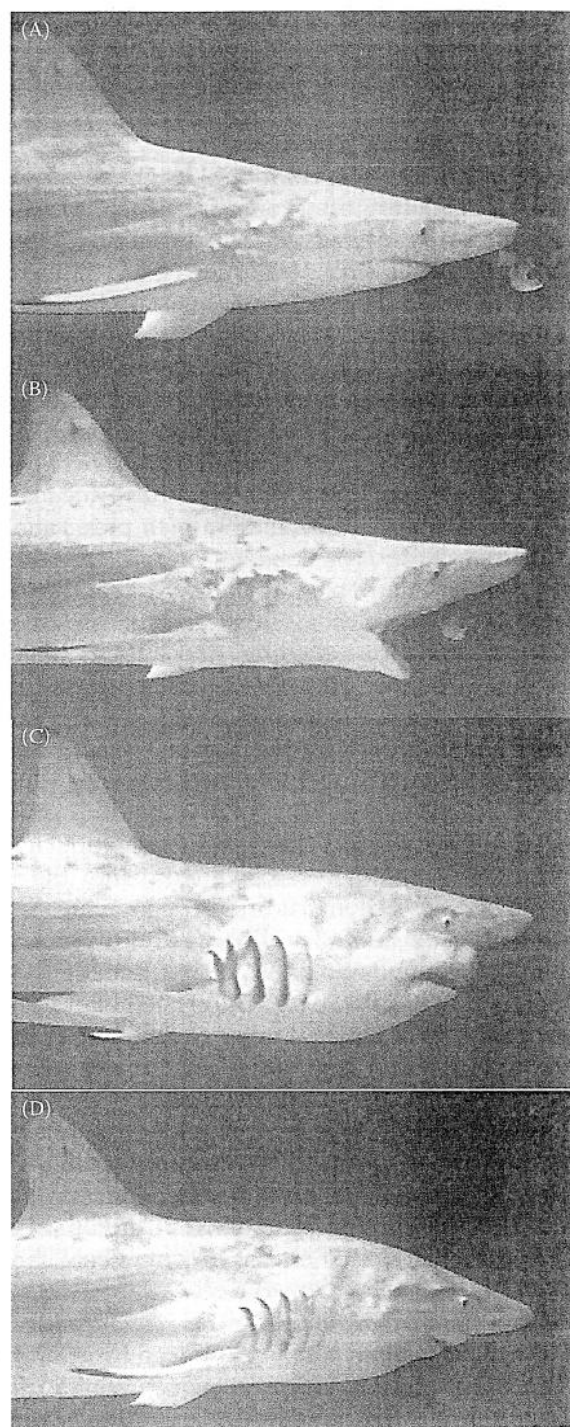

FIGURE 6.2

Food capture sequence of the blacktip shark, *Carcharhinus limbatus*. (A) Start of prey capture before mandible depression or cranial elevation. (B) The expansive phase characterized by mandible depression and head elevation. The slight bulge below the lower jaw is the basihyal being depressed. (C) During the compressive phase, the upper jaw is protruded (note bulge of upper jaw) and the mandible elevated as the prey is engulfed. The pharyngohyoid apparatus is depressed as the food is being transported posteriorly. (D) During the recovery phase, the upper jaw is retracted (partially retracted here), and the hyoid is mostly elevated.

substrate also extends the distance over which suction is effective; consequently, a predator can be effective further from the prey (Nauwelaerts et al., 2007). The prevalence of suction capture in batoids (Belbenoit and Bauer, 1972; Collins et al., 2007; Dean and Motta, 2004a,b; Sasko et al., 2006; Wilga and Motta, 1998b) might be related to the fact that fish often comprise a significant portion of the diet in many rays and skates, particularly in larger individuals (Abd El-Aziz, 1986; Ajayi, 1982; Babel, 1967; Barbini et al., 2010; Belbenoit and Bauer, 1972; Bray and Hixon, 1978; Ebert et al., 1991; Edwards, 1980; Funicelli, 1975; Holden and Tucker, 1974; Lucifora et al., 2000; Muto et al., 2001; Skjeraasen and Bergstad, 2000; Smale and Cowley, 1992). Rapid suction combined with jaw protrusion might be an effective way to catch such elusive prey. Suction feeding might also be better suited for feeding off the bottom, allowing batoids to pick prey from the substrate.

Biting, which may accompany ram feeding, may also occur when an elasmobranch approaches its prey or food, ceases swimming, and simply bites the prey or pieces off the prey. The cookie-cutter shark, *Isistius brasiliensis*, shows a unique biting behavior in which it employs its modified pharyngeal muscles, upper jaw, and hyoid and branchial arches to suck onto its prey of pelagic fishes or marine mammals. Forming a seal with its fleshy lips, it then sinks its hooklike upper teeth and sawlike modified lower teeth into the prey and twists about its longitudinal axis to gouge out a plug of flesh, leaving a craterlike wound (Compagno, 1984; Jones, 1971; LeBoeuf et al., 1987; Papastamatiou et al., 2010; Shirai and Nakaya, 1992). The related kitefin shark, *Dalatias licha*, has dentition similar to that of the cookie-cutter shark and apparently feeds in the same manner (Clark and Kristof, 1990), as does the Greenland shark, *Somniosus microcephalus*. The latter apparently slowly stalks unsuspecting seals at breathing holes in the ice. Its slow movements and cryptic coloration may facilitate an element of surprise. Skomal and Benz (pers. obs.) observed Greenland sharks grasping seal carcasses in their jaws while oriented vertically in the water column. The sharks slowly rolled their bodies left and right allowing the band of closely opposed and elevated lower jaw teeth to carve out large hunks of flesh. In addition to ingesting whole sea turtles, Mediterranean white sharks, *Carcharodon carcharias*, and tiger sharks, *Galeocerdo cuvier*, in Shark Bay, Western Australia, often bite off pieces of the turtle, including limbs, often resulting in the turtle surviving (Fergusson et al., 2000; Heithaus et al., 2002b).

Continuous ram filter feeding, such as in the basking shark, *Cetorhinus maximus*, occurs when the shark continuously swims forward with the mouth open. In this manner, these sharks will actively seek and locate zooplankton patches on the surface. Basking sharks forage

for longer periods in patches with high zooplankton density, and these high-density patches produce the most prolonged area-restricted searching during which the sharks follow convoluted swimming paths to stay within the plankton patches (Sims and Merrett, 1997; Sims and Quayle, 1998; Sims et al., 1997). The whale shark, *Rhincodon typus*, can employ intermittent suction filter feeding, generating suction with aperiodic pulses (Clark and Nelson, 1997; Diamond, 1985; Martin and Naylor, 1997; Sanderson and Wassersug, 1993; Taylor et al., 1983). Whale sharks can also use continuous ram filter feeding or hang vertically in the water column. In the latter case, they will suck prey into the mouth or rise vertically out of the water and sink back under water, thus creating an inflow of water and prey into their open mouths (Budker, 1971; Colman, 1997; Gudger, 1941a,b; Motta et al., 2010; Springer, 1967). The feeding behavior of the megamouth shark, *Megachasma pelagios*, has been inferred from its morphology. Although its feeding was speculated to employ ram (Taylor et al., 1983) or suction (Compagno, 1990), a more recent anatomical study proposed engulfment feeding similar to that of rorqual and humpback whales. During this behavior, the shark employs a low-velocity, high-volume suction during which the prey and water are drawn into the mouth. The continuous ram swimming then distends the elastic buccopharyngeal cavity. The engulfed prey and water are then driven across the gill rakers when the mouth is closed and the buccopharyngeal cavity compressed (Figure 6.3) (Nakaya et al., 2008).

6.3.2 Evolution of the Feeding Mechanism

The stem gnathostomes and early chondrichthyans had a jaw apparatus quite unlike modern sharks. In these, the upper jaw was braced against the braincase at multiple locations. This type of jaw suspension, termed *autodiastyly*, was possibly the ancestral type for the Chondrichthyes. Autodiastyly is characterized by a nonsuspensory hyoid arch that articulated with the palatoquadrate, with the hyoid arch being similar in morphology to the branchial arches. The palatoquadrate had ethmoidal and orbital articulations with the cranium (Figure 6.4) (Grogan and Lund, 2000; Lund and Grogan, 1997; reviewed in Wilga, 2002, and Wilga et al., 2007). The earliest sharks, the cladoselachians, had a large and almost terminal mouth with multicuspid teeth, relatively small labial cartilages, and a long palatoquadrate and Meckel's cartilage. The upper jaw of these sharks had an ethmoidal and a large postorbital articulation between the upper jaw and the cranium, as well as a hyomandibula that supposedly contributed little to jaw support. This type of jaw support is termed *amphistylic*. The body and caudal fin of these sharks were similar to modern fast-swimming pelagic sharks
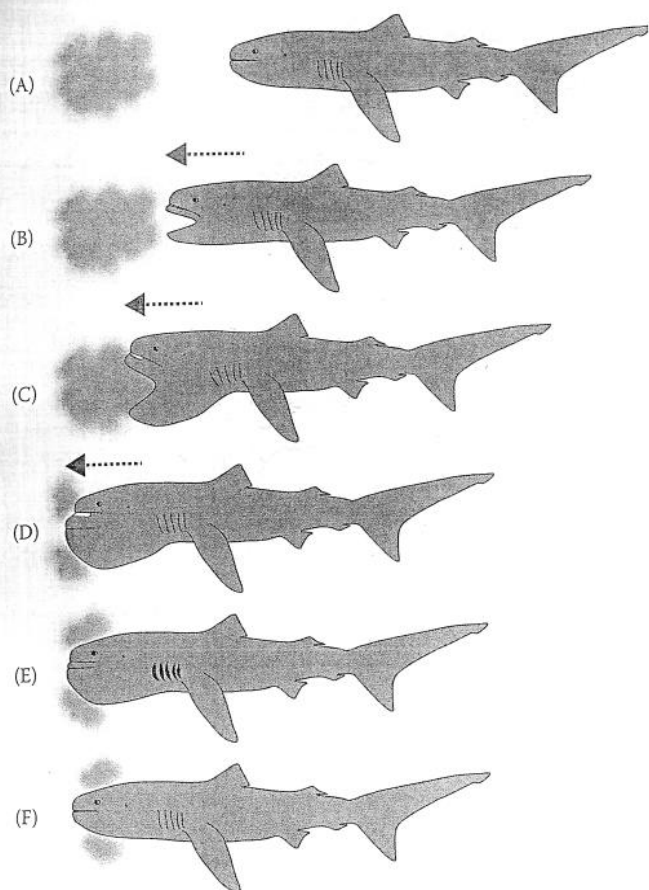
and shearing (but see Section 6.5). In the modern galean sharks, the ethmoidal articulation between the ethmoid process of the palatoquadrate and the ethmoid region of the cranium is the only anterior connection to the cranium, and it is joined by an ethmopalatine ligament, but the hyomandibula is thought to contribute more to jaw support than the anterior ligaments (Figure 6.6). This type of jaw suspension is termed *hyostylic* (Figure 6.4) (Carroll, 1988; Schaeffer, 1967; reviewed in Wilga, 2002, 2005). Some groups of squalomorph sharks, including *Chlamydoselachus*, Squaliformes, and Hexanchiformes, have an orbitostylic jaw suspension in which the orbital process articulates with the orbital wall while the hyomandibula contributes significantly to support of the jaws (Maisey, 1980; Wilga, 2002, 2005). Hexanchiform sharks, however, retained the postorbital articulation while acquiring the orbitostylic articulation and therefore possess two jaw suspension types, orbitostyly and amphistyly (Wilga, 2002; Wilga et al., 2007). The batoids have a euhyostylic jaw suspension, which is perhaps the most kinetic jaw system. This type has no cranial–palatoquadrate articulation, the hyomandibula is the sole means of support for the jaws, and the hyoid arch is "broken up," with the hyomandibula losing its connection to the ceratohyal (Compagno, 1999; Miyake and McEachran, 1991; Wilga, 2002, 2005). The hyostylic and euhyostylic jaw suspension plays a key role in the functioning of the elasmobranch feeding mechanism; therefore, from a biting ancestor there were multiple forays into biting, suction, and filter-feeding behaviors (Figure 6.6) (Wilga et al., 2007).

FIGURE 6.3
Engulfment feeding of the megamouth shark *Megachasma pelagios*. (From Nakaya, K. et al., *J. Fish Biol.*, 73, 17–34, 2008. With permission.)

(Figure 6.5). Their teeth were apparently suited for seizing and tearing prey rather than shearing or sawing, and it is speculated that they captured prey by biting, although suction may have played a role in prey capture (Carroll, 1988; Lund and Grogan, 1997; Moy-Thomas and Miles, 1971; Schaeffer, 1967; Wilga, 2002, 2005; Wilga et al., 2007; but see Maisey, 2008, for an alternative view). The xenacanthids that followed also had an amphistylic jaw suspension, a grasping dentition, long jaws, and a large gape suggesting a biting or ram-feeding mechanism (Carroll, 1988; Wilga, 2002; but see Maisey, 2008). The ctenacanthid sharks that followed likewise had an amphistylic jaw suspension, but they gave rise to the neoselachians, which include all modern sharks, skates, and rays (Figure 6.4).

During the evolution of modern elasmobranchs there was a general trend that involved shortening of the jaws and increased kinesis of the jaw suspension, facilitating upper jaw protrusion. Modern sharks have a subterminal mouth, shorter jaws, more movable hyomandibula that suspends the jaws, more protrusible upper jaw with a smaller otic process, and a dentition suited for sawing

6.3.3 Functional Morphology of the Feeding Mechanism

6.3.3.1 Sharks

Despite numerous studies on the anatomy of the head and cranium (e.g., Allis, 1923; Compagno, 1988; Daniel, 1915, 1934; Edgeworth, 1935; Frazzetta, 1994; Gadow, 1888; Gohar and Mazhar, 1964; Goodey, 1910; Goto, 2001; Lightoller, 1939; Luther, 1909; Marinelli and Strenger, 1959; Moss, 1972, 1977b; Motta and Wilga, 1995, 1999; Nobiling, 1977; Shirai and Okamura, 1992; Waller and Baranes, 1991; Wu, 1994), the functional morphology of the feeding mechanism is only understood for some representative species and is perhaps best understood for the carcharhiniform, squaliform, and orectolobiform sharks.

The feeding mechanism is perhaps best known in the spiny dogfish, *Squalus acanthias*, and the lemon shark, *Negaprion brevirostris*. As previously discussed, squaloids have an orbitostylic jaw suspension in which the hyomandibula suspends the jaws from the cranium, and the palatoquadrate articulates with the orbital
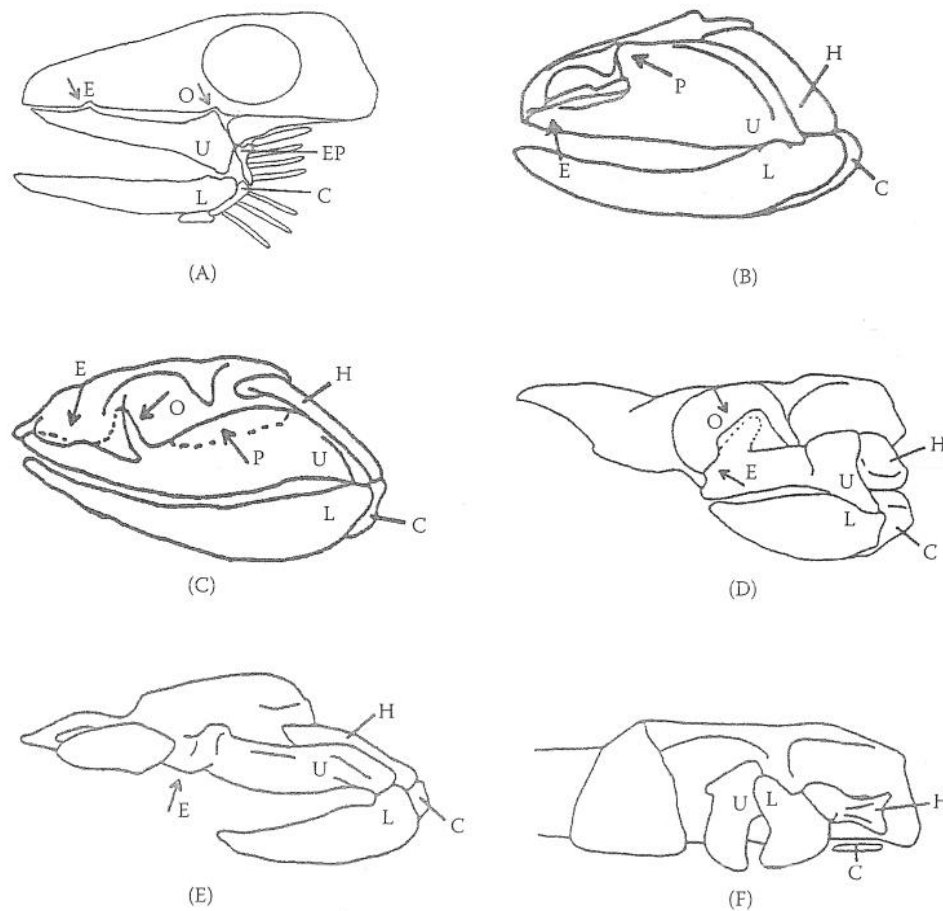
FIGURE 6.4
Left lateral views of select gnathostomes showing articulations involved with the jaw suspension. (A) Autodiastylic ancestor; (B) *Pleuracanthus*, Xenacanthida; (C) *Chlamydoselachus*, Chlamydoselachida; (D) *Squalus*, Squaliformes; (E) *Sphyrna*, Carcharhiniformes; (F) *Rhinobatos*, Batoidea. *Abbreviations:* C, ceratohyals; E, ethmoidal articulation; EP, epihyal; H, hyomandibula; O, orbital articulation; L, lower jaw; P, postorbital articulation; U, upper jaw. (From Wilga, C.D., *Biol. J. Linn. Soc.*, 75, 483–502, 2002. With permission.)

wall of the cranium by a relatively long orbital process (Figure 6.7) (Maisey, 1980; Marinelli and Strenger, 1959; Wilga and Motta, 1998a). The lemon shark has a hyostylic suspension in which the jaws are suspended from a more posteroventrally oriented hyomandibula, in contrast to the more laterally directed hyomandibula of the dogfish (Figure 6.8). The orbital process of the lemon shark is bound somewhat more loosely to the cranium by the elastic ethmopalatine ligament. The distal hyomandibula is braced against the mandibular knob of the mandible, and the ceratohyal is ligamentously bound to the distal hyomandibula and the mandible (Moss, 1965, 1972, 1977b; Motta and Wilga, 1995). In both species, the hyomandibula is ligamentously bound to the ceratohyal and in turn to the ventral basihyal, which rests somewhat dorsal to the mandibular symphysis.

Electromyographic analyses reveal that during jaw opening a relatively conservative series of events occurs in both species. Similar to the expansive phase described for teleost fishes (Lauder, 1985; Liem, 1978), the cranium is elevated by contraction of the epaxialis muscle, although cranial elevation need not occur (Motta et al., 1991, 1997; Wilga and Motta, 1998a) (Figures 6.9 and 6.10). Almost simultaneously, the mandible is depressed, primarily by the action of the coracomandibularis muscle, and the basihyal–ceratohyal apparatus begins to depress due to contraction of the coracoarcualis and coracohyoideus muscles. The branchial apparatus is depressed by the action of the coracobranchiales muscles. In the dogfish, in particular, the labial cartilages are extended as the mandible is depressed and laterally occlude the mouth (Motta et al., 1991, 1997; Wilga and Motta, 1998a). The compressive phase begins at peak gape as the mouth is maximally open, which is followed by the beginning of upper jaw protrusion and elevation of the mandible. Jaw adduction in both species is accomplished by contraction of the quadratomandibularis muscle. Various
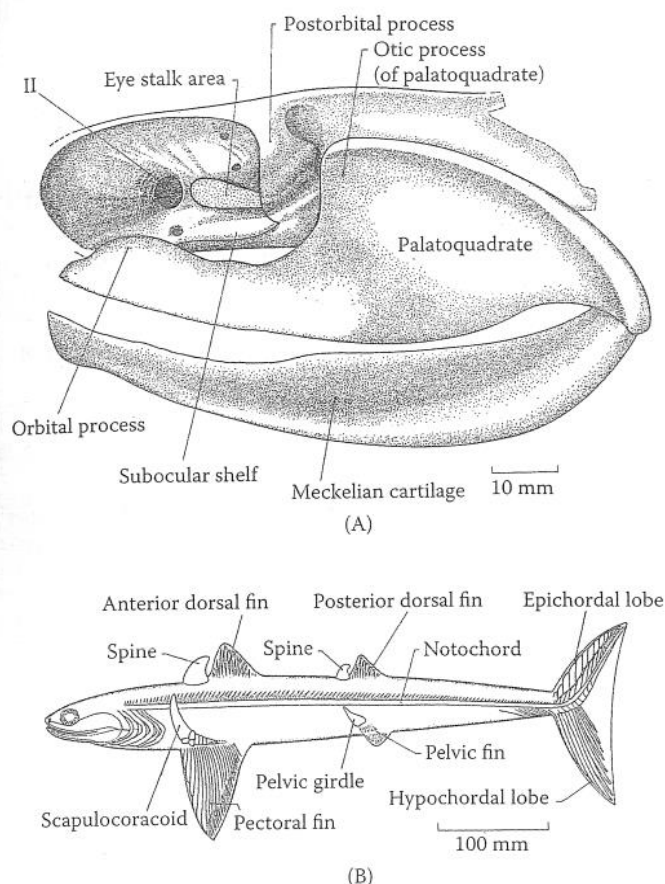
FIGURE 6.5

(A) Restoration of the neurocranium of *Cladodus*, and (B) restoration of *Cladoselache fyleri*. The cladodont palatoquadrate in panel A had a large otic process that is not well represented in the whole animal reconstruction shown in (B). The narrow suborbital ramus also extends anteriorly to the rostrum. (From Moy-Thomas, J.A. and Miles, R.S., *Paleozoic Fishes*, Chapman & Hall, London, 1971. With permission.)

FIGURE 6.6

(See color insert.) Morphoclinal transition predicted for the evolution of jaw suspension and feeding modes in chondrichthyans. Biting appears to be the basal feeding mode. Other feeding modes evolved with hyostyly, orbitostyly, and euhyostyly. *Abbreviations:* C, ceratohyals; E, ethmoidal articulation; H, hyomandibula; L, palatobasal articulation; M, lower jaw; O, orbital articulation; P, palatoquadrate; R, cranium; T, postorbital articulation; B, bite feeding; F, filter feeding; S, suction feeding. (From Wilga, C.D. et al., *Integr. Comp. Biol.*, 47, 55–69, 2007. With permission.)

combinations of the preorbitalis and levator palatoquadrati muscles that are particular to each taxon protrude the upper jaw. In squaliform sharks, such as in *Squalus acanthias*, the preorbitalis muscle (homologous to the ventral preorbitalis in carcharhiniform sharks; see Compagno, 1988, and Moss, 1972) is horizontally directed, representing the ancestral condition (Wilga, 2005). The contraction of the preorbitalis produces an anteriorly directed force near the posterior region of the jaw (Figure 6.11). This forces the orbital process of the upper jaw to slide ventrally along the orbital wall and the ethmopalatine groove to protrude the upper jaw. As the upper jaw is protruding, the orbital process slides ventrally within the sleevelike ethmopalatine ligament until the ligament becomes taut, at which time the upper jaw protrusion is complete. As the upper jaw protrudes, the entire jaw moves anteroventrally while the hyomandibula passively follows. The distal end of the hyomandibula is pulled ventrally and only
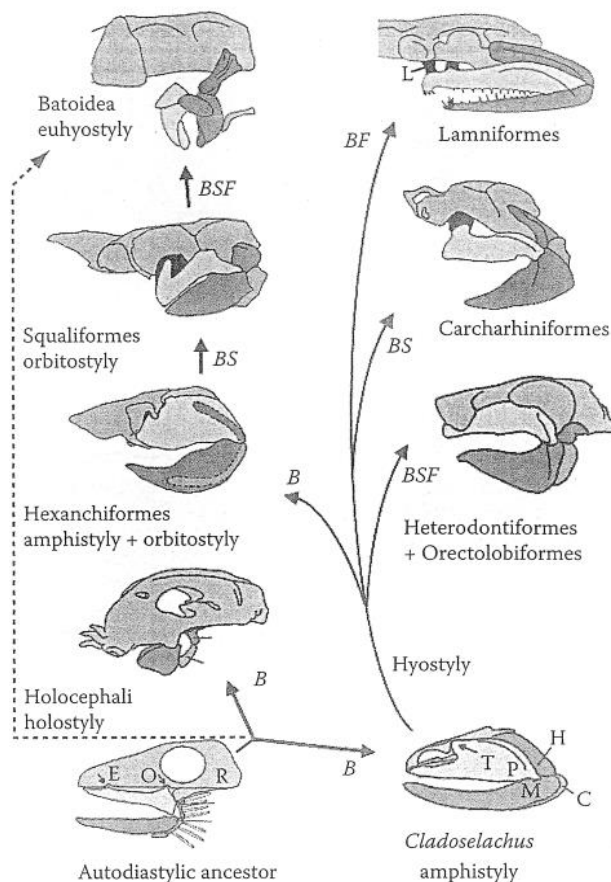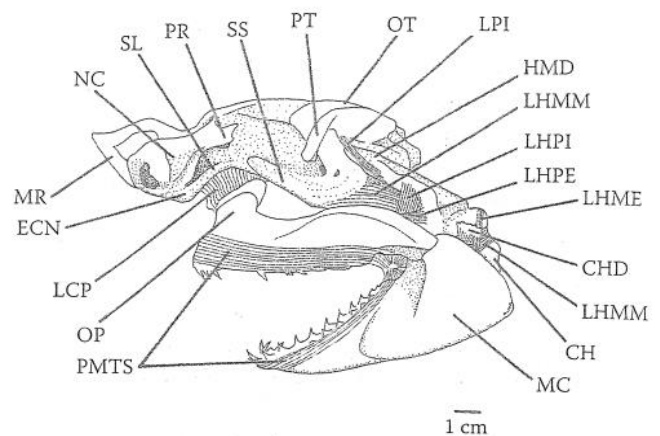
slightly anteriorly. In species with laterally or anteriorly directed hyomandibulae (e.g., *Chiloscyllium plagiosum*, *Squalus acanthias*), the distal ends of the hyomandibulae are adducted during jaw opening. In contrast, in sharks with posteriorly directed hyomandibulae such as *Isurus oxyrinchus*, *Carcharhinus plumbeus*, and *Negaprion brevirostris*, the distal ends of the hyomandibulae swing outward, forward, and downward, resulting in lateral expansion of the hyoid and increasing the gape width (Wilga, 2008). Because the action of an adductor muscle is to bring two elements closer together, contraction of the quadratomandibularis not only elevates the lower jaw but may also pull the upper jaw away from the cranium toward the lower jaw. In this way, the quadratomandibularis may assist the preorbitalis in protruding the upper jaw (Wilga and Motta, 1998a).
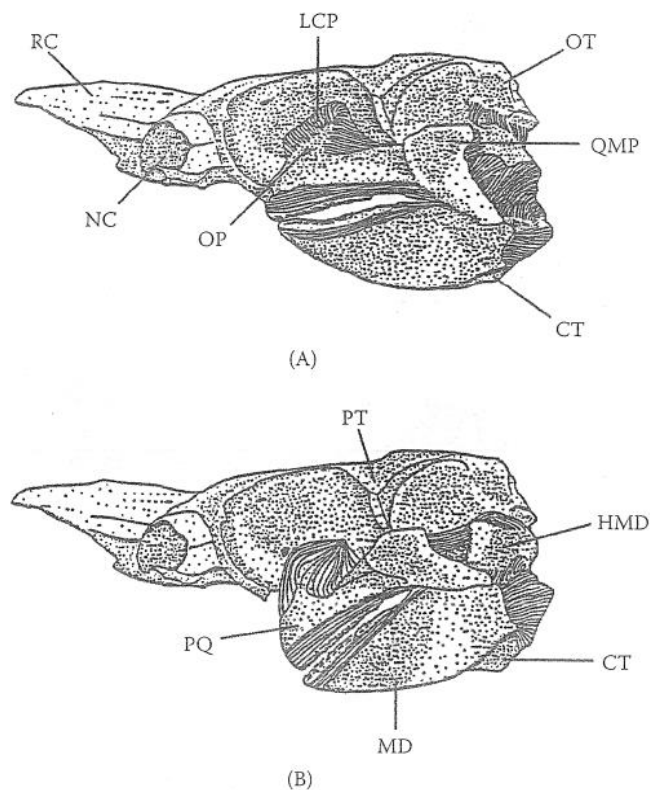
FIGURE 6.7

Left lateral view of the neurocranium, jaws, and hyoid arch of a 74.5-cm TL spiny dogfish, *Squalus acanthias*, with the skin and muscles removed. (A) At resting position, and (B) at peak upper jaw protrusion. *Abbreviations:* CT, ceratohyals; HMD, hyomandibula; LCP, ethmopalatine ligament; MD, mandible or lower jaw; NC, nasal capsule; OP, orbital process of palatoquadrate; OT, otic capsule of cranium; PQ, palatoquadrate cartilage or upper jaw; PT, postorbital process; QMP, quadratomandibularis process of palatoquadrate; RC, rostral cartilage. (From Wilga, C.D. and Motta, P.J., *J. Exp. Biol.*, 201, 1345–1358, 1998. With permission.)

FIGURE 6.8

Left lateral view of the neurocranium, jaws, and hyoid arch of a 122-cm TL lemon shark, *Negaprion brevirostris*, with the skin and muscles removed. Tendons and ligaments are indicated. *Abbreviations:* CH, ceratohyals; CHD, constrictor hyoideus dorsalis tendon; ECN, ectethmoid condyle; HMD, hyomandibula; LCP, ethmopalatine ligament; LHME, external hyoid–mandibular ligament; LHMM, medial hyoid–mandibular ligament; LHPE, external hyomandibula–palatoquadrate ligament; LHPI, internal hyomandibula–palatoquadrate ligament; LPI, postspiracularis ligament; MC, Meckel's cartilage or lower jaw; MR, medial rostral cartilage; NC, nasal capsule; OP, orbital process of palatoquadrate; OT, otic capsule; PMTS, palatoquadrate–mandibular connective tissue sheath; PR, preorbital process; PT, postorbital process; SL, suborbital ledge; SS, suborbital shelf. (From Motta, P.J. and Wilga, C.D., *J. Morphol.*, 226, 309–329, 1995. With permission.)

The mechanism of upper jaw protrusion in carcharhiniform sharks differs slightly from that in squaliform sharks. The carcharhiniform mechanism has been proposed in several studies (Frazzetta, 1994; Frazzetta and Prange, 1987; Luther, 1909; Moss, 1972) and has largely been supported in functional studies of feeding in *Negaprion brevirostris*, and the bonnethead shark, *Sphyrna tiburo* (Motta et al., 1997; Wilga, 1997; Wilga and Motta, 2000). Carcharhiniform sharks have a derived condition in which the levator palatoquadrati muscle is oriented more anteroposteriorly instead of dorsoventrally as in dogfish (Figure 6.9) (Compagno, 1988; Moss, 1972; Nakaya, 1975). In this orientation, the levator palatoquadrati muscle can assist the dorsal and ventral preorbitalis muscles (carcharhiniform sharks have two divisions of the preorbitalis muscle) in protruding the upper jaw (Figure 6.10). The dorsal division of the preorbitalis pulls the palatoquadrate ventrally as the ventral division of the preorbitalis and the levator palatoquadrati muscles pull it anterodorsally. Similar to the dogfish, the orbital process of the palatoquadrate is forced to glide on the ethmopalatine groove, and the resultant reaction force drives the upper jaw anteriorly and ventrally to protrude it. As the upper jaw is protruded, the ropelike ethmopalatine ligament unfolds (it is folded in the resting position) until it becomes taut, halting upper jaw protrusion. As the upper jaw protrudes, the jaws and the distal end of the hyomandibula also swing anteroventrally but to a greater extent than in the spiny dogfish, and the distal ceratohyal and basihyal complex pivots posteroventrally (Motta and Wilga, 1995; Motta et al., 1997; Wilga, 2005; Wilga and Motta, 2000). Contraction of the quadratomandibularis muscle might also assist upper jaw protrusion as described above (Moss, 1965). Lamnid sharks such as *Carcharodon carcharias* have shifted the insertion of the preorbitalis and levator hyomandibularis muscles so they have more forceful and controlled movement of the upper jaw, and white sharks are known to protrude and retract the upper jaw several times during a gape cycle (Tricas and McCosker, 1984; Wilga, 2005). Numerous functions for protrusion have been proposed, including more efficient biting of the prey, gouging of the upper jaw into large prey, reorientation of the teeth, simultaneous
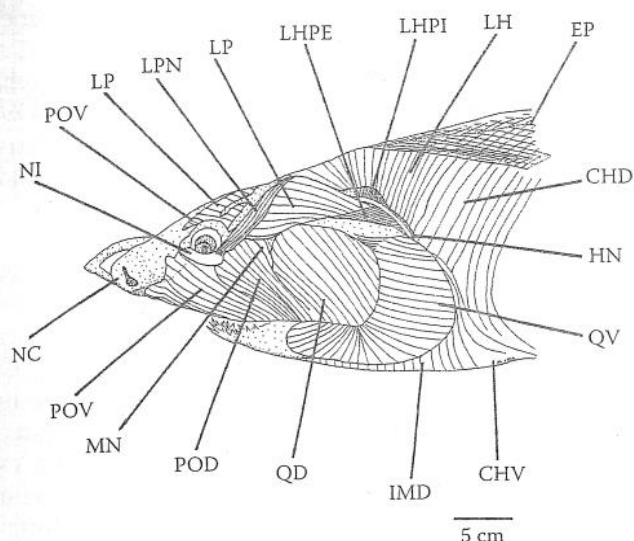
FIGURE 6.9

Left lateral view of the head and muscles of a 229-cm TL lemon shark, *Negaprion brevirostris*, with the skin removed and muscle fiber direction indicated. Myosepta of the epaxialis muscle (W-shape) are indicated in addition to the muscle fiber direction. The chondrocranial–palatoquadrate connective tissue sheath is removed. *Abbreviations:* CHD, constrictor hyoideus dorsalis; CHV, constrictor hyoideus ventralis; EP, epaxialis; HN, hyomandibular nerve; IMD, intermandibularis; LH, levator hyomandibularis; LHPE, external hyomandibula–palatoquadrate ligament; LHPI, internal hyomandibula–palatoquadrate ligament; LP, levator palatoquadrati; LPN, levator palpebrae nictitantis; MN, mandibular branch of trigeminal nerve; NC, nasal capsule; NI, nictitating membrane; POD, dorsal preorbitalis; POV, ventral preorbitalis; QD, quadratomandibularis dorsal; QV, quadratomandibularis ventral. (From Motta, P.J. and Wilga, C.D., *J. Morphol.*, 226, 309–329, 1995. With permission.)

closing of the upper and lower jaws, and reducing the time to close the jaws on the prey, to name a few. Only one function, reducing the time to close the jaws, has been experimentally verified (reviewed in Motta, 2004; Wilga, 2005).

Peak hyoid depression occurs in the latter half of the compressive phase. In *Squalus acanthias, Negaprion brevirostris,* and *Sphyrna tiburo* the mandible meets the maximally protruded upper jaw either with the food grasped between the teeth or after the food has been engulfed and passes through the buccal cavity. Finally, the recovery phase occurs as the palatoquadrate is retracted into its cranial seat. In the dogfish, the dorsoventrally oriented levator palatoquadrati assists in its retraction, whereas in the carcharhinids the elastic ethmopalatine ligament assists. It is not known if the ethmopalatine ligament of squaloids is elastic. In both species, however, the levator hyomandibularis retracts the hyomandibula, helping to elevate the entire jaw apparatus (Motta et al., 1997; Wilga and Motta, 1998a, 2000; see Wilga, 2005, for a discussion of the ethmopalatine ligament and jaw support in lamniform sharks).
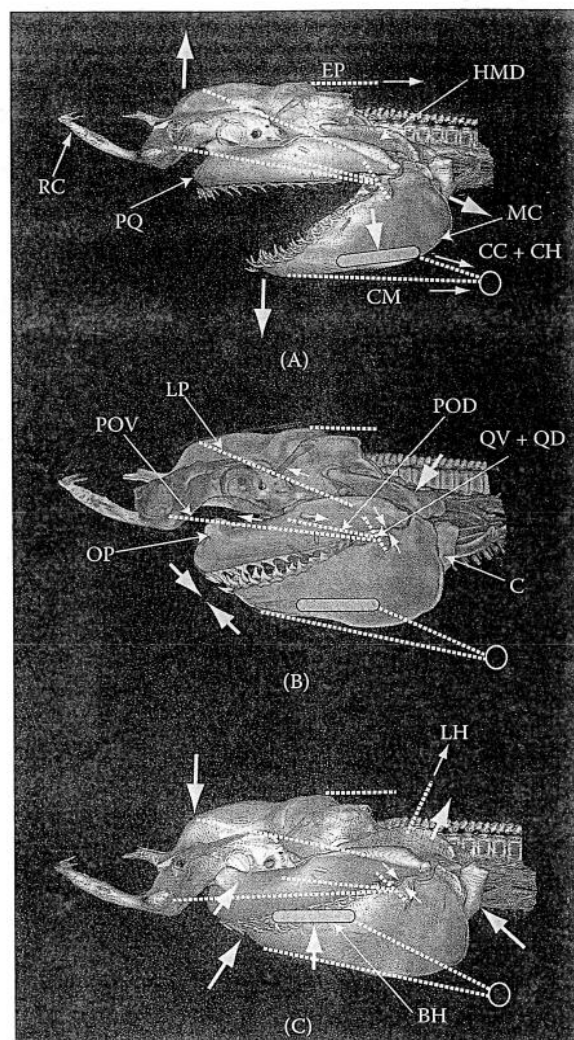

FIGURE 6.10

A reconstruction of chondrocranial, mandibular, and hyoid arch kinetics during feeding in the blacktip shark *Carcharhinus limbatus*. (A) Expansive phase, characterized by depression of the mandible, elevation of the cranium, hyoid depression, and movement of the hyomandibula such that its anterior end is depressed along with the basihyal and its posterior end pivots about its joint with the distal hyomandibula. (B) Compressive phase, characterized by elevation of the mandible to the protruded upper jaw and anteroventral movement of the distal hyomandibula. (C) Recovery phase, characterized by hyomandibular and palatoquadrate retraction, elevation of the basihyal, and depression of the cranium. The cranial elements were manipulated into the approximate anatomical positions for the CT scan; however, the hyomandibula and basihyal were most likely not depressed to the extent possible during a feeding event. Consequently, the anterior end of the ceratohyal is not fully depressed. The branchial arches are not manipulated and their movement is not indicated. Dotted white lines indicate approximate muscle origins and insertions, large arrows indicate the movement of specific elements, and small arrows indicate direction of muscle contraction. *Abbreviations:* BH, basihyal; C, ceratohyals; CC, coracoarcualis; CH, coracohyoideus; CM, coracomandibularis; EP, epaxialis; HMD, hyomandibula; LH, levator hyomandibularis; LP, levator palatoquadrati; MC, Meckel's cartilage or lower jaw; OP, orbital process of the palatoquadrate; POD, dorsal preorbitalis; POV, ventral preorbitalis; PQ, palatoquadrate cartilage or upper jaw; QD, quadratomandibularis dorsal; QV, quadratomandibularis ventral; RC, rostral cartilage.
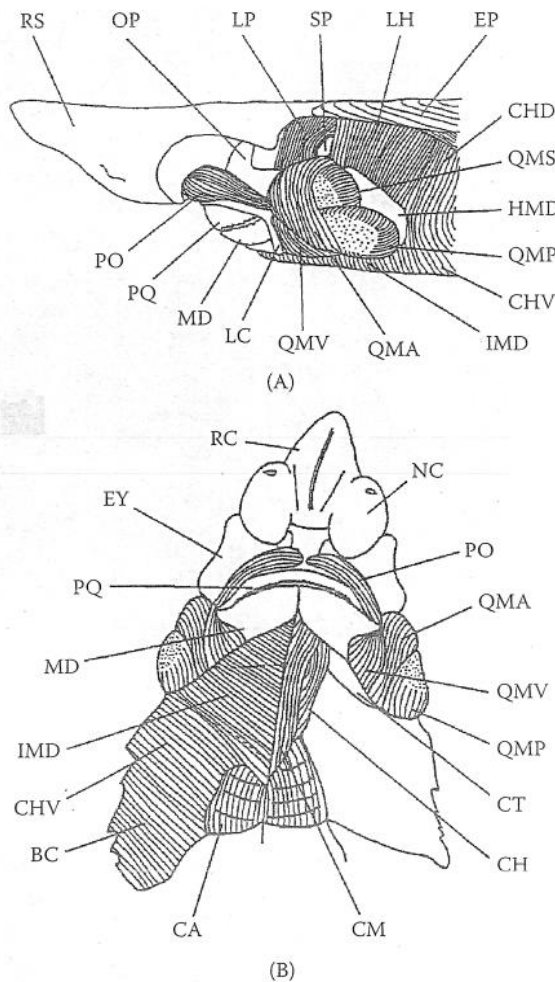
FIGURE 6.11

(A) Left lateral view (74.5-cm TL) and (B) ventral view (60-cm TL) of the head of the spiny dogfish, *Squalus acanthias*, with the skin and eye removed and muscle fiber direction indicated. Skin over the rostrum and cranium is left intact. Myosepta only of the epaxialis muscle are indicated. Raphe overlying quadratomandibularis is indicated by stippling. Anterior and posterior margins of the interhyoideus (deep to intermandibularis) are indicated by dotted lines. *Abbreviations:* BC, branchial constrictors; CA, coracoarcualis; CH, coracohyoideus; CHD, constrictor hyoideus dorsalis; CHV, constrictor hyoideus ventralis; CM, coracomandibularis; CT, ceratohyals; EP, epaxialis; EY, eye; HMD, hyomandibula; IMD, intermandibularis; LC, labial cartilages; LH, levator hyomandibularis; LP, levator palatoquadrati; MD, mandible or lower jaw; NC, nasal capsule; OP, orbital process of palatoquadrate; PO, preorbitalis; PQ, palatoquadrate or upper jaw; QMA, quadratomandibularis anterior; QMS, quadratomandibularis superficial; QMP, quadratomandibularis posterior; QMV, quadratomandibularis ventral; RC, rostral cartilage; RS, rostrum; SP, spiracularis. (From Wilga, C.D. and Motta, P.J., *J. Exp. Biol.*, 201, 1345–1358, 1998. With permission.)

The kinematic sequence described above is similar to that reported for carcharhiniform sharks such as the blacknose (*Carcharhinus acronotus*), blacktip (*C. limbatus*), swell (*Cephaloscyllium ventriosum*), and Caribbean reef (*Carcharhinus perezi*) sharks, although cranial elevation and upper jaw protrusion may be lacking in some bites (Ferry-Graham, 1997a, 1998a; Frazzetta and Prange, 1987; Motta and Wilga, 2001). This differs somewhat for surface feeding in the lamnid white shark, *Carcharodon carcharias*, in that peak upper jaw protrusion occurs well before the lower jaw is completely elevated, and cranial depression may not occur until the recovery phase rather than during the compressive phase (Tricas, 1985; Tricas and McCosker, 1984). Prey capture, manipulation, and transport events in *Negaprion brevirostris*, *Squalus acanthias*, and *Sphyrna tiburo* have a common kinematic and motor pattern sequence but are distinguishable from each other by their duration and relative timing of individual kinematic events. Manipulation and transport events are typically shorter than capture events, although crushing manipulation events may be extensive in some species (Motta and Wilga, 2001; Motta et al., 1997; Wilga, 1997; Wilga and Motta, 1998a,b, 2000).

The mechanics of suction feeding in sharks and rays is understood from kinematic and electromyographic analyses (Clark and Nelson, 1997; Edmonds et al., 2001; Ferry-Graham, 1997b, 1998b; Lowry and Motta, 2007, 2008; Lowry et al., 2007; Matott et al., 2005; Motta, pers. obs.; Motta et al., 2002, 2008; Nauwelaerts et al., 2008; Robinson and Motta, 2002; Wilga and Sanford, 2008; Wu, 1994). A variety of extant and primarily benthic elasmobranchs use inertial suction to some degree as their dominant feeding method: whitespotted bamboo shark (*Chiloscyllium plagiosum*) (Lowry and Motta, 2007, 2008; Nauwelaerts et al., 2008; Wilga and Sanford, 2008; Wilga et al., 2007); spiny dogfish (*Squalus acanthias*) (Wilga and Motta, 1998a; Wilga et al., 2007); leopard shark (*Triakis semifasciata*) (Ferry-Graham, 1998b; Lowry and Motta, 2008; Russo, 1975; Talent, 1976); wobbegong (*Orectolobus maculatus*), nurse shark (*Ginglymostoma cirratum*), whale shark (*Rhincodon typus*), and zebra shark (*Stegostoma fasciatum*) (Clark and Nelson, 1997; Matott et al., 2002, 2005, 2008, 2010; Motta, pers. obs.; Robinson and Motta, 2002; Wu, 1994); horn shark (*Heterodontus francisci*) (Edmonds et al., 2001; Strong, 1989); chain catshark (*Scliorhinus retifer*) (Ajemian and Sanford, 2007); little skates (*Leucoraja erinacea*) (Wilga et al., 2007); guitarfish (*Rhinobatos lentiginosus*) (Wilga and Motta, 1998b); cownose ray (*Rhinoptera bonasus*) (Sasko et al., 2006); lesser electric ray (*Narcine bancroftii*) (Dean and Motta, 2004a,b); spotted torpedo ray (*Torpedo marmorata*) (Belbenoit, 1986; Belbenoit and Bauer, 1972; Michaelson et al., 1979; Wilson, 1953); and perhaps the angel shark (*Squatina californica*) (Fouts and Nelson, 1999). Inertial suction-feeding elasmobranchs are found in at least eight families, often nested within clades that contain ram and compensatory suction feeders, indicating that specialization for inertial suction feeding has most likely evolved independently in several elasmobranch lineages (Motta and Wilga, 2001; Motta et al., 2002; Wilga et al., 2007).
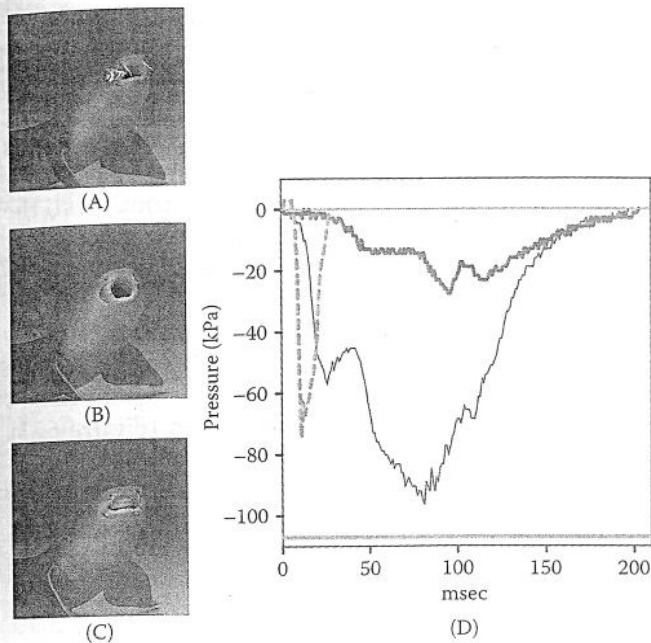
(A)

(B)

(C)

(D)

FIGURE 6.12
(See color insert.) Suction food capture in an 85-cm TL nurse shark, *Ginglymostoma cirratum*. (A) Mandible depression, which averages 26 ms, is occurring during the expansive phase. (B) Peak gape, which occurs at 32 ms, is visible with the food entering the mouth (36 ms). (C) Upper jaw protrusion is visible as the white band inside the mouth during the compressive phase. Total bite time averages 92 ms. (D) Three representative buccal pressure profiles from different semicaptive adult *Ginglymostoma cirratum* demonstrating the variability in suction performance during feeding. Some captures are extremely rapid with large subambient pressures (green dashed line), others can approach −1 atmosphere but be more prolonged (blue solid line), whereas others may generate little subambient pressure (red dash–dot line). The lower gray line indicates −1 atmosphere pressure at the average depth of the probe (~0.5 m). (From Motta, P.J. et al., *J. Morphol.*, 269, 1041–1055, 2008. With permission.)

Ginglymostoma cirratum (Ginglymostomatidae), *Triakis semifasciata* (Triakidae), and *Heterodontus francisci* (Heterodontidae) appear to exhibit an abbreviated kinematic sequence in which cranial elevation is reduced or lacking during many capture bites. In contrast, carcharhiniform and lamniform sharks usually consume relatively large prey with their ventrally located mouth, and as such they elevate the cranium and depress the mandible to open the mouth as wide as possible and direct the gape more anteriorly toward the prey. In contrast, *G. cirratum*, *T. semifasciata*, *H. francisci*, and perhaps most suction-feeding sharks primarily capture relatively small prey with a mouth that is almost terminal when maximally open (e.g., *G. cirratum*) or a mouth that is protruded anteroventrally to capture prey below them (e.g., *Squalus acanthias*). Consequently, lifting of the cranium during prey capture may not always be necessary (Lowry and Motta, 2007; Matott et al., 2005; Motta et al., 2002, 2008). In these suction-feeding sharks, the labial cartilages

protrude anteriorly as the lower jaw is depressed to effectively form a lateral enclosure of the mouth (Figure 6.12). This not only directs the suction anteriorly but may also prevent the food from escaping from the sides of the mouth (Edmonds et al., 2001; Ferry-Graham, 1997b, 1998b; Motta and Wilga, 1999; Wilga and Motta, 1998a).

In the suction-feeding whitespotted bamboo shark, *Chiloscyllium plagiosum*, the progression of the anterior to posterior expansion of the buccal, hyoid, and pharyngeal cavities is accompanied by sequential onset of subambient pressures in these cavities as the prey is drawn into the mouth. The increased velocity of hyoid area expansion is primarily responsible for generating peak subambient pressure in the buccal and hyoid regions (Wilga and Sanford, 2008). In the nurse shark, *Ginglymostoma cirratum*, peak subambient pressure is not related to shark size but instead to the rate of buccopharyngeal expansion (Motta et al., 2008). Buccopharyngeal expansion in these suction-feeding elasmobranchs appears to be mostly due to ventral expansion of the hyoid cavity, not lateral expansion, with the orientation of the hyomandibular cartilages making the difference (Wilga, 2010). Concomitant with an allometric increase in the relative contribution of suction over ontogeny in *C. plagiosum*, the hyoid muscles that expand the buccopharyngeal chamber hypertrophy (Lowry and Motta, 2007).

Not surprisingly, bite duration, from the beginning of mandible depression to retraction of the jaws to their resting position, is generally shorter for the suction-feeding sharks (*Chiloscyllium plagiosum*, 69 ms; *Ginglymostoma cirratum*, 100 ms; *Heterodontus francisci*, 113 to 148 ms; *Triakis semifasciata*, 150 to 180 ms) than for ram-feeding sharks (*Sphyrna tiburo*, 302 ms; *Negaprion brevirostris*, 309 ms; *Carcharhinus perezi*, 383 ms; *Cephaloscyllium ventriosum*, 367 to 419 ms; *Carcharodon carcharias*, 405 ms). Bite duration is 200 ms for suction-feeding and 280 ms for ram-feeding sequences in the dogfish. Time to maximum gape from mouth opening is similarly much faster in suction-feeding sharks (*Orectolobus maculatus*, 30 ms; *G. cirratum*, 32 ms; *H. francisci*, 47 to 64 ms) compared to the ram-feeding sharks (*N. brevirostris*, 81 ms; *C. perezi*, 120 ms; *S. tiburo*, 162 ms) (Edmonds et al., 2001; Ferry-Graham, 1997a; Lowry and Motta, 2008; Motta et al., 1997, 2002; Tricas, 1985; Tricas and McCosker, 1984; Wilga and Motta, 1998a,b; Wu, 1994). Faster buccopharyngeal expansion for suction-feeding sharks is expected because the dominant force that suction-feeding fishes exert on their prey is the fluid pressure gradient experienced by the prey (Wainwright and Day, 2007). The forces exerted on the prey can be elevated by increasing the rate of expansion or by reducing the size of the mouth aperture (Carroll et al., 2004; Lauder, 1980; Muller et al., 1982; Sanford and Wainwright, 2002; Svanback et al., 2002; Van Wassenbergh et al., 2006; Wainwright and Day, 2007; Wainwright et al., 2001a,b). Suction pressure

in specialized suction-feeding sharks can be large. *Chiloscyllium plagiosum* can generate subambient pressures as low as –99 kPa, and *Ginglymostoma cirratum* as low as –110 kPa. Nurse sharks may use a spit–suck manipulation to dismember larger prey (Matott et al., 2005; Motta and Wilga, 1999; Motta et al., 2002, 2008; Robinson and Motta, 2002; Tanaka, 1973; Wilga and Sanford, 2008). Despite large suction pressures, the parcel of water and consequently the prey that is effectively sucked into the mouth only extend a few centimeters in front of the mouth, although feeding just above the substrate can extend this effective distance approximately 2.5 times. As a result, these suction-feeding elasmobranchs need to closely approach their prey to capture them or to thrust their heads into crevices. This functional limitation may lead to stalking or ambushing of

prey or nocturnal foraging when they can more closely approach their prey (Ajemian and Sanford, 2007; Lowry and Motta, 2008; Motta et al., 2008; Nauwelaerts et al., 2007; Wilga et al., 2007).

Based on kinematic and cineradiograhic analysis and dissection, Wu (1994) proposed a mechanism for upper jaw protrusion in orectolobid sharks. First, the intermandibularis and interhyoideus muscles that span the inner margins of the mandible and ceratohyals, respectively, contract and medially compress the lower jaw and hyomandibulae. This results in a more acute symphyseal angle of the lower jaw such that the jaws move anteriorly similar to the change in height of a triangle when the base is shortened (Figure 6.13). As the lower jaw is depressed it pushes on the relatively large labial cartilages, swinging them laterally
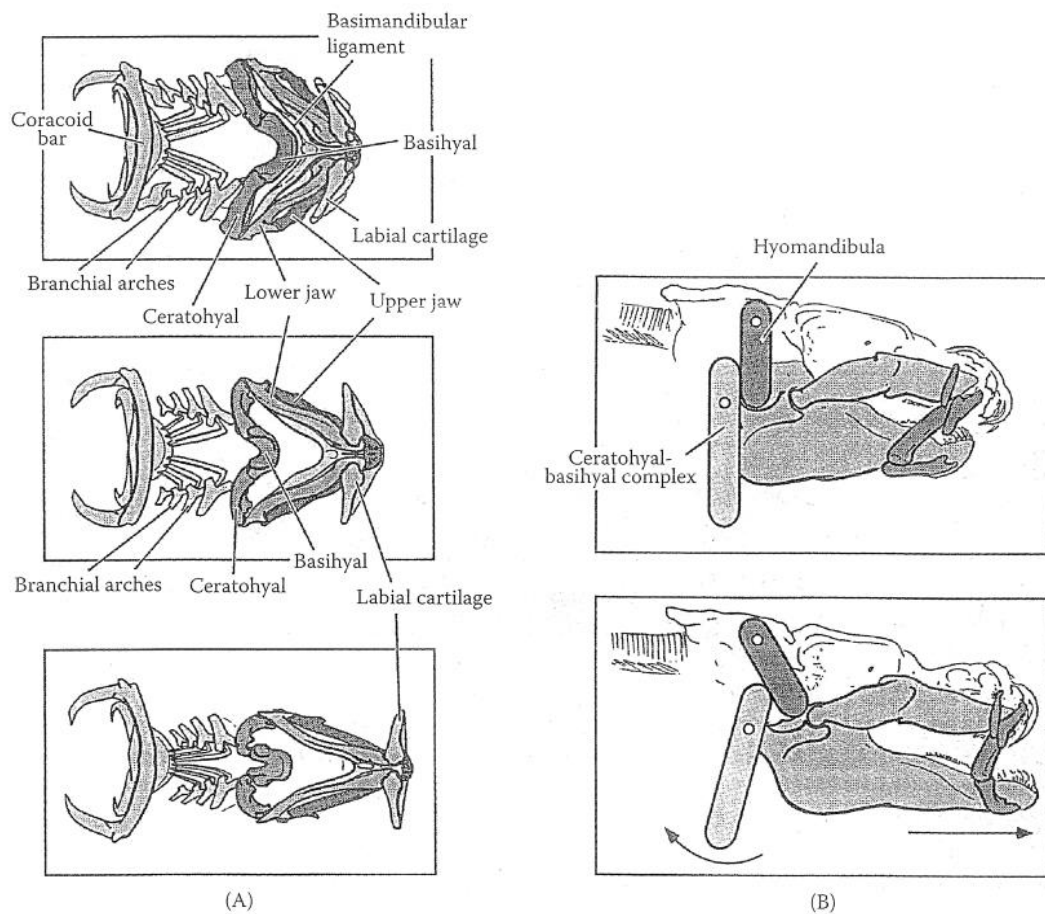
FIGURE 6.13

Feeding mechanism of *Orectolobus maculatus*. (A) Ventral view of the head, branchial arch, and pectoral girdle skeleton during jaw protrusion. In the top figure, the shark is shown with its mouth closed. In the center figure, the jaws are partly protruded, showing retraction of the basihyal, lateral compression of the jaw joints, and anterolateral swing of the labial cartilages. In the bottom figure, the jaws are completely protruded, showing the continued compression of the jaw joints and the branchial arches. The labial cartilages reach their maximum arc. (B) Schematic of the ceratohyal–hyomandibular mechanism of jaw protrusion. In the upper figure, the ceratohyal and the hyomandibula are represented as two links of a kinematic chain. In the lower figure, as the ceratohyal rotates around the posterior process of the lower jaw, the dorsal end pushes against the hyomandibula. The hyomandibula rotates forward against the mandibular knob and pushes the lower jaw forward. (From Wu, E.H., *J. Morphol.*, 222, 175–190, 1994. With permission.)
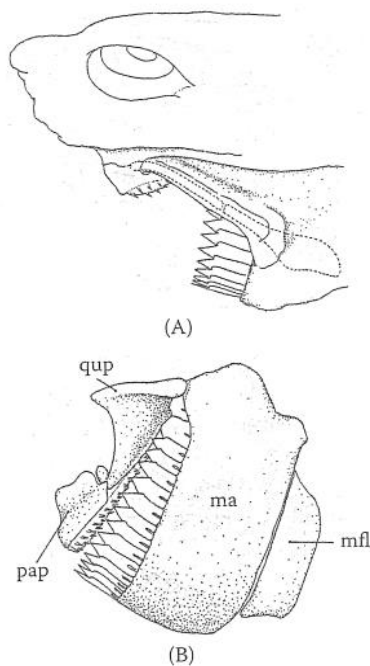
FIGURE 6.14
(A) Lateral view of the mouth of *Isistius brasiliensis* with the upper jaw protruded. Labial cartilages are indicated by broken line. (B) Lateral view of the upper and lower jaw showing hinge on the upper jaw. *Abbreviations:* Ma, mandibula or lower jaw; mfl, mandibular flap (a flexible, weakly chondrified plate at its posteroventral edge); pap, palatine process of palatoquadrate; qup, quadrate plate of palatoquadrate. (From Shirai, S. and Nakaya, K., *Zool. Sci.*, 9, 811–821, 1992. With permission.)

FIGURE 6.15
(See color insert.) Diagram of the skeleton, muscles, and ligaments associated with jaw movements in the megamouth shark, *Megachasma pelagios*. *Abbreviations:* bh, basihyal; ch, ceratohyals; hy, hyomandibula; mc, Meckel's cartilage; nc, neurocranium; pq, palatoquatrate. (From Nakaya, K. et al., *J. Fish Biol.*, 73, 17–34, 2008. With permission.)

and anteriorly and moving the oral aperture forward to form a round mouth opening. In addition, Wu proposed that the ceratohyals rotate around a process on the lower jaw, pushing the hyomandibulae anteroventrally, which in turn pushes the jaw articulation ventrally and anteriorly to protrude the jaws (Figure 6.13). This putative mechanism awaits electromyographic confirmation.

The cookie-cutter shark, *Isistius brasiliensis*, employs a unique behavior and mechanism to gouge out pieces of its prey. It anchors itself to the prey with its hooklike upper teeth and sinks its large sawlike lower teeth into the prey as it apparently sucks onto its prey, forming a seal with its fleshy lips. Twisting about its longitudinal axis, it gouges out a piece of flesh, leaving a craterlike wound (Compagno, 1984; Jones, 1971; LeBoeuf et al., 1987; Shirai and Nakaya, 1992). The upper jaw of this small shark is reduced in size and composed of two pieces: an anterior section that can pivot dorsally and a posterior section. The lower jaw is relatively large and robust (Figure 6.14). Presumably the upper jaw pivots at this juncture when the shark has gripped its prey with its upper jaw, allowing the shark to pivot dorsally about this joint and sink its large lower jaw teeth into the prey.

The adductor mandibulae and preorbitalis muscles are modified, apparently to facilitate the gouging function of the lower jaw (Shirai and Nakaya, 1992).

The megamouth shark, *Megachasma pelagios*, is apparently a slow, weak swimmer that filter feeds on small, deepwater prey such as euphausid shrimp. This shark has a large terminal mouth, no labial cartilage, densely packed papillose gill rakers, and relatively small gill openings, and the upper jaw is very protrusible. Anatomical investigation suggests that bioluminescent tissue in its mouth likely attracts prey. The shark has long palatorostral and ethmopalatine ligaments and long hyomandibular and ceratohyal cartilages. Together with a stretchy skin, these features give it a very kinetic jaw mechanism that is capable of extreme jaw protrusion and lateral expansion and depression. The large gape creates a low-velocity, high-volume suction that pulls the prey into the mouth. As the shark swims forward, the water and prey are forced into the distended buccopharyngeal cavity by ram; when the cavity is fully distended, the mouth is closed and the water is forced over the gill rakers, filtering out the prey (Figures 6.3 and 6.15). Thus, this shark uses a combination of suction, ram, and engulfment, similar to that of balenopterid whales (Nakaya et al., 2008).

The basking shark, *Cetorhinus maximus*, has slender jaws that are hardly protrusible. The jaws of *C. maximus* swing ventrally on the cranium and spread apart to form a circular hooplike mouth. When the mouth is open, two rows of bristle-like gill rakers stretch across each gill slit with an inter-raker distance of about 0.8 mm. The rakers do not greatly impede water flow through the gills and out the large gill openings but catch microscopic crustaceans. The filtering apparatus of the basking shark is better suited for a higher rate of water flow than the megamouth shark, and the former is better suited for sustained, powerful swimming, which may average 0.85 m/s as it ram filter feeds (Clark and Nelson, 1997; Compagno, 1990; Gudger, 1941a,b; Matthews and Parker, 1950; Taylor et al., 1983; Sims, 2000, 2008). Seasonal change in feeding morphology occurs in *C. maximus*. The gill raker sieve is apparently shed sporadically and nonsynchronously each year during late autumn or winter, a period during which the sharks were believed not to feed; however, some basking sharks have been caught with gill rakers in autumn and winter, and it is now evident that basking sharks can continue to feed at plankton densities much lower than previously thought possible (Francis and Duffy, 2002; Parker and Boeseman, 1954; Sims, 1999, 2008; Sims et al., 1997).

The whale shark, *Rhinocodon typus*, employs either a ram or pulsatile suction-filtering mechanism during which the shark may swim at (0.3 to 1.5 m/s) or below (0.2 to 0.5 m/s) the surface, or they may slow down and even cease swimming, assuming a horizontal or nearly vertical position to suction food into the mouth (Clark and Nelson, 1997; Heyman et al., 2001; Motta et al., 2010; Nelson and Eckert, 2007; Taylor, 2007). The diet of the whale shark is primarily composed of plankton, which they filter through 20 unique filtering pads that occlude the pharyngeal openings. A reticulated mesh lies on the proximal surface of the pads; the openings average 1.2 mm in diameter (Figure 6.16). These sharks can feed on fish eggs that are smaller in diameter than the pore openings of the pads (Heyman et al., 2001; Hoffmayer et al., 2007). This may be due to cross-flow filtration whereby the pads lie at an acute angle to the incoming water and plankton. If this mechanism does occur, the plankton would accumulate at the posterior end of the buccopharyngeal chamber while the water would exit through the pads. Such a mechanism would reduce clogging of the pads and concentrate the food into a bolus for swallowing (Motta et al., 2010).

6.3.3.2 Batoids

The feeding mechanics of batoids differs from that of sharks in cranial anatomy and function. The hyoid arch of batoids is modified in that the hyomandibula is the only major support for the jaws (euhyostylic jaw suspension) and the basihyal and ceratohyal are disconnected and separated ventrally from the hyomandibulae, becoming more or less degenerate or lost (Compagno, 1999; Heemstra and Smith, 1980; Miyake and McEachran, 1991). This decoupling of the jaws and hyomandibulae from the branchial arches may have increased the role of the branchial arches in feeding. Prey can now be processed by rhythmic contractions of the branchial and jaw arches to create a highly controlled and coordinated flow of water, essentially a "hydrodynamic tongue" for the delicate separation of edible and inedible materials (Dean et al., 2005, 2007b). Furthermore, while the cranial muscles of batoids are generally similar to sharks, the homologies of some are unclear (e.g., the "X" muscle of electric rays), the muscles are depressed in form (e.g., preorbitalis), some muscles may be lacking (e.g., intermandibularis), and some muscles may be unique to batoids (e.g., coracohyomandibularis) (Miyake et al., 1992).

There are very few studies on the feeding mechanism of batoids; three involve the guitarfish (*Rhinobatos lentiginosus*), the lesser electric ray (*Narcine bancroftii*), and the cownose ray (*Rhinoptera bonasus*). The guitarfish captures its food by suction. The suction captures, manipulation bites, and suction transport of the food through the buccal cavity are all similar in the relative sequence of kinematic and motor activity but differ in the absolute muscle activation time, the presence or absence of muscle activity, and in the duration of muscle activity (Figure 6.17). A preparatory phase, which is often present prior to food capture, is marked by activity of the levator palatoquadrati muscle as the upper jaw is being retracted. The expansive phase is characterized by mouth opening, during which posteroventral depression of the lower jaw is initiated by the coracomandibularis. Midway through the expansive phase, the hyomandibula is depressed ventrally by the coracohyomandibularis and occasionally by the depressor hyomandibularis, which expands the orobranchial cavity. Movement of the food toward the mouth occurs during the activity of the hyomandibular depressors. The compressive phase begins with elevation of the lower jaw and the beginning of upper jaw protrusion. Maximum upper jaw protrusion is attained just prior to complete closure of the jaws. The compressive phase is represented by motor activity in the jaw adductors. Protrusion appears to be a coordinated effort of the quadratomandibularis and preorbitalis. The quadratomandibularis not only elevates the lower jaw but also protrudes the upper jaw by pulling the upper jaw ventrally toward the lower jaw. As the preorbitalis pulls the jaws anteroventrally, the upper jaw is protruded and the lower jaw is elevated by the quadratomandibularis until the jaws are closed. In the final recovery phase, the head and jaws are returned to their resting position. The upper jaw is retracted by the levator palatoquadrati
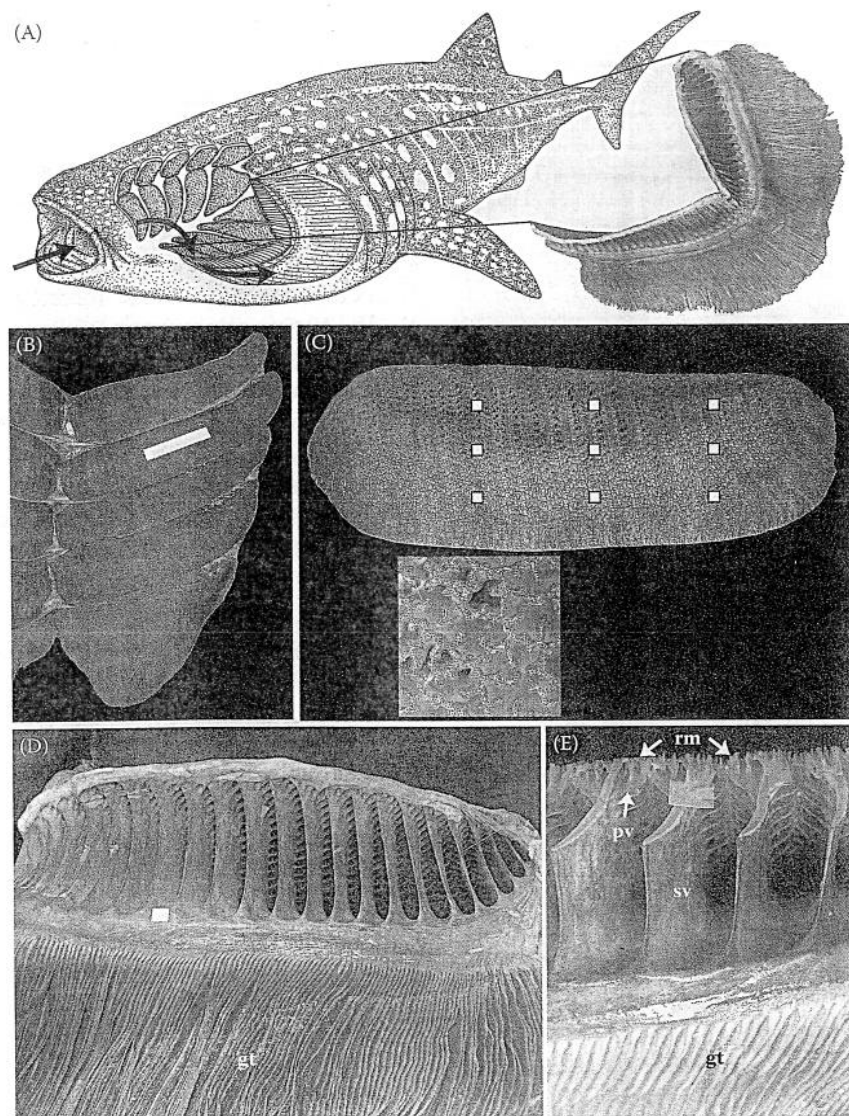
FIGURE 6.16
(See color insert.) (A) Schematic representation of a surface ram filter feeding whale shark, *Rhincodon typus*, showing the approximate position of the filtering pads and the direction of water flow through them. Inset shows a lateral view of the vanes deep to the filtering mesh, as well as the primary gill filaments on the first branchial arch over which the water flows. (B) Gross morphology of the whale shark filtering pads. Dorsal view of the lower filtering pads of a shark of approximately 622-cm TL. The fifth most posterior lower pad at the bottom is triangular in shape, and the lateral side of the pads is to the left. The lateral raphe between the lower and upper pads is visible toward the left. All other soft tissue has been removed. White ruler is 15 cm. (C) The upper second filtering pad of a shark of approximately 593-cm TL. Because it is an upper pad, lateral is to the left and posterior toward the top. Upper pads are not as falcate on their medial margin as the lower pads. The 1-cm squares indicate areas sampled to measure mesh diameter, and the inset is a representative 1-cm square area showing the irregularly shaped holes of the reticulated mesh. (D) External view of the first upper left pad of 622-cm TL shark with lateral margin toward the left. Note that the secondary vanes direct water laterally into the parabranchial chamber and over the gill tissue (gt) before it exits the pharyngeal slit (not shown). White square is 1 cm. (E) Close-up of a section through the third left lower filtering pad of 622-cm TL shark showing the reticulated mesh (rm), primary vanes (pv), secondary vanes (sv), and gill tissue (gt). Water flow is through the mesh, between the primary and secondary vanes, and over the gill tissue. White square is 1 cm. (From Motta, P.J. et al., *Zoology*, 113, 199–212, 2010. With permission.)

and the hyomandibula is retracted by the levator hyomandibularis. Hyomandibular elevation also elevates the jaws because the mandible is attached to the hyomandibula. The cranium is finally elevated to its resting position by the epaxialis and the levator rostri (Wilga and Motta, 1998b).

The lesser electric ray, *Narcine bancroftii*, has a remarkably protrusible and versatile mouth that it uses to probe beneath the substrate and suction feed on benthic invertebrates such as polychaete worms. Based on high-speed videographic analysis and anatomical dissection, Dean and Motta (2004a,b) proposed a novel mechanism for jaw
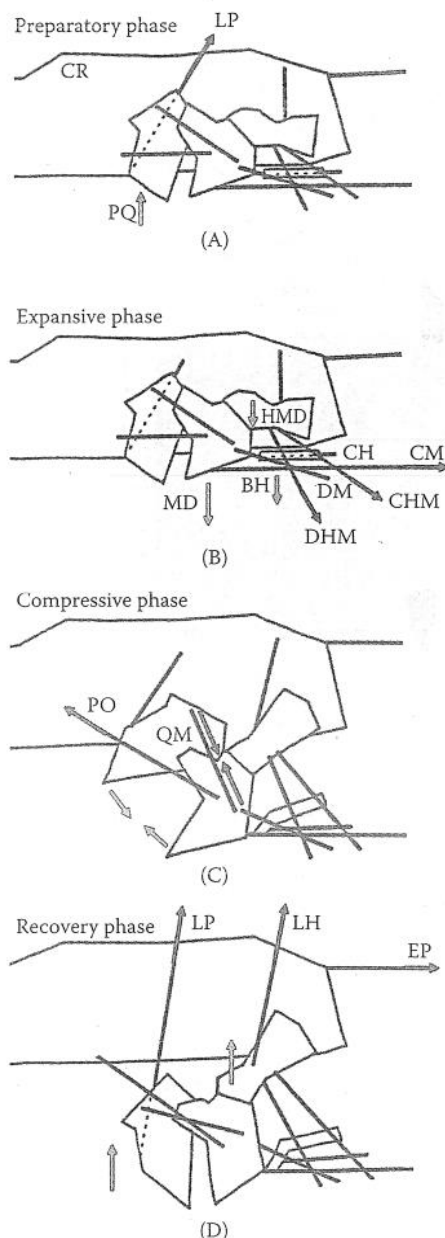
FIGURE 6.17
Schematic diagram of the functional components involved in jaw protrusion and jaw retraction during suction capture in *Rhinobatos lentiginosus*. (A) Upper jaw retraction during the preparatory phase; (B) lower jaw and hyomandibular depression during the expansive phase; (C) upper jaw protrusion and lower jaw elevation during the compressive phase; (D) hyomandibular, upper jaw, and lower jaw retraction during the recovery phase. Solid black lines represent muscles, and dark gray arrows indicate their direction of travel. Open elements represent skeletal elements, and their direction of movement is indicated by light gray arrows. *Abbreviations:* BH, basihyal; CH, coracohyoideus; CHM, coracohyomandibularis; CM, coracomandibularis; CR, cranium; DHM, depressor hyomandibularis; DM, depressor mandibularis; EP, epaxialis; HMD, hyomandibula; LH, levator hyomandibularis; LP, levator palatoquadrati; MD, mandible or lower jaw; PO, medial preorbitalis; PQ, palatoquadrate or upper jaw; QM, anterior quadratomandibularis. (From Wilga, C.D. and Motta, P.J., *J. Exp. Biol.*, 201, 3167–3184, 1998. With permission.)

protrusion that is similar to that proposed for *Orectolobus maculatus* by Wu (1994). During protrusion, which can be up to 100% of head length, the stout hyomandibulae are moved medioventrally, transmitting that motion to the attached mandible. The hyomandibular motion results in a medial compression of the entire jaw complex, shortening the distance between the right and left posterior corners of the jaws and forming a more acute symphyseal angle. As the angle between the mandibles is decreased, the jaws are forced anteroventrally during the expansive phase, in a manner similar to a scissor jack (Figure 6.18). The euhyostylic jaw suspension permits a degree of ventral protrusion that is impossible in the orectolobid sharks. The food item and sand are consequently sucked into the buccal region before maximum protrusion is reached. Suction pressures of ≤31 kPa can be generated in this manner. Food processing, when present, involves repeated, often asymmetrical, protrusion of the jaws, while sand is expelled from the spiracles, gills, and mouth. A pronounced difference between this mechanism and that of sharks is the degree of asymmetrical control during protrusion, which may be due to the highly subdivided and duplicated cranial musculature of batoids, the jaws being suspended only by the hyomandibula, the lack of an ethmopalatine ligament, and a flexible jaw symphysis (Dean and Motta, 2004a,b; Dean et al., 2007b; Gerry et al., 2008). In fact, bilateral implantation of electromyographc leads in four species of elasmobranchs revealed the greatest asymmetry of muscle firing in the batoid *Leucoraja erinacea* compared to three other shark species (Gerry et al., 2008). It should be noted, however, that the morphological restrictions that permit the unique protrusion mechanism of *N. bancroftii*, including the coupled jaws and narrow gape, most likely constrain its dietary breadth (Dean and Motta, 2004a,b).

Cownose rays are pelagic rays that feed on benthic invertebrates such as mollusks and crustaceans (Collins et al., 2007; Nelson, 1994; Orth, 1975; Schwartz, 1989; Smith, 1980). Food is captured by suction in a conservative series of expansive, compressive, and recovery phases similar to that of other elasmobranchs, then crushed between the platelike teeth (Figure 6.19). Prey is excavated by repeated opening and closing of the jaws to fluidize the surrounding sand and prey. The food is then surrounded laterally by the mobile cephalic lobes, which are anterior extensions of the pectoral fins, and sucked into the mouth. The cephalic lobes, which are also covered with electroreceptive ampullae (Mulvany, pers. comm.), may be used to herd elusive prey into the range of the mouth, as well. During capture, the spiracle, mouth, and gill movements are timed such that water enters only the mouth (Sasko et al., 2006). In mobulid rays, the cephalic lobes are paired and presumably used to direct water flow and plankton into the terminal mouth of these filter feeding rays (Sasko et al., 2006).
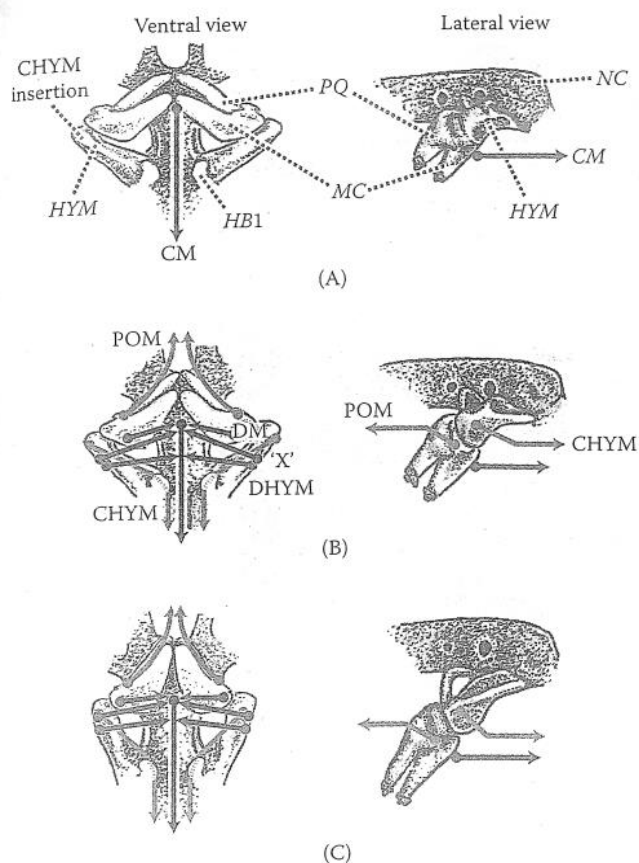
FIGURE 6.18
Proposed muscular basis of jaw protrusion for *Narcine bancroftii* based on muscle morphology and manipulations of fresh specimens. The protrusion mechanism is illustrated in ventral (left column) and left lateral (right column) view, with anterior up and to the left, respectively. Only contracting muscles are labeled (dark arrows), and dashed arrows denote skeletal structures (note that the coracohyomandibularis tendon runs beneath the first hypobranchial). The lower jaw depresses slowly (A), before protrusion onset (B) and peak protrusion (C). Lower jaw depression is effected by the coracomandibularis (CM), followed by medial compression of the jaws and hyomandibulae through coracohyomandibularis (CHYM), depressor hyomandibularis (DHYM), depressor mandibularis (DM), and 'X' ('X') muscle contraction. The halves of the upper jaw may also be adducted and extended by the preorbitalis medialis (POM). *Abbreviations:* HB1, first hypobranchial; HYM, hyomandibula; MC, Meckel's cartilage; NC, neurocranium; PQ, palatoquadrate. (From Dean, M. and Motta, P.J., *J. Morphol.*, 262, 462–483, 2004. With permission.)

6.4 Feeding Biomechanics

6.4.1 Skeletal Materials and Mechanics

Chondrichthyans are unique in that their skeletons consist of a combination of mineralized and unmineralized cartilage. Nearly all other vertebrates (agnathans withstanding) possess unmineralized cartilage as the developmental precursor to soon-to-be bony skeletal elements and at the articular surfaces of load-bearing
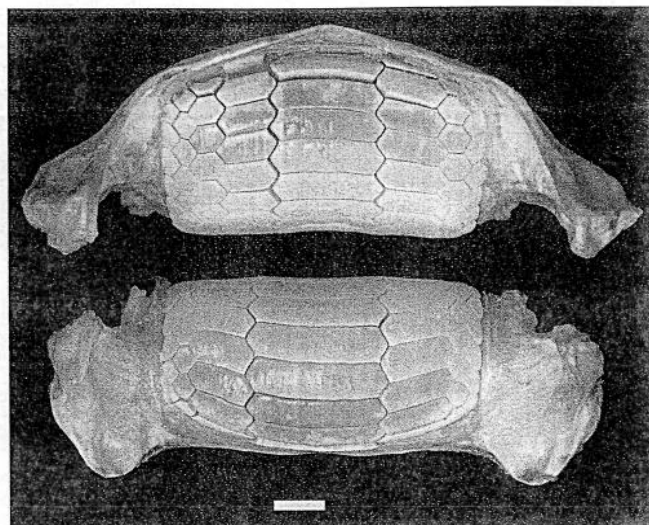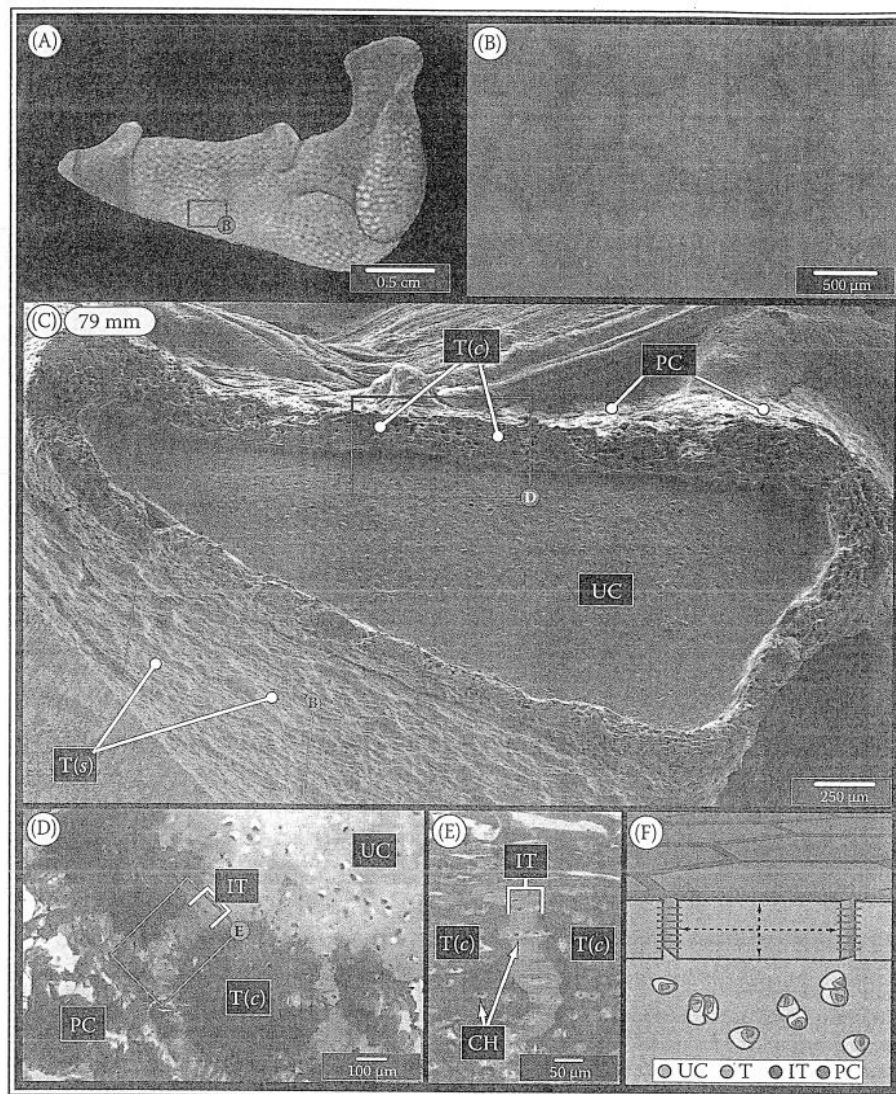

FIGURE 6.19
Posterior view of the upper and lower tooth plates of a cownose ray *Rhinoptera bonasus* (disk width ~60 cm) showing the imbricated tooth plates. The jaws are separated to better show the tooth plates. Scale bar is 1 cm.

joints, as well as mineralized cartilage as an ephemeral tissue that exists solely at the cartilage–bone interface of developing skeletal elements. Not only is chondrichthyan cartilage a composite of mineralized and unmineralized forms, but the latter is also a composite of solid and liquid phases consisting of chondrocytes in a gelatinous extracellular matrix (ECM) permeated with collagen fibers (Dean and Summers, 2006; Liem et al., 2001). Mineralized chondrichthyan cartilage is quite stiff due to the presence of calcium phosphate hydroxyapatite, whereas unmineralized chondrichthyan cartilage is remarkably elastic due to high concentrations of proteoglycans within the ECM. Negatively charged glycosaminoglycan side chains (e.g., chondroitin sulfate and keratin sulfate) on the proteoglycans attract water, which infiltrates the ECM and causes the tissue to swell. This swelling is resisted by the collagen network and mineralized cortex, thereby creating turgor. Water is forced out of the ECM during compression only to rush back into the matrix once the force is removed, due to polar attractions with the glycosaminoglycan side chains. The tissue is brought back to its original state provided that the loading has not resulted in plastic deformation (Carter and Wong, 2003; Liem et al., 2001).

The structural arrangement of the mineralized and unmineralized cartilage in skeletal elements of elasmobranch feeding mechanisms consists of a cortical mesh of mineralized tiles known as tesserae that surround a soft core of unmineralized tissue (Figure 6.20) (Kemp and Westrin, 1979; Orvig, 1951; Summers, 2000). Mineralization in holocephalans also consists of tesserae, but these are arranged in lamellar sheets that pass

FIGURE 6.20

(See color insert.) Anatomy of the tessellated lower jaw skeleton of an elasmobranch; lettered and inset red boxes reference other panels in the figure (e.g., the box in panel A references panel B). Elasmobranch skeletal elements are tiled superficially with abutting mineralized blocks called tesserae (T) (panel A: microCT scan, left lateral view; panel B: cleared and stained tissue), overlain by a fibrous perichondrium (PC) and surmounting a monolithic core of uncalcified cartilage (UC) (panel C: cryoSEM cross-section). Tesserae can be seen in cross-section [T(c)] at the top of the image and in surface view [T(s)], covered by perichondrium, at the bottom. At higher magnifications (panels D and E: hematoxylin and eosin stained cross-sections), the margins of tesserae are less regular, and vital chondrocytes (CH) can be seen in mineralized lacunae in tesserae and extending into the intertesseral fibrous joints (IT). The tessellated skeleton can therefore be thought of simply as unmineralized cartilage wrapped in a composite fibro-mineral bark (panel F: schematic cross-section). (From Dean, M.N. et al., *J. Anat.*, 215, 227–239, 2009. With permission.)

through skeletal elements, the mechanical properties and homology of which are less well understood (Lund and Grogan, 1997; Rosenberg, 1998). Individual tesserae exhibit diverse forms, but all are roughly polygonal; those of the round stingray, *Urobatis halleri*, are hexagonal in shape and rectangular in cross-section (Dean et al., 2009a; Kemp and Westrin, 1979). Tesserae consist of an outer crystalline layer of prismatic calcification, which is connected to the perichondrium via Sharpey's fibers, and an inner layer of globular calcification consisting of fused spherules of hydroxyapatite (Dean and Summers, 2006; Kemp and Westrin, 1979; Summers, 2000); globular calcification may also appear within the ECM (Dean and Summers, 2006).

Tesserae are linked together via collagenous ligaments and contain live chondrocytes in lacunae which are connected via canaliculi that presumably facilitate intercellular communication and nutrient diffusion (Dean et al., 2010; Kemp and Westrin, 1979; Moss, 1977a; Orvig, 1951; Rosenberg, 1998; Summers, 2000).
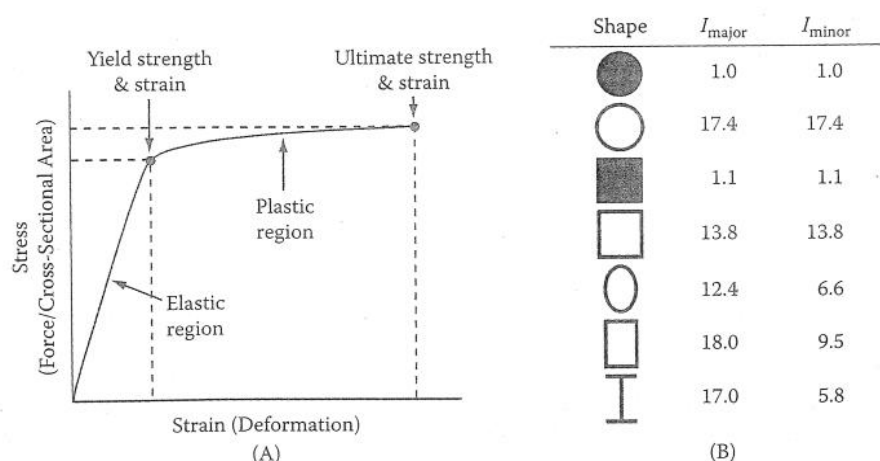
Shape	I_{major}	I_{minor}
	1.0	1.0
	17.4	17.4
	1.1	1.1
	13.8	13.8
	12.4	6.6
	18.0	9.5
	17.0	5.8
	(B)	

FIGURE 6.21

(A) Representative stress–strain curve indicating the elastic and plastic regions of material behavior. The slope of the elastic region is the stiffness (Young's modulus) of the material. The transition point from the elastic to plastic regions represents the yield strength and strain, after which the material has undergone permanent deformation. Ultimate strength and strain occur at the point of material failure. The area under the stress–strain curve represents the quantity of work required to cause material failure (work to fracture). (Adapted from Liem, K.F. et al., *Functional Anatomy of the Vertebrates: An Evolutionary Perspective*, 3rd ed., Brooks Cole, Belmont, CA, 2001.) (B) Second moments of area along the major and minor axes of representative geometric cross-sections. Wall thickness of hollow sections is constant, and the major axis is 1.5× the length of the minor axis in asymmetrical sections. (Adapted from Wainwright, S.A. et al., *Mechanical Design in Organisms*, Princeton University Press, Princeton, NJ, 1976.)

Tesserae develop embryonically as globular calcification surrounds "strings" of chondrocytes aligned parallel to the perichondral surface of the jaw (Dean et al., 2009a; Summers, 2000). The initial deposition of mineral occurs in association with collagen fibrils and appears to be related to alkaline phosphatase activity (Eames et al., 2007). Tesserae thicken by continuing to engulf chondrocytes at the endochondral surface in globular mineral while the calcification at the perichondral surface attains a more organized crystalline structure; tesserae widen by continued accretion of mineral at the surfaces of the intertesseral joints. Through this process, the tesserae of *U. halleri* were observed to increase in size by two to three times over ontogeny (Dean et al., 2009a).

Chondrichthyan mineralization differs from that of bony vertebrates in several key ways. Chondrocytes at the mineralizing front do not hypertrophy or form columns perpendicular to the perichondral surface, and mineral in chondrichthyans occurs in association with both Type I and II collagen, whereas vertebrate bone contains exclusively Type I collagen (Currey, 2008; Dean et al., 2009a; Eames et al., 2007; Kittiphattanabawon et al., 2010; Rama and Chandrakasan, 1984). Unlike vertebrate bone, chondrichthyan cartilage is incapable of remodeling (Ashhurst, 2004; Clement, 1992). The tessellated design of the skeleton therefore appears to be a means of facilitating growth in a system that does not reabsorb calcium. If the mineralized cortex of an elasmobranch jaw was solid it would not be able to accommodate growth of the ECM without remodeling.

Tesselation allows for increases in ECM volume as the individual tesserae grow via mineral deposition on all surfaces (Dean et al., 2009a).

The composite nature of the mineralized and unmineralized portions of skeletal elements in the elasmobranch feeding mechanism yields emergent mechanical properties that would otherwise not be found in a single-phase structure. The mineralized cortex confers stiffness, while the unmineralized core confers damping, two properties that are generally at odds in isolated materials (Dean et al., 2009b,c; Meyers et al., 2008). Both the type (material properties) and distribution (structural properties) of materials within skeletal elements determine their mechanical performance, which is inherently linked to aspects of ecological performance (e.g., jaw performance and prey capture). Material properties are reflected by the stiffness (*E*, Young's modulus) of those materials, whereas structural properties are reflected by their second moment of area (*I*), the contribution of a structure's cross-sectional shape to its resistance to bending. Young's modulus is the slope of the elastic region of a material's stress–strain curve, and the second moment of area is the distribution of material about the neutral axis of a skeletal element in the direction of loading (Figure 6.21):

$$E = \frac{Stress}{Strain} \tag{6.1}$$

$$I = \int y^2 dA \tag{6.2}$$

Material and structural properties are combined in an elegantly simple way to determine a structure's overall resistance to bending, otherwise known as *flexural stiffness*:

$$\text{Flexural stiffness} = E \times I \qquad (6.3)$$

By parsing flexural stiffness into the mutual contributions of material and structural properties, the selective pressures on skeletal material type and shape can be delineated. Although only investigated in a few species, jaw shape demonstrates clear relationships with feeding ecology. Cortical thickening of the jaws via deposition of multiple layers of tesserae has been identified in large or durophagous sharks and rays, all of which tend to have high bite forces associated with the consumption of functionally difficult prey (Dingerkus et al., 1991; Summers, 2000; Summers et al., 1998). Cortical thickening directly impacts the second moment of area, which is greatest in durophagous species such as the spotted eagle ray, *Aetobatus narinari*, and horn shark, *Heterodontus francisci* (Figure 6.22). The second moment of area is highest near the symphysis and lateral margins of the jaws in *A. narinari* ($I_{max} \sim 8000$ mm^4) and beneath the posterior molariform teeth and jaw joint in *H. francisci* ($I_{max} \sim 2000$ mm^4), in which the second moment of area increases by three orders of magnitude over ontogeny. Although the jaws of *A. narinari* are more heavily mineralized, the mineral in the jaws of *H. francisci* is better positioned to resist bending; jaw mineral in *H. francisci* and *A. narinari* resists bending 35× and 20× better than a solid rod of equivalent cross-sectional area, respectively (moment ratio = $I_{specimen}/I_{circle}$) (Summers et al., 2004). The moment ratios of *H. francisci* and *A. narinari* are higher than those of various piscivorous species, such as the goblin shark, *Mitsukurina owstoni*; sandtiger shark, *Carcharias taurus*; crocodile shark, *Pseudocarcharias kamoharai*; salmon shark, *Lamna ditropis*; and shortfin mako shark, *Isurus oxyrinchus* ($I_{specimen}/I_{circle}$, 5 to 18) (Goo et al., 2010). Feeding ecology aside, all of the species investigated thus far exhibit similar changes in the second moment of area along the lengths of the upper and lower jaws, have peaks in the second moment of area beneath the jaw joints and anterior biting surfaces of the jaws, and their
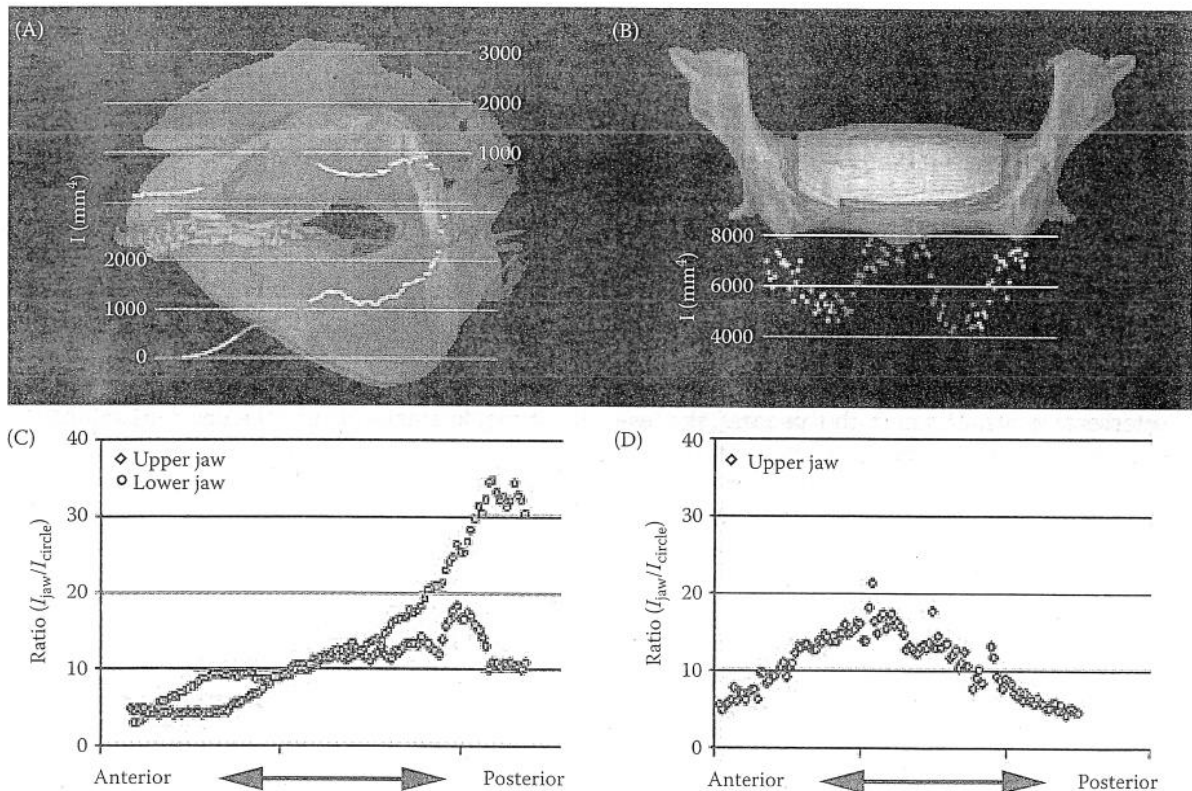
FIGURE 6.22
(See color insert.) (A) Second moment of area of the cross-section of the upper and lower jaws of the horn shark, *Heterodontus francisci*, and (B) upper jaw of the spotted eagle ray, *Aetobatus narinari*. The *x*-axis position of each point on the graph corresponds to the position of the section through jaws in the background. Points corresponding to sections with teeth involved in crushing hard prey are in red. (C) Moment ratio (ratio of the second moment of area of the jaw cross-section to the second moment of area of a circle with the same cross-sectional area) plotted vs. position along the jaw for the upper and lower jaws of *H. francisci*. (D) Moment ratio vs. position along the jaw for the upper jaw of *A. narinari*. (Adapted from Summers, A.P. et al., *J. Morphol.*, 260, 1–12, 2004. With permission.)

high moment ratios are correlated with orthogonal orientation between the major axis of the jaws and occlusal surface of the teeth (Goo et al., 2010; Summers et al., 2004).

Although cortical thickening is the principal means of stiffening the jaws of cartilaginous fish, trabecular reinforcement is also found in myliobatid stingrays and the lesser electric ray, *Narcine bancroftii*. Trabeculae, a means of optimizing weight and strength found throughout animal skeletons, are mineralized struts that pass through the lumen of a skeletal element, connecting and transmitting stress between its cortical layers. These struts are orthogonal to the tooth plates in the jaws of myliobatid stingrays so as to resist jaw flexion during hard prey consumption (Summers, 2000). Trabeculae in *N. bancroftii* are found near the jaw joints and symphyses and in the hyomandibulae near their joints with the cranium. Those oriented transverse to applied loads resist jaw flexion as in the myliobatids, whereas those in the parasymphyseal regions of the jaws form cross-braces parallel to the occlusal surface that resist buckling during ballistic protrusion of the jaws into the sediment in search of prey (Figure 6.23) (Dean et al., 2006). Although these reinforcements certainly play a role in maintaining the functional integrity of the feeding mechanism, their presence prior to birth in the cownose ray, *Rhinoptera bonasus*, and in the planktivorous manta ray, *Manta birostris*, suggests that they are phylogenetic in origin and not functionally induced (Summers, 2000).

As with structural properties, the material properties of chondrichthyan skeletons have seldom been examined. The dentine and enameloid in elasmobranch teeth range in stiffness from 22.49 to 28.44 GPa and 68.88 to 72.61 GPa, respectively (Table 6.1) (Whitenack et al., 2010). Mineralized jaw cartilage from the round stingray, *Urobatis halleri*, has a stiffness of 4.05 GPa, which is at the low end of the range of stiffness for vertebrate bone (Table 6.1) (Currey, 1987; Currey and Butler, 1975; Erickson et al., 2002; Hudson et al., 2004; Kemp et al., 2005; Rath et al., 1999; Rho et al., 2001; Wroe et al., 2008). The stiffness of unmineralized jaw cartilage ranges from 0.029 to 0.056 GPa and is generally greater than that of mammalian articular cartilage but exhibits little correlation with feeding ecology in durophagous and piscivorous species (Table 6.1) (Jagnandan and Huber, 2010; Laasanen et al., 2003; Summers and Long, 2006; Tanne et al., 1991). Selective pressure for mechanical adaptation in unmineralized jaw cartilage may be weak due to the principal role of mineralized cartilage in withstanding stress (Ferrara et al., 2011). Mineral content is the single largest determinant of stiffness in calcified connective tissues; as little as a 16% increase in mineral content can cause a 95% increase in the stiffness (Porter et al., 2006). Regardless, variation in the properties of unmineralized jaw cartilage may be associated with water and collagen content (Porter et al., 2006).

Structural analysis of whole shark jaws (including mineralized and unmineralized portions) has identified correlations among their mechanical performance, feeding ecology, and chondrichthyan evolution. Fahle and Thomason (2008) found that jaw viscoelasticity in the lesser spotted dogfish, *Scyliorhinus canicula*, decreases over ontogeny, which may contribute to an ontogenetic dietary shift toward harder and larger prey in adults. Using finite element analysis (FEA), Ferrara et al. (2011) determined that the mechanical performance of the jaws varies with gape angle such that species consuming large prey must have jaws better able to withstand stress. Finally, Wroe et al. (2008) used FEA to simulate the mechanical performance of the jaws of the white shark, *Carcharodon carcharias*, using realistic cartilaginous jaw models and hypothetical bony jaw models to explore the mechanical consequences of the loss of bone in the chondrichthyan skeleton. As expected, bony jaws exhibited higher stress and lower strain, but bite force was only 4.4% lower for cartilaginous jaws, suggesting that the adoption of a more compliant skeletal system has not compromised the biting performance of cartilaginous fishes (Wroe et al., 2008).

6.4.2 Musculoskeletal Lever Mechanics

Assuming that the jaws are functioning as rigid levers, the mechanical determinants of feeding performance are the forces produced by the cranial muscles and the leverage with which they act (a.k.a. mechanical advantage). Force generation (F_I, force input) is a function of muscular structure and geometry, whereas mechanical advantage (*MA*) determines the proportion of that force that is transmitted either to the fluid medium during jaw abduction or to prey items during jaw adduction (F_O, force output):

$$F_O = F_I \times MA \tag{6.4}$$

Although expansive phase force generation plays a pivotal role in suction feeding performance (see Section 6.3.3.1), the output force of the mandibular lever system during jaw adduction represents none other than bite force. In recent years, bite force has become an increasingly relied upon measure of vertebrate feeding performance because it affects prey capture energetics and dietary diversity within species, as well as the partitioning of dietary and reproductive resources among species. High bite forces improve prey capture efficiency by reducing prey handling time and enabling the consumption of relatively large prey, thereby improving the net energy return per feeding event (Herrel et al., 2001b; van der Meij et al., 2004; Verwaijen et al., 2002). High bite forces are also frequently associated with reduced dietary diversity, niche specialization, and ontogenetic dietary shifts because high-performance
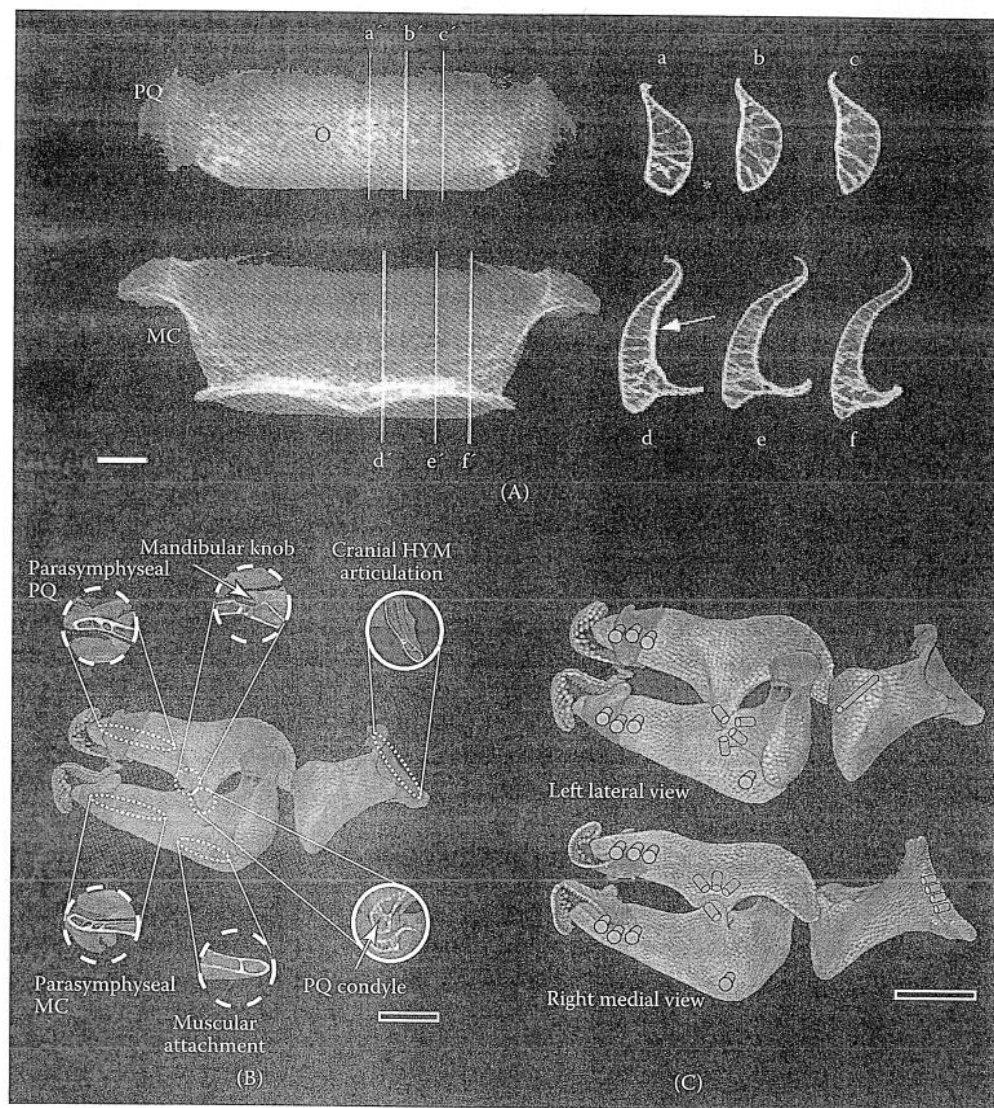
FIGURE 6.23

(A) Radiograph of the palatoquadrate (PQ) and Meckel's cartilage (MC) of an adult cownose ray, *Rhinoptera bonasus*, with the tooth plates removed (scale bar, 1 cm). The lower (MC) and upper (PQ) jaws are shown in anteroposterior and dorsoventral view, respectively, and the crushing area of the tooth plates would have been near the bottom of both images. Parasagittal sections are shown on the right (anterior on left, dorsal on top), with each section taken in approximately the plane indicated by the corresponding section line and trabecular reinforcement evident in all sections. An area of high tooth wear on the upper jaw is indicated by an asterisk, and an area of particularly thick prismatic cartilage on the lower jaw is indicated by an arrow. Hollow trabeculae can be seen end-on in some areas of the whole jaw radiographs, as indicated by the black circle on the upper jaw. (From Summers, A.P., *J. Morphol.*, 243, 113–126, 2000. With permission.) (B) Trabeculation in the jaws and hyomandibula of the lesser electric ray *Narcine bancroftii* (scale bar, 1 cm). Expanded white circles illustrate trabeculation within a given area with text indicating relevant regional landmarks; solid circles present elements in lateral view (in the same orientation as the larger image of the jaws and hyomandibula), while dashed circles provide a dorsal view. *Abbreviations:* HYM, hyomandibula; MC, Meckel's cartilage; PQ, palatoquadrate. (C) The orientation of groups of trabeculae shown schematically in left lateral (top) and right lingual (bottom) views, with trabeculae represented as columns (scale bar, 1 cm). (From Dean, M.N. et al., *J. Morphol.*, 267, 1137–1146, 2006. With permission.)

biting facilitates access to functionally difficult (large or hard) prey resources. This may reduce interspecific competition, because the lower absolute performance capacities of sympatric species preclude them from consuming such prey (Anderson et al., 2008; Christiansen and Wroe, 2007; Clifton and Motta, 1998; Hernandez and Motta, 1997; Herrel et al., 2002, 2004; Huber et al., 2006, 2009; Kolmann and Huber, 2009; Wainwright, 1988; Wyckmans et al., 2007). Although the relationship between bite force and fitness has not been directly quantified, Lappin and Husak (2005) and Husak et al. (2006) have demonstrated that bite force in male lizards is correlated with territory size and access to female conspecifics such that potential reproductive output

TABLE 6.1

Material Properties of Connective Tissues in Elasmobranchs and Other Vertebrates

Major Group	Species	Tissue	Young's Modulus (GPa)[a]	Ultimate Strength (MPa)[a]	Hardness (GPa)[a]	Source
Petromyzontiformes	*Petromyzon marinus*	Cartilage (annular)	0.001	—	—	Courtland et al. (2003)
Elasmobranchimorphii	*Sphyrna tiburo*	Dentine (orthodentine)	22.490	—	0.970	Whitenack et al. (2010)
Elasmobranchimorphii	*Carcharias taurus*	Dentine (osteodentine)	28.440	—	1.210	Whitenack et al. (2010)
Elasmobranchimorphii	*Carcharodon carcharias*	Dentine (osteodentine)	—	—	0.250	Chen et al. (2008)
Elasmobranchimorphii	*Carcharias taurus*	Enameloid	72.610	—	3.200	Whitenack et al. (2010)
Elasmobranchimorphii	*Carcharodon carcharias*	Enameloid	—	—	1.500	Chen et al. (2008)
Elasmobranchimorphii	*Sphyrna tiburo*	Enameloid	68.880	—	3.530	Whitenack et al. (2010)
Elasmobranchimorphii	*Urobatis halleri*	Cartilage (jaw, mineralized)	4.050	—	—	Wroe et al. (2008)
Elasmobranchimorphii	*Carcharhinus limbatus*	Cartilage (jaw, unmineralized)	0.051	—	—	Huber (unpublished data)
Elasmobranchimorphii	*Heterodontus francisci*	Cartilage (jaw, unmineralized)	0.056	—	—	Jagnandan and Huber (2010)
Elasmobranchimorphii	*Negaprion brevirostris*	Cartilage (jaw, unmineralized)	0.043	—	—	Jagnandan and Huber (2010)
Elasmobranchimorphii	*Rhinoptera bonasus*	Cartilage (jaw, unmineralized)	0.029	41.000	—	Summers and Long (2006)
Elasmobranchimorphii	*Carcharhinus falciformis*	Cartilage (vertebrae)	0.560	24.300	—	Porter et al. (2006)
Elasmobranchimorphii	*Carcharhinus plumbeus*	Cartilage (vertebrae)	0.400	23.700	—	Porter et al. (2006)
Elasmobranchimorphii	*Centrophorus granulosus*	Cartilage (vertebrae)	0.430	20.800	—	Porter et al. (2006)
Elasmobranchimorphii	*Isurus oxyrinchus*	Cartilage (vertebrae)	0.330	11.900	—	Porter et al. (2006)
Elasmobranchimorphii	*Sphyrna zygaena*	Cartilage (vertebrae)	0.520	23.800	—	Porter et al. (2006)
Elasmobranchimorphii	*Torpedo californica*	Cartilage (vertebrae)	0.025	4.600	—	Porter et al. (2006)
Osteichthyes	*Clupea harengus*	Bone (rib)	3.5–19.0	155.000	—	Rho et al. (2001)
Osteichthyes	*Lepidosiren paradoxa*	Dentine	—	—	0.430	Currey and Abeysekera (2003)
Osteichthyes	*Lepidosiren paradoxa*	Petrodentine	—	—	2.490	Currey and Abeysekera (2003)
Amphibia	*Cryptobranchus alleganiensis*	Bone (femur)	22.300	—	—	Erickson et al. (2002)
Amphibia	*Cyclorana alboguttata*	Bone (tibiofibula)	8.800	—	—	Hudson et al. (2004)
Reptilia	*Crocodylus sp.*	Bone (frontal)	5.600	—	—	Currey (1987)
Reptilia	*Varanus xanthematicus*	Bone (femur)	22.800	—	—	Erickson et al. (2002)
Aves	*Gallus gallus*	Bone (tibia)	0.600	—	—	Rath et al. (1999)
Aves	*Phoenicopterus ruber*	Bone (tarsometatarsus)	27.800	—	—	Currey (1987)
Mammalia	*Homo sapiens*	Bone (femur)	123.406	—	—	Currey and Butler (1975)
Mammalia	*Canis lupus familiaris* (pit bull)	Bone (humerus)	3.200	—	—	Kemp et al. (2005)
Mammalia	*Bos taurus*	Cartilage (articular, tibia)	0.0001	—	—	Laasanen et al. (2003)
Mammalia	*Canis lupus familiaris*	Cartilage (articular, mandible)	0.092	—	—	Tanne et al. (1991)
Mammalia	*Loxodonta africana*	Dentine	7.700	—	0.430	Currey (1998); Currey and Abeysekera (2003)
Mammalia	*Homo sapiens*	Dentine	19.890	—	0.920	Waters (1980); Mahoney et al. (2000)
Mammalia	*Bos taurus*	Enamel	73.000	—	3.000	Currey (1998); Currey and Abeysekera (2003)
Mammalia	*Homo sapiens*	Enamel	87.500	—	3.900	Habelitz et al. (2001)

[a] Non-elasmobranch tissues with more than one value per major group represent minimum and maximum known values for that major group

(based on female fecundity and probability of insemination) is greater for individuals with higher bite forces. An inquiry of this type has not been conducted in cartilaginous fishes.

6.4.2.1 Muscle Force and Leverage

The force produced by a muscle (P_O, maximum tetanic tension; F_I of Equation 6.4) is determined by the specific tension (T_S) and geometric arrangement of its fibers, the latter of which is approximated by its cross-sectional area (CSA):

$$P_O = T_S \times CSA \qquad (6.5)$$

Specific tension is the maximum stress (force per unit area) that a muscle fiber can generate. Although likely an oversimplification (Hernandez and Morgan, 2009), for the purposes of biomechanical modeling cartilaginous fishes are considered to have either "white" or "red" jaw muscles. White muscles contain glycolytic fibers that produce greater power (18.3 W/kg) and stress (28.9 N/cm²) than their red counterparts (6.6 W/kg and 14.2 N/cm²), although the latter are oxidative and dramatically better at resisting fatigue (Curtin et al., 2010; Lou et al., 2002). Current estimates of the specific tension of chondrichthyan muscle are based on axial myomeres and may underestimate the physiological capacity of jaw adductors. "Superfast" isoforms of masticatory myosin capable of producing greater stress than locomotory muscles have been identified in the jaw adductors of numerous vertebrates, including the blacktip shark, *Carcharhinus limbatus* (Hoh, 2002; Qin et al., 2002).

Masticatory myosin aside, there is preponderance of white muscle tissue in the jaw adductors of cartilaginous fishes with limited exception. The deepest subdivisions of the jaw adductors of carcharhinid and orectolobiform sharks and holocephalan ratfishes have red fibers, which are believed to be associated with rhythmic respiratory movements of the jaw apparatus and stabilization of the jaw joint, respectively (Huber et al., 2008; Motta, pers. obs.). The only group possessing jaw adductors dominated by red muscle tissue are the myliobatid stingrays such as the cownose ray, *Rhinoptera bonasus*, in which the fatigue resistance of this oxidative tissue likely aids in the rhythmic crushing of epibenthic fauna (Gonzalez-Isais, 2003; Peterson et al., 2001; Smith and Merriner, 1985). However, all other parameters held constant, a chondrichthyan with "white" jaw adductors can generate static bite forces approximately two times greater than one with "red" jaw adductors, due to differences in specific tension.

Muscles in which the fibers are arranged parallel to the mechanical line of action are the norm among cartilaginous fish. The cross-sectional areas of these parallel-fibered muscles can be estimated rather simply from digital images of muscle sections taken perpendicular to the principal fiber direction through the center of mass. The prevalence of parallel fibered muscles in cartilaginous fish is believed to be due to the low pullout strength of the tessellated cartilaginous skeleton, which necessitates the presence of aponeurotic surface insertions for cranial muscles. These broad insertions decrease the applied stress by spreading muscular force over a considerable skeletal area (Liem and Summers, 1999; Summers et al., 2003). Tendinous point insertions, such as those of pinnate muscles in which fibers insert onto a central tendon at acute angles, are likely to cause considerable point stresses and local instability along the tessellated skeleton. Not surprisingly, pinnate muscles are fairly rare among cartilaginous fishes; nonetheless, the few known examples generally occur in concert with skeletal structures that ameliorate the stresses created by tendinous point insertions.

Estimating the force produced by a pinnate muscle requires a more elaborate calculation of cross-sectional area due to the angular insertion of muscle fibers onto a central tendon. In such cases, it is necessary to determine "physiological" cross-sectional area, which estimates the portion of the muscle making a mechanically relevant input to a musculoskeletal system by accounting for the fact that some of the force generated by muscle fibers not parallel to the central line of action of the muscle will be lost during contraction. Physiological cross-sectional area is calculated as:

$$PCSA = \frac{\text{Muscle mass}}{\text{Muscle density}} \times \cos\Theta \times \frac{1}{\text{Fiber length}} \qquad (6.6)$$

in which Θ is the average angle of pinnation from the central tendon of the muscle and the density of fish muscle is 1.05 g/cm³ (Powell et al., 1984; Wainwright, 1988). Although this loss of force may sound problematic, pinnate muscles actually generate greater forces than comparably sized parallel muscles because pinnate architecture allows greater packing of muscle fibers per unit volume. In fact, pinnate fiber architecture is typical of the primary jaw adductors of most bony fishes (Gans and Gaunt, 1991; Liem et al., 2001; Winterbottom, 1974). Parallel-fibered muscles are not without their merit, however. The fibers of parallel muscles typically have more sarcomeres arranged in series, facilitating larger, more rapid contractions, which is advantageous for consumers of elusive prey (Liem et al., 2001).

Given the force-generating advantages of pinnate muscles, it is no surprise that some cartilaginous fishes have found ways to circumvent the problem of pinnate muscle-point stress on a cartilaginous skeleton. Pinnate muscle architecture has been found in the feeding mechanisms

of carcharhinid and orectolobiform sharks, myliobatid stingrays, and holocephalan ratfishes. Subdivisions of the dorsal quadratomandibularis muscle in the lemon shark, *Negaprion brevirostris*, and blacktip shark, *Carcharhinus limbatus*, gradually shift to pinnate fiber architecture during early ontogeny; however, the central tendons of these subdivisions insert onto the mid-lateral raphe of the quadratomandibularis, avoiding interaction with the tessellated skeleton (Huber et al., 2006; Motta and Wilga, 1995). The mid-lateral raphe is a connective tissue sheath onto which fibers from the dorsal and ventral divisions of the quadratomandibularis merge.

There are numerous tendons throughout the feeding musculature of the nurse shark, *Ginglymostoma cirratum*, and cownose ray, *Rhinoptera bonasus*, both of which possess heavily mineralized jaws that presumably preclude the problems associated with tendinous point insertions (Motta and Wilga, 1999; Summers, 2000). The adductor complex of *R. bonasus* is particularly unique in that the major subdivision (adductor mandibulae major) is a multipinnate muscle that originates from its antimere beneath the lower jaw and extends parallel to the occlusal surface until wrapping around the corner of the lower jaw and inserting onto the upper jaw via a stout tendon. This tendon-wrapping redirects the adductor force perpendicular to the occlusal plane, thereby yielding bite force from a muscle not inherently positioned to do so (Figure 6.24). Fibrocartilaginous pads found where the muscle–tendon complex wraps around the corners of the jaw are believed to be mechanical responses to compressive and shear loading, analogous to the "wrap around" tendons of mammals such as the bovine deep digital flexor tendon (Summers, 2000; Summers et al., 2003). The presence of red muscle fibers and pinnate architecture in the jaw adductors of *R. bonasus* appears to be a way of optimizing fatigue resistance and force production in its feeding mechanism. The jaws of holocephalan ratfishes are barely (if at all) mineralized, necessitating an altogether different solution to the problem of pinnate muscle-point stress on a cartilaginous skeleton. The adductor mandibulae anterior of these fish is a bipinnate muscle that inserts onto the lower jaw via a tendinous sling that twists as it wraps beneath the mandible (Figure 6.25). Fiber pinnation angle increases over ontogeny, serving to maintain isometric force production despite hypoallometric growth of cranial volume, while the twisted tendon topology equalizes strain throughout the muscle such that all of its fibers operate at equal positions on their length–tension curves regardless of the size of the gape (Dean et al., 2007a; Didier, 1995; Huber et al., 2008).

As one might expect, the forces produced by the cranial muscles of sharks exhibit significant correlations with feeding mode and ecology. Suction feeders tend to have hypertrophied abductors of the oropharyngeal
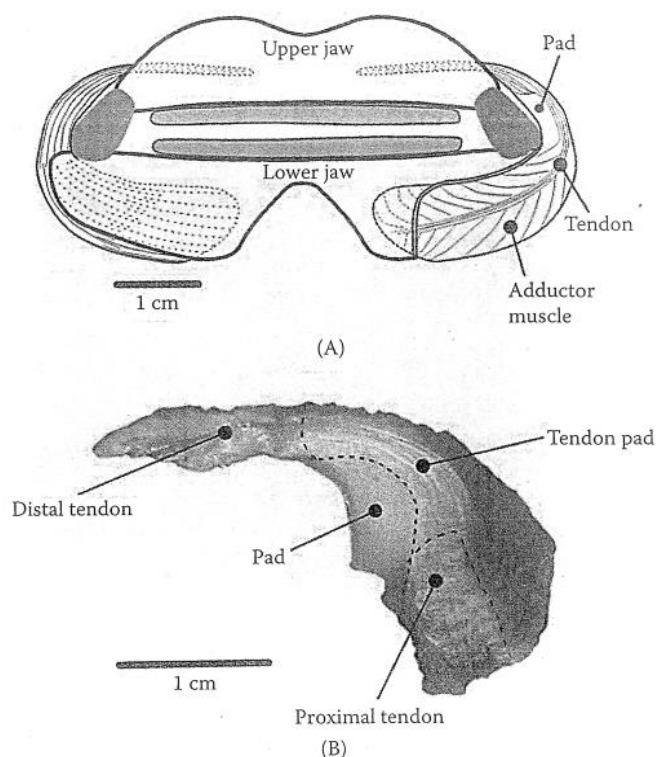

FIGURE 6.24

(A) Ventral view of the jaws of the cownose ray, *Rhinoptera bonasus*, dissected to show the position of the adductor mandibularis medialis muscle and the associated tendon. The right side of the ventral margin of the lower jaw (Meckel's cartilage) has been cut away and the muscle sectioned along its long axis to reveal the central tendon. The upper and lower jaws are connected by strong, short ligaments shown in dark gray. (B) Photograph of a section of the tendon showing the fibrocartilaginous pad and the linear fibers of the tendon lateral to it. The orientation of the tendon is approximately the same as in the right side of panel A. (From Summers, A.P. et al., *Cell Tissue Res.*, 312, 221–227, 2003. With permission.)

cavity, whereas those taxa relying on some variant of a biting mechanism tend to have hypertrophied jaw adductors. Heterodontiform and orectolobiform sharks exhibit remarkable suction and biting performance, having hypertrophied virtually everything in their heads (Edmonds et al., 2001; Huber et al., 2005; Motta and Wilga, 1999; Motta et al., 2008; Nobiling, 1977; Ramsay and Wilga, 2007; Wilga and Sanford, 2008). Interestingly, Habegger et al. (in review) found jaw adductor size to be a significant predictor of bite force in a phylogenetically informed analysis of chondrichthyan feeding biomechanics, suggesting that species having higher than expected bite forces for their body size have achieved this through convergent evolution of hypertrophied jaw adductors. Nonetheless, size is not the only thing that matters; muscle position can play a significant role in determining function (Maas et al., 2004). Ancestrally, the preorbitalis muscle of sharks originated posterior to the nasal capsule and inserted onto the mid-lateral
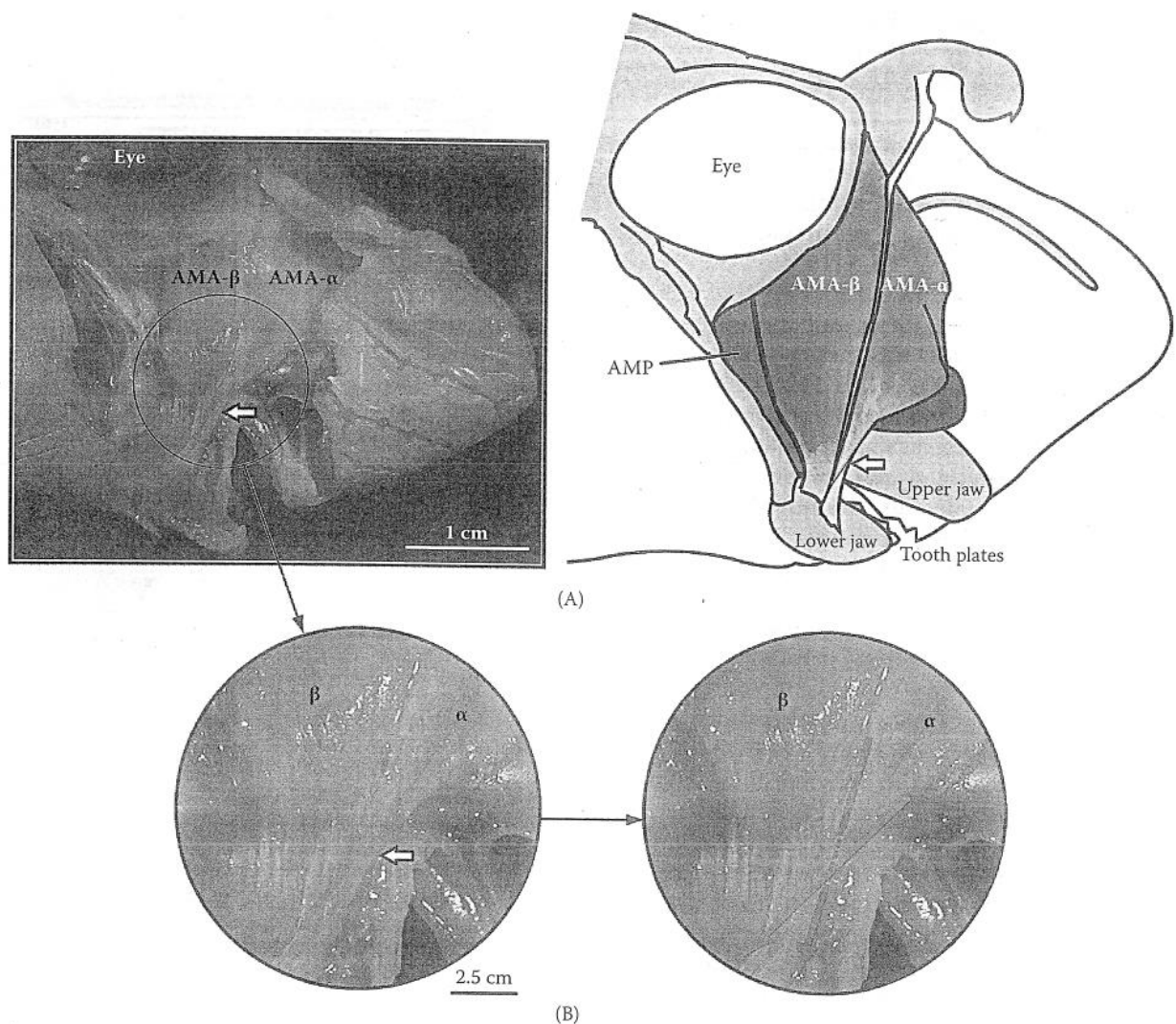
FIGURE 6.25

(See color insert.) Right lateral view of the cranial musculature of the spotted ratfish, *Hydrolagus colliei*. (A) The schematic on the right illustrates the musculature labeled on the left. (B) The tendon (circled in panel A) has been magnified to show the twisted portion. Although all three adductors insert on the lower jaw, only the anterior adductor (AMA-α) exhibits a pronounced twist in its tendon (its approximate middle indicated by a white arrow in A and B) where the anterior face (red arrow) inserts more posteriorly than the posterior face (blue arrow). *Abbreviations:* AMA-α, anterior subdivision of the adductor mandibulae anterior; AMA-β, posterior subdivision of the adductor mandibulae anterior; AMP, adductor mandibulae posterior. (From Dean, M.N. et al., *J. Exp. Biol.* 210, 3395–3406, 2007. With permission.)

raphe of the quadratomandibularis muscle. Horizontal orientation enabled the preorbitalis to actuate upper jaw protrusion, which facilitates rapid jaw closure and gouging of prey and is further augmented in carcharhinid sharks by the derived motor pattern and horizontal orientation of the levator palatoquadrati (Frazzetta, 1994; Motta et al., 1997; Wilga, 2005; Wilga et al., 2001). However, heterodontiform and orectolobiform sharks possess a derived vertical preorbitalis which inserts onto the lower jaw anterior to the quadratomandibularis, giving this muscle higher leverage over jaw adduction. Consequently, species such as the horn shark, *Heterodontus francisci*, and whitespotted bamboo shark,

Chiloscyllium plagiosum, have among the highest leverage jaws of all cartilaginous fishes (Table 6.2) (Habegger et al., in review; Huber, 2006; Huber et al., 2005, 2008; Wilga, 2005; Wilga et al., 2001).

Positioning muscles perpendicular to their associated skeletal element is a key way to optimize force transmission in lever systems, as illustrated by the preorbitalis muscles of heterodontiform and orectolobiform sharks. Recent work by Ferrara et al. (2011) has demonstrated a novel role of the mid-lateral raphe in maintaining the orthogonal arrangement of the musculoskeletal elements in shark feeding mechanisms as well. Through computational modeling of jaw

TABLE 6.2

Morphometrics, Biomechanical Parameters of the Feeding Mechanism, and Dietary Categorizations of Various Cartilaginous Fishes

Scientific Name	TL (cm)	Mass (g)	PBL (cm)	HW (cm)	HH (cm)	JL (cm)	AM CSA (cm²)	Ant MA	Post MA	Ant BF (N)	Post BF (N)	% Cephalopod	% Decapod	% Fish	% Mollusk	Trophic Level
Carcharhinus acronotus[a]	103	—	—	—	—	7.3	7.2	0.33	1.18	67	270.1	0	1.2	98.2	0.6	4.2
Carcharhinus leucas[b]	285	192,976	47.4	41.1	40.8	29.0	112.0	0.37	1.10	2128	5914	0.5	2.6	52.3	0.2	4.3
Carcharhinus limbatus[c]	152	9833	34.0	26.0	17.0	15.6	30.0	0.42	1.33	423	1083	4.1	2.1	88.9	0.1	4.2
Carcharodon carcharias[d]	250	240,000	42.2	45.0	17.9	24.1	78.4	0.40	1.36	1602	3131	3.6	1.8	35.5	0.4	4.5
Chiloscyllium plagiosum[e]	71	1219	10.2	7.5	4.9	3.9	4.0	0.44	0.83	93	168	2.3	33.5	30.3	7.8	3.7
Chimaera monstrosa[f]	41	310	5.0	3.8	5.2	2.2	1.3	0.69	1.13	34	61	0.0	34.4	0.0	17.2	3.2
Etmopterus spinax[g]	38	191	6.3	3.9	2.8	2.7	0.7	0.57	0.95	21	28	19.7	22.7	33.3	0.0	3.8
Eusphyra blochii[a]	132	—	—	—	—	7.8	7.1	0.26	0.93	52.1	171.8	4	12.8	82.9	0	4.1
Galeus melastomus[g]	71	742	9.9	6.1	3.5	1.8	0.7	0.33	0.84	12	30	3.8	32.3	32.9	0.0	3.7
Heptranchias perlo[e]	85	1614	11.9	7.0	8.0	9.0	13.2	0.34	0.95	245	845	40.0	13.3	40.0	0.0	4.2
Heterodontus francisci[h]	63	1616	8.7	9.5	7.5	7.5	5.4	0.55	1.21	117	318	0.1	27.0	0.0	71.3	3.2
Hydrolagus colliei[i]	46	515	5.4	4.0	6.7	0.9	1.9	0.68	1.80	89	175	20.0	17.2	0.1	34.4	3.2
Negaprion brevirostris[e]	61	1219	10.3	7.0	6.0	5.6	4.0	0.36	0.98	79	220	0.0	4.3	92.9	0.0	4.2
Rhizoprionodon terraenovae[a]	88	—	—	—	—	6.7	4.6	0.3	1.18	38.6	157.7	1.8	31.6	66.4	0.1	4
Sphyrna lewini[a]	257	—	—	—	—	14.6	23.4	0.24	0.76	207.4	623.1	15.5	22	61.9	0.1	4.1
Sphyrna mokarran[j]	286	—	—	—	—	20.4	68.3	0.26	0.84	642.2	1839.4	3.3	11.2	43.5	0.0	4.3
Sphyrna tiburo[k]	88	2920	14	8.6	5.2	5.8	3.5	0.22	0.84	18.2	71.1	2.2	71.5	1.6	0.0	3.2
Sphyrna tudes[a]	93	—	—	—	—	6.0	5.1	0.24	0.88	38.4	139	0	83.3	16.7	0	3.6
Sphyrna zygaena[a]	263	—	—	—	—	16.3	32.1	0.12	1.01	288.5	1210	68.9	0.4	29.8	0	4.2
Squalus acanthias[l]	55	673	9.9	3.2	7.4	3.6	1.6	0.20	0.50	12	30	5.2	3.5	41.6	0.4	3.9

Note: Individuals represent the highest mass-specific bite force among the adults sampled for each species, other than the lemon shark, for which no adult data are available.

Abbreviations: AM CSA, adductor mandibulae cross-sectional area; Ant BF, anterior bite force; Ant MA, anterior mechanical advantage; HH, head height; HW, head width; JL, jaw length; PBL, prebranchial length; Post BF, posterior bite force; Post MA, posterior mechanical advantage; TL, total length.

[a] Cortés (1999); Mara (2010).
[b] Habegger et al. (in review); Cortés (1999).
[c] Cortés (1999); Huber et al. (2006).
[d] Cortés (1999); Wroe et al. (2008).
[e] Cortés (1999); Huber (2006).
[f] Claes, Huber, and Mallefet (unpublished data); MacPherson (1980); Mauchline and Gordon (1983).
[g] Claes, Huber, and Mallefet (unpublished data); Cortés (1999).
[h] Cortés (1999); Kolmann and Huber (2009).
[i] Mauchline and Gordon (1983); Huber et al. (2008); Dunn et al. (2010).
[j] Cortés (1999); Huber et al. (2009); Mara (2010).
[k] Mara (2010); Mara et al. (2010).
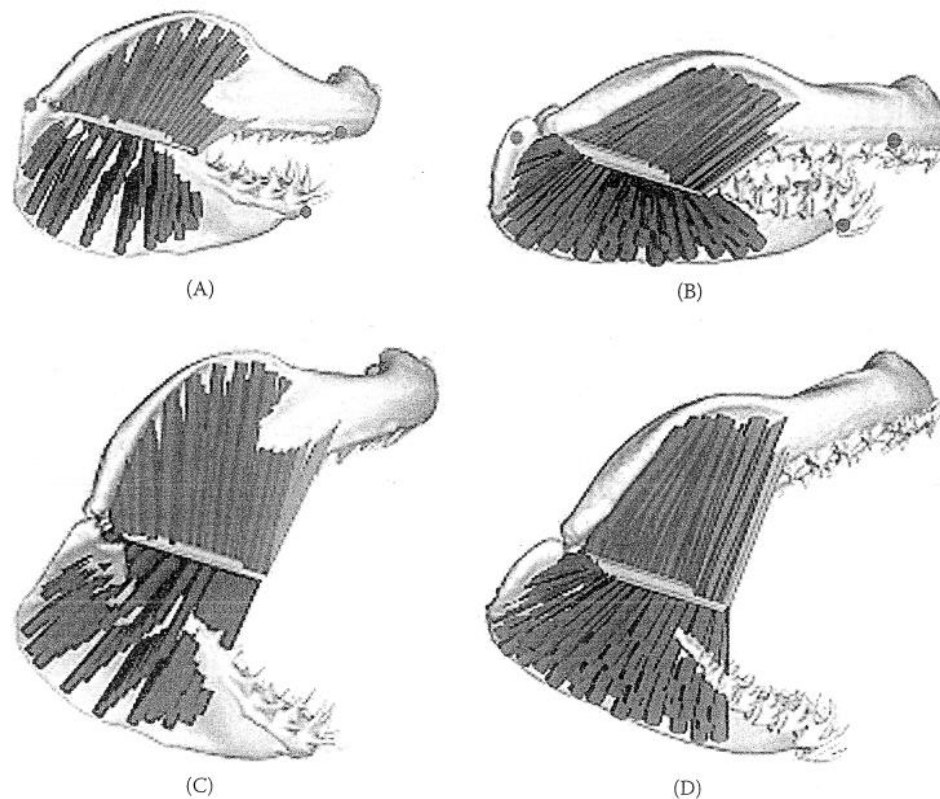[l] Cortés (1999); Huber and Motta (2004).

FIGURE 6.26
(See color insert.) Arrangement of muscle fibers in finite element models (FEMs) of the jaws of (A, C) white sharks, *Carcharodon carcharias*, and (B, D) sandtiger sharks, *Carcharias taurus*, at 15° (A, B) and 55° (C, D) gape angles. Each jaw adductor muscle group inserts on the mid-lateral raphe (yellow) and is represented by a series of trusses that are used to approximate muscle forces and insertion angles of muscle fibers. In both species, the angle of muscle trusses becomes more orthogonal at 55° due to their insertion on the MLR. Truss colors correspond to the following muscle groups: blue, dorsal quadratomandibularis (QMD); orange, medial division of dorsal quadratomandibularis (sandtiger only); green, preorbitalis; red, ventral quadratomandibularis. (From Ferrara, T.L. et al., *J. Biomech.*, 44(3), 430–435, 2011. With permission.)

mechanics in the white shark, *Carcharodon carcharias*, and sandtiger shark, *Carcharias taurus*, Ferrara et al. (2011) found that bite force increases as gape increases because the angle between the adductor muscle fibers and the lower jaw becomes increasingly orthogonal due to their insertion on the mid-lateral raphe (Figure 6.26). This is in stark contrast to models of mammalian jaw mechanics, in which bite force decreases significantly at wider gapes due to increasingly acute adductor insertion angles (Bourke et al., 2008; Dumont and Herrel, 2003). The muscle arrangement characteristic of shark jaw adductors therefore creates the potential to maintain jaw leverage and generate high bite forces across a much wider range of gape angles than is observed in mammalian predators.

Jaw leverage is most commonly investigated through analyses of mechanical advantage (MA), the ratio of a jaw's in-lever distance (L_I) to its out-lever distance (L_O):

$$MA = \frac{L_I}{L_O} \qquad (6.7)$$

The in-lever is the distance from the jaw joint to the point of insertion of a particular muscle, whereas the out-lever is the distance from the jaw joint to a relevant bite point such as the anteriormost tooth of the functional row (Figure 6.27). The ratio of these distances determines the proportion of the force applied *to* the lever system (i.e., muscle force) that will be transmitted *by* the lever system (i.e., bite force). Though conceptually simple, mechanical advantage is difficult to determine in cartilaginous fishes because the aponeurotic attachments of most jaw adductors do not have a clear insertion points. Muscle insertions must be approximated from the intersection of the muscle's mechanical line of action with the jaw, which can be determined by following the principal fiber direction through the muscle's center of mass. The presence of multiple adductor divisions then requires calculation of a resultant in-lever based on a weighted average of the individual in-levers and their respective forces. Mechanical advantage can subsequently be calculated as the ratio of the weighted in-lever to a relevant out-lever (Huber et al., 2005).
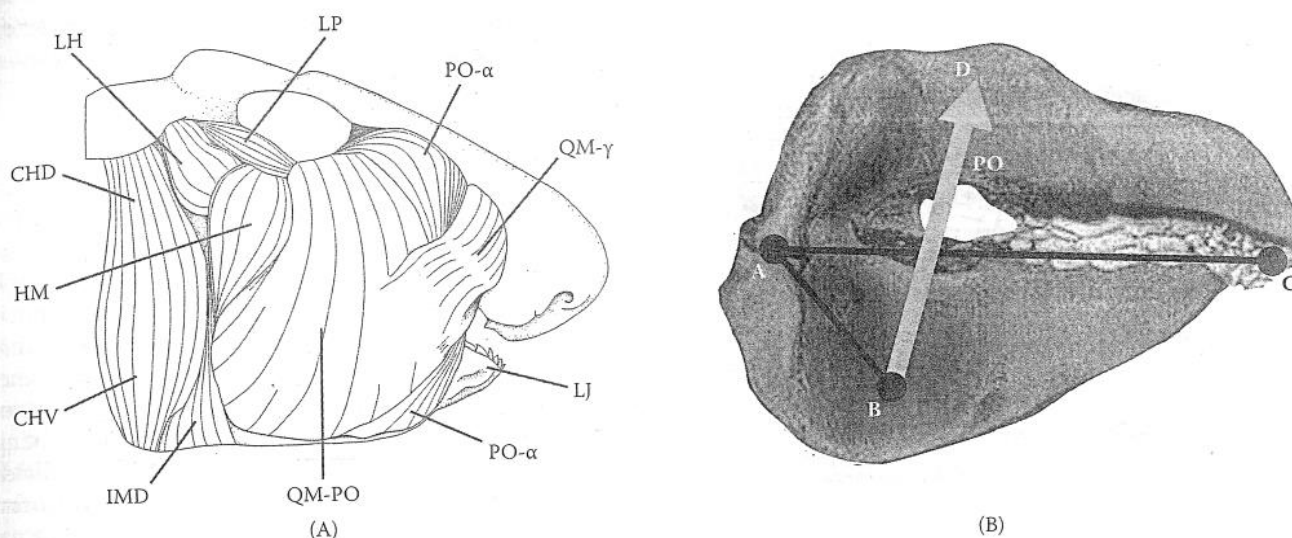
FIGURE 6.27

(A) Right lateral view of the cranial musculature of the horn shark, *Heterodontus francisci. Abbreviations:* CHD, dorsal hyoid constrictor; CHV, ventral hyoid constrictor; HM, hyomandibulo–mandibularis; IMD, intermandibularis; LH, levator hyomandibularis; LJ, lower jaw; LP, levator palatoquadrati; QM–PO, quadratomandibularis–preorbitalis complex; PO-α, preorbitalis-α; QM-γ, quadratomandibularis-γ; (B) Right lateral view of the jaws of *H. francisci* indicating measurements used in calculating mechanical advantage: A–B, resolved in-lever for jaw adduction; A–C, out-lever; B–D, adductive muscle force vector; PO, maximum tetanic tension. (From Kolmann, M.A. and Huber, D.R., *Zoology*, 112, 351–361, 2009. With permission.)

Methodological complications aside, mechanical advantage exhibits a strong ecomorphological signal among cartilaginous fishes. Those species that consume a significant amount of functionally difficult (large or hard) prey typically have mechanical advantage ratios ≥ 0.40, while those specializing on soft-bodied prey typically have mechanical advantages ratios ≤ 0.40 (Table 6.2). Four of the top five mechanical advantage ratios among cartilaginous fish are durophagous taxa, with the holocephalans *Chimaera monstrosa* and *Hydrolagus colliei* ranking highest (0.69 and 0.68, respectively). Despite the lack of mechanical advantage data for batoids, Summers (2000) proposed that asymmetrical jaw adductor contraction and fused jaw symphyses in the durophagous cownose ray, *Rhinoptera bonasus*, create a "nutcracker" mechanism capable of amplifying the force produced by the adductor musculature (mechanical advantage > 1.0) (Figure 6.28). Blue crabs, *Callinectes sapidus*, constitute 72% of the diet of the bonnethead shark, *Sphyrna tiburo*, yet it has a rather low mechanical advantage (0.22), suggesting that chemical digestion may play a greater role than mechanical processing in its durophagous ecology (Cortes, 1999; Mara, 2010; Mara et al., 2010). In fact, hammerhead sharks in general have low-leverage feeding mechanisms (mechanical advantage, 0.12 to 0.26) (Table 6.2), which is consistent with other species in which diet is dominated by elusive prey such as teleosts, cephalopods, and other elasmobranchs (Mara, 2010). Although force transmission is of obvious importance for prey capture, low-leverage jaws can

be advantageous to consumers of elusive prey because force and velocity are inversely proportional in mechanical lever systems (De Schepper et al., 2008; Wainwright et al., 2000; Westneat, 1994). Low-leverage jaws reach higher angular velocities, which can be augmented by increasing adductor muscle mass at any mechanical advantage, thereby aiding in the capture of elusive prey (Van Wassenbergh et al., 2005; Wainwright and Shaw, 1999). Nonetheless, very-high-leverage jaws appear to be a luxury that only predators of sessile benthic epifauna can afford.

Ecomorphological variation among jaw leverage, feeding modality, and prey type has been well documented in teleost fishes as well (Hernandez and Motta, 1997; Turingan et al., 1995; Wainwright et al., 2000, 2004; Westneat, 2004). Although durophagous specialists such as the scarid parrotfishes have mechanical advantage ratios approaching 1.0, those teleosts with mechanical advantage ratios greater than 0.34 are considered to have "high-leverage" jaws (Wainwright et al., 2004; Westneat, 2004). Yet, the average mechanical advantage ratio of the cartilaginous fishes that have been investigated is 0.42, begging the question of whether or not cartilaginous fishes inherently have higher leverage feeding mechanisms. The adductor mandibulae complex develops from cranial somitomeres in association with the first visceral arch in cartilaginous and bony fishes (Liem et al., 2001). Although the palatoquadrate and Meckel's cartilages of the first visceral arch develop into the upper and lower jaws
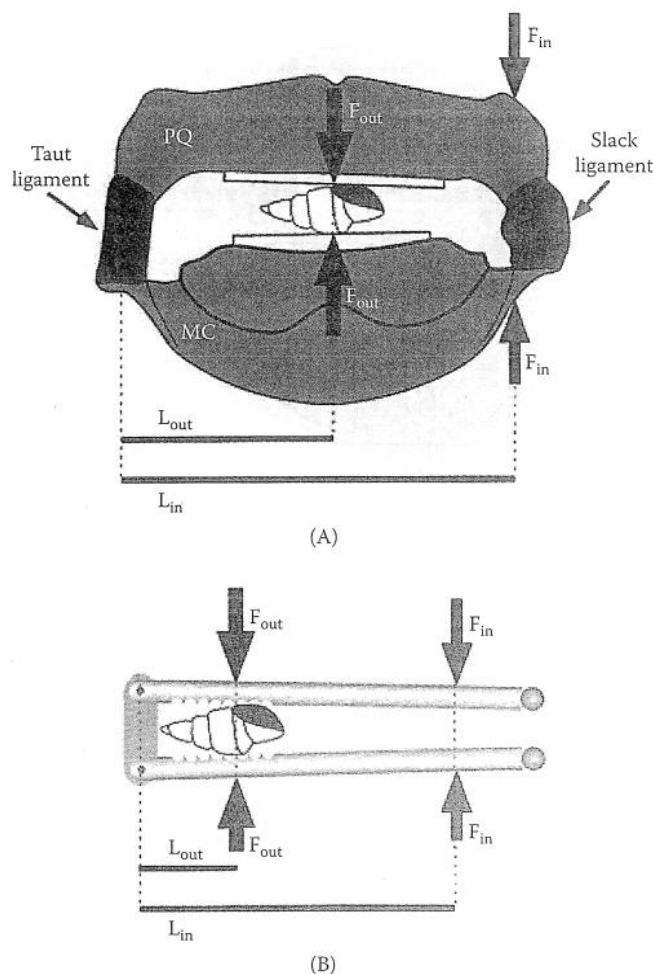
FIGURE 6.28

(A) Ventral view of the jaws of the cownose ray, *Rhinoptera bonasus*, illustrating the "nutcracker" model of the bite force amplification proposed by Summers (2000). A gastropod is shown between the tooth plates, acted upon by a second-class lever powered by the jaw adductors. The ligaments between the upper and lower jaws, shown in black, serve as the fulcrum of the lever system. (B) A nutcracker of similar proportions showing the principles of the second-order lever system. (From Summers, A.P., *J. Morphol.*, 243, 113–126, 2000. With permission.)

of chondrichthyans, these elements are incorporated into the jaw joint and suspensorium of teleosts, and the upper and lower jaws are subsequently derived from dermal bones (de Beer, 1932; Liem et al., 2001). Consequently, the adductor mandibulae complex develops posterior to the teleost lower jaw and inserts via tendons that extend past the jaw joint, whereas this muscle complex develops in direct association with the chondrichthyan lower jaw. Specific adaptations for teleostean jaw leverage notwithstanding, the chondrichthyan adductor mandibulae complex is located relatively more anteriorly and is inherently in a position of higher leverage. This may ultimately be of great significance, as Friedman (2009) has demonstrated that fish with high-leverage jaws experienced lower extinction intensity during the mass extinction event at the end of the Cretaceous Period.

6.4.2.2 Bite Force

As previously mentioned, bite force has become a frequently used measure of vertebrate feeding performance because it directly impacts the acquisition of dietary and reproductive resources (Anderson et al., 2008). Cartilaginous fishes are a particularly interesting group in which to examine bite force because they span seven orders of magnitude in size, representing an ideal clade in which to examine the effects of changing body size on feeding performance. In addition, many species consume functionally difficult prey that may be quite large or composed of structural materials that are harder than the cartilaginous endoskeleton (Currey, 1980; Huber et al., 2009; Kolmann and Huber, 2009; Summers and Long, 2006; Wainwright et al., 1976; Wroe et al., 2008). Whether these feats of prey capture are a byproduct of large body size or are the result of size-specific selection for enhanced feeding performance (allometric growth) is largely unknown (Huber et al., 2009).

The bite forces of apex predators such as the white shark (*Carcharodon carcharias*), bull shark (*Carcharhinus leucas*), and great hammerhead (*Sphyrna mokarran*) rank among the highest of all extant vertebrates (Table 6.2), and the extinct *Carcharodon megalodon* may have had the highest bite force of any predator in vertebrate evolutionary history (Habegger et al., in review; Huber et al., 2009; Mara, 2010; Wroe et al., 2008). Recent phylogenetically informed analyses of numerous species spanning five orders of magnitude in size have determined that these tremendous bite forces can be attributed to large body size, not size-specific adaptations for high-performance feeding; bite force scales isometrically with body mass among species (Habegger et al., in review; Huber et al., 2009). It is likely that the high absolute bite forces generated by these larger shark species allow them to overcome constraints set by prey durability, thereby eliminating the selective pressure for size-specific adaptation (e.g., positive allometry of jaw adductor force or leverage) at large sizes. Huber et al. (2009) identified a possible transition point for this change in selective pressure at approximately 100 N of bite force, above which the slope of the relationship between bite force and body mass among species decreases dramatically. In other words, bite force increases with size more rapidly among smaller shark species perhaps because their lower bite forces represent a greater constraint with respect to the physical properties of their prey. Interestingly, a recent analysis of the cutting performance of teeth from 14 species

of extant and extinct sharks found the highest force required to penetrate a range of prey items to be 114 N (Whitenack and Motta, 2010).

Perhaps the most intriguing examples of feeding performance among cartilaginous fishes are those that consume hard prey, as the physical properties of such prey items represent a significant ecological constraint and the prey may be even harder than their own skeletons. Most durophagous chondrichthyans are small benthic predators that likely experience selective pressure for high-performance biting due to the physical demands of their trophic niche. As one might expect, durophagous species such as the spotted ratfish, *Hydrolagus colliei*, and horn shark, *Heterodontus francisci*, have the highest mass-specific bite forces of all species, and durophagy is significantly correlated with high mass-specific bite forces over evolutionary history (Habegger et al., in review; Huber et al., 2008, 2009; Mara et al., 2010). Surprisingly, the piscivorous sharpnose sevengill shark, *Heptranchias perlo*, has a very high mass-specific bite force, which appears to be a function of disproportionately large jaw adductors occupying deep fossae in the upper and lower jaws, characteristic of the ancestral cranial morphotype for sharks (Compagno, 1977; Huber, 2006). The bonnethead shark, *Sphyrna tiburo*, has one of the lowest mass-specific bite forces of all species, again suggesting that its durophagous ecology can be attributed to behavioral handling of prey as well as digestive enzymes, and not the pulverizing of prey (Habegger et al., in review; Huber et al., 2008, 2009; Mara, 2010; Mara et al., 2010). As with mechanical advantage, hammerhead sharks generally have low size-specific bite forces, although this low performance does not appear to be a consequence of the evolution and expansion of the cephalofoil (Mara, 2010). Although bite force has seldom been examined in batoids, at 60-cm disk width the cownose ray, *Rhinoptera bonasus*, can generate bite forces of at least 200 N, which is 20× greater than the forces at which their coquina clam prey (*Donax* sp.) begin to fracture, but considerably less than the force needed to crush large oysters and clams (Fisher et al., 2011; Maschner, 2000; Sasko, 2000; Sasko et al., 2006).

Phylogenetic analyses have identified jaw adductor cross-sectional area, mechanical advantage, and widening of the head as the biomechanical correlates of high mass-specific biting performance over chondrichthyan evolutionary history (Habegger et al., in review). This corroborates previous studies that have posited that a suite of morphological characters has convergently evolved among durophagous cartilaginous fishes, including hypertrophied jaw adductors, high-leverage jaws, and a pavement-like dentition (whether of individual teeth as in elasmobranchs or tooth plates as in holocephalans), with well-mineralized jaws and fused mandibular symphyses present among some taxa as well (Huber et al., 2005, 2008; Summers, 2000; Summers

et al., 2004). Although a pavement-like dentition is common among durophagous chondrichthyans, it must be noted that the interaction between biting performance and tooth morphology is little understood. Sustained adductor contraction, force amplification through asymmetrical biting, and cyclical loading of prey items have been identified as behavioral correlates of durophagy in these species as well (Huber et al., 2005; Summers, 2000; Wilga and Motta, 2000). Phylogenetic analyses have also indicated that evolution toward increased bite force has gone hand in hand with the evolution of wider heads among sharks (Habegger et al., in review; Huber et al., 2009). These results corroborate findings on the blacktip shark, *Carcharhinus limbatus*; horn shark, *Heterodontus francisci*; spotted ratfish, *Hydrolagus colliei*; and other vertebrate lineages in which head width is an excellent predictor of biting performance as it best approximates the cross-sectional area of the jaw adductors (Herrel et al., 1999, 2001a, 2002, 2004, 2005; Huber et al., 2006, 2008; Kolmann and Huber, 2009; Verwaijen et al., 2002).

6.4.2.3 Scaling of Feeding Biomechanics

Organismal performance changes over ontogeny as the musculoskeletal systems underlying animal behavior change in relative size and shape. As performance is largely a determinant of ecology, ontogenetic changes in the former can influence the latter. Thus, a thorough understanding of organismal ecology requires knowledge of how the functional integrity of morphological systems is maintained or enhanced during growth (Kolmann and Huber, 2009; Schmidt-Nielsen, 1984). Inquiries of this type are made through analyses of scaling patterns, which indicate the rate of change of morphological and performance measures with respect to body size. The null hypothesis of scaling analyses is one of geometric similarity, in which the chosen dependent parameter grows isometrically (in direct proportion) relative to body size, whereas positive or negative allometry indicates relatively faster or slower growth, respectively. Evidence of allometric growth is generally thought to indicate selective pressure for deviation from geometric similarity (Herrel and Gibb, 2006). For example, positive allometry of feeding performance is associated with ontogenetic dietary shifts and niche partitioning because enhanced performance enables the consumption of functionally difficult prey that other species, or younger members of the same species, cannot consume (Aguirre et al., 2003; Hernandez and Motta, 1997; Herrel and O'Reilly, 2006). Alternatively, positive allometry of feeding performance during early life history stages allows juveniles to rapidly reach adult performance levels, after which selective pressure for allometry maybe relaxed (Habegger et al., in review). Scaling relationships are examined by comparing the

observed slope of a relationship to the hypothetical isometric slope, which is the ratio of the exponents of the dependent and independent variables in the analysis. The isometric slope for a comparison of bite force against total length is 2.0 because bite force is a function of the cross-sectional area of the jaw muscles (x^2) and total length is a linear function (x^1). Given this logic, the isometric conditions for biomechanical parameters such as bite force and muscle force, in-levers and out-levers, and mechanical advantage are 2, 1, and 0 respectively.

Positive allometry of bite force has now been identified in horn sharks, *Heterodontus francisci*; blacktip sharks, *Carcharhinus limbatus*; juvenile bull sharks, *Carcharhinus leucas*; and spotted ratfish, *Hydrolagus colliei*. This is consistent with intraspecific findings from other vertebrates (Binder and Van Valkenburgh, 2000; Erickson et al., 2003; Habegger et al., in review; Hernandez and Motta, 1997; Herrel and Gibb, 2006; Herrel et al., 1999; Huber et al., 2006, 2008; Kolmann and Huber, 2009; Meyers et al., 2002). The biomechanical determinants of these scaling patterns were positive allometry of jaw adductor cross-sectional area in the three shark species and positive allometry of mechanical advantage at the anterior or posterior bite point in *H. francisci*, *C. limbatus*, *H. colliei*, and juvenile *C. leucas* (Habegger et al., in review; Huber et al., 2006, 2008; Kolmann and Huber, 2009). Conversely, isometry of bite force has been identified within adult *C. leucas* and from interspecific analyses of shark species spanning five orders of magnitude of size (Habegger et al., in review; Huber et al., 2009). These findings contrast with interspecific analyses of other vertebrate clades that have identified positive allometry of bite force among bats and turtles (Aguirre et al., 2002; Herrel et al., 2002), but negative allometry within carnivoran mammals (Christiansen and Wroe, 2007).

The collective results of scaling analyses within and among shark species suggest that positive allometry of bite force in small species or during the early ontogeny of large species plays a key role in determining adult performance and the ability to capture functionally difficult prey, and it may confer a competitive advantage over isometric ontogenetic trajectories, providing access to *relatively* competitor-free trophic niches earlier in life (Figure 6.29). For example, consumption of hard or large prey increases ontogentically in *Heterodontus francisci*, *Carcharhinus limbatus*, and *Carcharhinus leucas*,
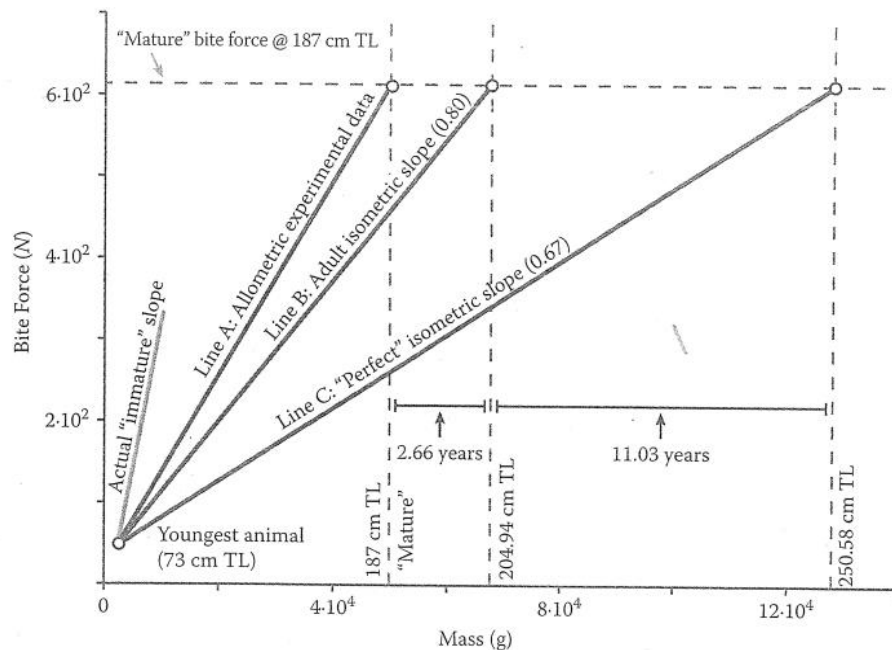

FIGURE 6.29

Simulation of bite force (N) with respect to body mass (g) in the bull shark, *Carcharhinus leucas*, illustrating the selective advantage gained due to the period of positive allometry early in its life history. Line A is drawn between this study's smallest animal (73 cm TL) and the smallest examined "mature" animal (187 cm TL). This is compared to lines B and C—bearing the experimentally calculated adult slope (0.80) and a perfectly isometric slope (0.67), respectively—to determine the masses (vertical dashed lines) at which animals on these curves would reach line A's adult bite force (horizontal dashed line). These masses are converted to units of time based on Branstetter and Stiles' (1987) equations for bull shark growth. The simulation indicates that the early growth rate of bull shark bite force allows it to reach mature bite forces many years before hypothetical isometric members of the same cohort; this performance and time gain could therefore have been a major driver in the evolution of positive allometry in shark species. Furthermore, the slope of line A is an underestimate of the allometric slope for all sampled juvenile *C. leucas* (short gray line on the far left of the graph), so this effect could be even more pronounced over the course of the life history of *C. leucas*. (From Habegger, M.L. et al., *Zoology*, in review. With permission of Elsevier.)

and positive allometry of bite force allows *H. francisci* to begin consuming purple sea urchins, *Strongylocentrotus purpuratus*, during its second year of life, whereas an isometric ontogenetic trajectory would have delayed access to this resource for at least another year (Bethea et al., 2004; Cliff and Dudley, 1991; Kolmann and Huber, 2009; Strong, 1989). Thus, selective pressure for size-related performance adaptations may be expected in small species or the young of large species, whereas extremely large sharks likely experience reduced pressure because the sheer magnitude of their bite forces is great enough to overcome the physical constraints of any prey item. The discrepancy between interspecific analyses of sharks and other vertebrate groups may be due to the fact that sharks simply reach larger sizes and have larger absolute bite forces than other groups of vertebrates.

6.4.3 Biomechanics of Chondrichthyan Jaw Suspension Mechanisms

Jaw suspension has historically been regarded as a major determinant of jaw kinesis in chondrichthyan feeding mechanisms (Huxley, 1876; Moss, 1977b; Wilga, 2002, 2008). Although Wilga (2002) found little correlation between the diversity of extant jaw suspension mechanisms and hyomandibular morphology with upper jaw protrusion ability, it can be expected in a macroevolutionary sense that the transition from Paleozoic forms to neoselachians has brought about increased movement of the jaws relative to the cranium, and that this undoubtedly plays a key role in the predatory ability of modern elasmobranchs (Carroll, 1988; Dean and Motta, 2004b; Frazzetta and Prange, 1987; Maisey, 2008; Motta and Wilga, 2001; Moy-Thomas and Miles, 1971; Schaeffer, 1967; Tricas and McCosker, 1984; Wilga et al., 2001).

While the postorbital articulation of extinct taxa such as *Cobelodus*, *Orthacanthus*, and *Pucapampella* is believed to have severely restricted palatoquadrate protrusion (Maisey, 2008), that of the hexanchid sharks readily disengages facilitating limited dorsoventral protrusion (Compagno, 1988; Wilga, 2002), and the remaining 99.6% of modern elasmobranchs lack a postorbital articulation altogether. Spanning the continuum of jaw suspensions, it is clear that euhyostylic batoids are capable of far greater jaw protrusion than amphistylic hexanchids, although the hyostylic and orbitostylic sharks show no conclusive pattern (Figure 6.6) (Dean and Motta, 2004b; Wilga, 2002). Among those species that have been experimentally investigated, the length of the ethmopalatine ligament, or its absence in the case of euhyostylic batoids, appears to be the primary determinant of jaw protrusion distance (Wilga, 2002).

Despite the ambiguity between suspension type and jaw mobility, hyomandibular morphology and behavior have been linked with other aspects of elasmobranch feeding. During prey capture, depression of the basihyal cartilage pulls the ceratohyal cartilages posteroventrally, causing rotation of the hyomandibular cartilages about the cranium. The short, laterally directed hyomandibulae of the whitespotted bamboo shark, *Chiloscyllium plagiosum*, and spiny dogfish, *Squalus acanthias*, as well as the anteriorly directed hyomandibulae of the little skate, *Leucoraja erinacea*, are depressed ventrally and compressed medially during this sequence. Although hyomandibular adduction temporarily delays peak suction pressure generation, the combined effect of ventral and medial movement of the hyomandibulae is expansion of the oropharyngeal cavity and hydraulic transport of water and prey into the mouth (Wilga, 2008; Wilga and Sanford, 2008). The posteriorly directed hyomandibulae of the shortfin mako shark, *Isurus oxyrinchus*, and sandbar shark, *Carcharhinus plumbeus*, swing ventrolaterally during feeding, causing expansion of the hyoid arch and an increase in the area of the mouth opening (Wilga, 2008). Although it is difficult to determine which hyomandibular orientation is plesiomorphic among modern elasmobranchs, it appears that the laterally directed hyomandibulae of heterodontiform, orectolobiform, and squaliform sharks facilitate suction feeding, whereas the posteriorly directed hyomandibulae of carcharhiniform, lamniform, and hexanchiform sharks facilitate a large gape for the biting of large prey (Wilga, 2008).

The general kinematic pattern of the hyoid arch experimentally verified by Wilga (2008) suggests that the hyomandibulae are acting in tension, which is reassuring considering that they have been referred to as "suspensory" elements for well over a century. Huber (2006) verified this role via biomechanical modeling of jaw suspensions in hyostylic species (e.g., horn shark, *Heterodontus francisci*; whitespotted bamboo shark, *Chiloscyllium plagiosum*; lemon shark, *Negaprion brevirostris*) and an amphistylic species (e.g., sharpnose sevengill shark, *Heptranchias perlo*). The hyomandibular and anterior craniopalatine articulations (ethmoidal/orbital) of *H. francisci*, *C. plagiosum*, and *H. perlo* are loaded in tension and compression, respectively, the magnitude of which is proportional to the force generated by the preorbitalis muscle (other adductor muscles act between the jaws with no net effect on suspensorial elements). In these species, the preorbitalis attaches in front of the anterior craniopalatine articulation, which remains intact throughout the gape cycle. Contraction of the preorbitalis compresses the upper jaw into the articulation and generates a torque about this point that rotates the posterior region of the upper jaw anteroventrally, pulling the hyomandibular cartilages in tension. Conversely, *N. brevirostris* is capable of protruding the upper jaw far enough to disengage its ethmoidal articulation (Motta and Wilga, 1995). In the absence of anterior craniopalatine contact, contraction of the preorbitalis and levator

palatoquadrati causes upward translation of the jaws and compression of the hyomandibulae (Huber, 2006). Thus, it appears that the hyomandibulae are tensile elements among species in which the anterior cranio-palatine articulation remains intact during feeding, and they act as compressive elements among species in which the anterior craniopalatine articulation either disengages (some carcharhinid and lamniform sharks) (Motta and Wilga, 1995; Wilga, 2005) or is absent altogether (batoids) (Huber, 2006). The euhyostylic batoids possess several novel jaw and hyomandibular muscles that appear to pivot the jaws and hyomandibulae about the cranium, allowing for high-precision, asymmetrical movements of the feeding mechanism (Dean and Motta, 2004a; Dean et al., 2005; McEachran et al., 1996; Wilga and Motta, 1998b). Furthermore, trabecular reinforcement in the jaws and hyomandibulae of the lesser electric ray, *Narcine bancroftii*, resist buckling, as the jaws are ballistically protruded into the sediment in search of prey (Dean et al., 2006). Although a suspensorial modeling analysis has not been performed for the euhyostylic mechanism, these findings corroborate the role of the hyomandibulae as compressive elements in batoids.

These suspensorial mechanics are suggestive of a broad evolutionary pattern in elasmobranch feeding mechanisms. The amphistylic jaw suspension of *Heptranchias perlo* restricts jaw protrusion, thereby reducing selective pressure for well-developed preorbitalis muscles; consequently, the hyomandibulae and craniopalatine articulations of *H. perlo* experience negligible loading (Huber, 2006). Although not homologous, the amphistylic jaw suspensions of modern hexanchid sharks and archaeostylic Paleozoic species are mechanically analogous (Maisey, 2008). The postorbital articulation of these Paleozoic forms precluded jaw protrusion (Maisey, 2008), so it can be assumed that these sharks also lacked well-developed preorbitalis muscles. Given that the force generated by the preorbitalis is the primary determinant of suspensorial loading (Huber, 2006), neither of these groups is therefore likely to have experienced selective pressure for structural modifications to their long, thin, poorly calcified, posteriorly directed hyomandibular cartilages. Thus, the hyoid arch retained the appearance of the postmandibular visceral arch from which it was derived (Maisey, 1980; Mallat, 1996; Zangerl and Williams, 1975). When the postorbital articulation was lost in neoselachians via reduction of the otic and postorbital processes of the upper jaw and cranium, respectively (Carroll, 1988; Maisey and de Carvalho, 1997; Schaeffer, 1967), architectural changes to the preorbitalis (enlargement, subdivision, reorientation) would have facilitated enhanced force production and jaw kinesis. Enhanced force production by the preorbitalis may then have provided the mechanical impetus for structural modifications to the

hyomandibular cartilages and the evolution of hyostyly in neoselachians. During this process, the hyomandibular cartilages became shorter, thicker, and rotated anteriorly into a more orthogonal position relative to the cranium, and they developed deep articular facets against the cranium, facilitating directionally specific motion (Cappetta, 1987; Schaeffer, 1967; Wilga, 2002). The increase in load-bearing ability of the hyomandibular cartilages and enhanced jaw kinesis associated with the evolution of hyostyly appear to have increased the functional versatility of the feeding mechanism, resulting in the evolution of ram, suction, biting, and filter-feeding mechanisms in modern elasmobranchs (Moss, 1977b).

Although the holocephalans have a much simpler jaw suspension mechanism, it would be remiss to neglect them in this discussion because they are one of the more curious groups of chondrichthyans. The upper jaw of holocephalans fuses to the nasal, trabecular, and parachordal cartilages of the cranium early in development, resulting in an akinetic holostylic jaw suspension (Grogan et al., 1999; Wilga, 2002). The fused upper jaw is located directly below the vaulted ethmoidal region of the cranium; along with hypermineralized tooth plates, these are considered adaptations for durophagy in holocephalans (Didier, 1995; Grogan and Lund, 2004). Many holocephalans regularly consume hard prey despite the fact that their feeding mechanisms are poorly if at all mineralized. Because hard prey can generate large bite reaction forces and unmineralized cartilage has poor compressive stiffness, the unique cranial morphotype of holocephalans is believed to stabilize the feeding mechanism against dorsoventral flexion, thus representing a wholly different strategy for cranial stability than is found among elasmobranchs (Huber et al., 2008; Wroe et al., 2008).

6.5 Tooth Form and Function

6.5.1 Arrangement and Terminology

Elasmobranch teeth are arranged in rows on the palatoquadrate and Meckel's cartilage, such as in most sharks and many rays, or they form large pavement-like tooth plates for crushing prey, as in many batoids. Elasmobranch teeth are polyphyodont, meaning that they develop in rows similar to the teeth of bony fishes and are replaced at a regular interval. A tooth in the functional position at the edge of the jaw and its replacement teeth constitute a tooth row (file, family). The number of tooth rows/families varies from 1 per jaw in some rays to more than 300 in the whale shark; in most sharks, there are 20 to 30 tooth rows. A

tooth series refers to a line of teeth along the jaw that is parallel to the jaw axis and includes teeth from all rows (Compagno, 1984; James, 1953; Reif, 1976, 1984). The rate of replacement is species specific; is affected by age, diet, seasonal changes, and water temperature; and may vary between the upper and lower jaw (Moss, 1967). Most species only replace a few teeth at a time, although the cookie-cutter shark, *Isistius brasiliensis*, differs in that its relatively large lower triangular teeth are shed together as a complete set (Strasburg, 1963). Replacement rates, as measured by the rate of movement of a tooth from the row lingual to the functional row to that of the functional row, vary from 9 to 12 days in the leopard shark, *Triakis semifasciata* (Reif et al., 1978); from 9 to 28 for the nurse shark, *Ginglymostoma cirratum*, in the summer and from 51 to 70 days in the winter (Luer et al., 1990; Reif et al., 1978); from 8 to 10 days for the lemon shark, *Negaprion brevirostris* (Moss, 1967); about 4 weeks for *Heterodontus* (Reif, 1976); and 5 weeks for *Scyliorhinus canicula* (Botella et al., 2009; Märkel and Laubier, 1969). Primitive chondrichthyan fishes, such as the Early Devonian *Leonodus carlsi*, are believed to have an extremely slow dental replacement rate (Botella et al., 2009). The teeth of myliobatid rays are arranged as a central file of thick, flattened, usually hexagonal teeth that are fused together and three lateral files of smaller teeth on each side. Other myliobatid rays, such as the spotted eagle ray, *Aetobatus narinari*, have only a central file of fused teeth on the upper and lower jaws, in which replacement teeth move toward the occlusal plane where they fuse and become functional (Figure 6.30). *Myliobatis* has three to ten rows of mature, unworn teeth behind the functional rows, and as they are replaced these teeth eventually pass aborally and are lost. *Aetobatus narinari* has an unusual condition in which the lower jaw teeth move anteriorly out of the crushing zone and remain attached to the tooth plate to form a spade-like appendage used to dig up prey items (Bigelow and Schroeder, 1953; Cappetta, 1986a,b; Summers, 2000; A. Collins, pers. comm.).

Within a jaw, homodont teeth are all the same shape and show no abrupt change in size. This is rare in recent and fossil sharks, but apparently exists in *Rhincodon* and *Cetorhinus*. Monognathic heterodonty refers to a significant change in size and shape of the teeth in different parts of the same jaw (upper or lower) and is common in recent and fossil sharks (Applegate, 1965; Compagno, 1988). Horn sharks (Heterodontidae) and bonnethead sharks (Sphyrnidae) both have anterior cuspidate teeth for grasping and posterior molariform crushing teeth (Figure 6.31) (Budker, 1971; Compagno, 1984; Nobiling, 1977; Peyer, 1968; Reif, 1976; Smith, 1942; Taylor, 1972). Carcharhinid sharks have dignathic heterodonty, with more cuspidate lower jaw teeth lacking serrations and more blade-like, serrated teeth in the upper jaw (Bigelow

and Schroeder, 1948; Compagno, 1984, 1988). Sexual heterodonty occurs in many elasmobranchs, and in many cases the teeth of adult males differ in shape from those of females and immature males. The dimorphism is often confined to the anterior teeth, and in the carcharhinoids it is mostly confined to species less than one meter in length. Sexual heterodonty in sharks and particularly rays appears to be related to courtship, during which the male holds onto a female with his mouth, rather than to feeding (Cappetta, 1986b; Compagno, 1970, 1988; Ellis and Shackley, 1995; Feduccia and Slaughter, 1974; Herman et al., 1995; Kajiura and Tricas, 1996; McCourt and Kerstitch, 1980; McEachran, 1977; Nordell, 1994; Smale and Cowley, 1992; Springer, 1967).
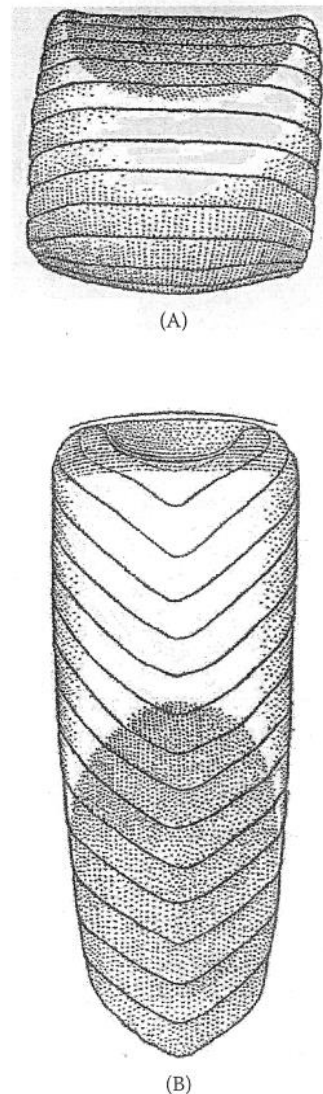

(A)

(B)

FIGURE 6.30

(A) Upper and (B) lower tooth plate of *Aetobatus narinari*. In the lower plate, the front tooth is lowermost. (From Bigelow, H.B. and Schroeder, W.C., *Mem. Sears Found. Mar. Res.*, 1(2), 1–588, 1953. Courtesy of the Peabody Museum of Natural History, Yale University.)
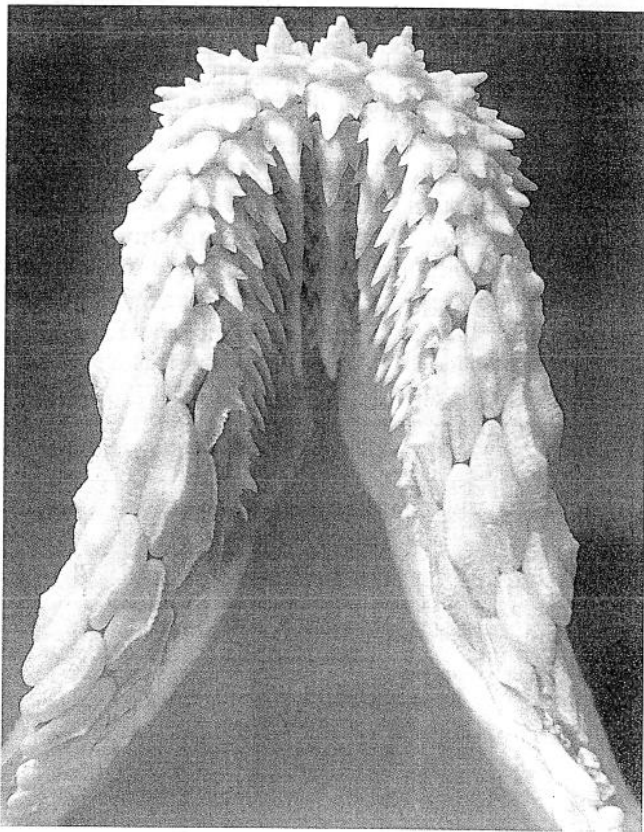
FIGURE 6.31
Dorsal view of the lower jaw teeth of the horn shark, *Heterodontus francisci*, showing the grasping teeth in the front of the jaw and the molariform or grinding teeth behind. Rostral tip of the jaw is at the top of the picture.

Ontogenetic heterodonty refers to ontogenetic changes in dentition, often associated with ontogenetic changes in diet. The shape of the teeth and number of tooth cusps in horn sharks (Heterodontidae) change with ontogeny. Rear replacement teeth gradually lose cusps, broaden at the base, and flatten along the crown. The more anterior recurved teeth have larger central cusps and fewer overall cusps with age. Juvenile Port Jackson shark, *Heterodontus portusjacksoni*, have more pointed teeth and apparently take more soft-bodied prey than the adults (Compagno, 1984; McLaughlin and O'Gower, 1971; Nobiling, 1977; Peyer, 1968; Reif, 1976; Shimada, 2002b; Smith, 1942; Taylor, 1972). White sharks less than 1.5 m TL (total length) have relatively long and narrow teeth with lateral cusplets (Hubbell, 1996). Smaller white sharks feed primarily on fish, while larger animals with broader teeth prefer marine mammals (Tricas and McCosker, 1984), a dietary switch that is reflected in the isotopic signature of their vertebrae (Estrada et al., 2006). Lamniform sharks have an embryonic peg-like dentition before parturition, and at about 30 to 60 cm TL they transition into the adult lamnoid type of dentition just before or after birth. The early stage of the adult dentition often possesses bluntly pointed crowns without distinct cutting edges, serrations, and lateral cusplets of the adult teeth. This is perhaps to prevent the developing embryos, which are often consuming eggs and embryos *in utero*, from damaging the mother's uterus (Shimada, 2002b).

6.5.2 Evolutionary and Functional Patterns

It is suggested that the earliest sharks for which there are no fossil teeth, just denticles (placoid scales), were microphagous filter feeders. Presumably with a selection for larger teeth there was a concomitant change to a macrophagous diet (Williams, 2001). Many of the early Paleozoic sharks, including the cladodont, xenacanthid, hybodont, and ctenacanthid lineages, had a dentition apparently suited for piercing, holding, and slashing. Most of the Early Devonian and Carboniferous sharks have a tooth pattern often referred to as "cladodont" in form (Figure 6.32). These grasping teeth have a broad base with a single major cusp and smaller lateral cusps and apparently slow replacement. In *Xenacanthus*, the lateral cusps are enlarged, and the central cusp is reduced. Hybodont and ctenacanthid sharks in general also had a tooth morphology, composed of two of more elongated cusps, that appears suited for piercing and holding prey. Even within these early lineages, as in modern forms, there were repeated evolutionary forays into a benthic lifestyle and development of crushing, pavement-like teeth (Cappetta, 1987; Carroll, 1988; Hotton, 1952; Moy-Thomas and Miles, 1971; Schaeffer, 1967; Williams, 2001; Zangerl, 1981).

The tooth microstructure of these ancestral lineages was characterized by a single crystallite enameloid monolayer with random crystallite orientation (Gillis and Donoghue, 2007). The lack of microstructural diversity in these teeth is believed to have limited the functional diversification of feeding mechanisms in non-neoselachian elasmobranchs because microstructural diversity is related to the mechanical integrity of the teeth (Preuschoft et al., 1974). Neoselachian elasmobranchs other than batoids possess teeth with a triple-layered enameloid structure consisting of a layer of single crystallite enameloid and layers of parallel-fibered enameloid and tangle-fibered enameloid; parallel-fibered enameloid is believed to resist crack propagation and confer tensile strength, whereas tangle-fibered enameloid confers compressive strength (Gillis and Donoghue, 2007; Preuschoft et al., 1974). Triple-layered enameloid has been identified in basal members of the neoselachian crown groups Galea and Squalea (Gillis and Donoghue, 2007; Reif, 1977). Though lacking this extent of microstructural diversification, certain highly predatory Paleozoic species
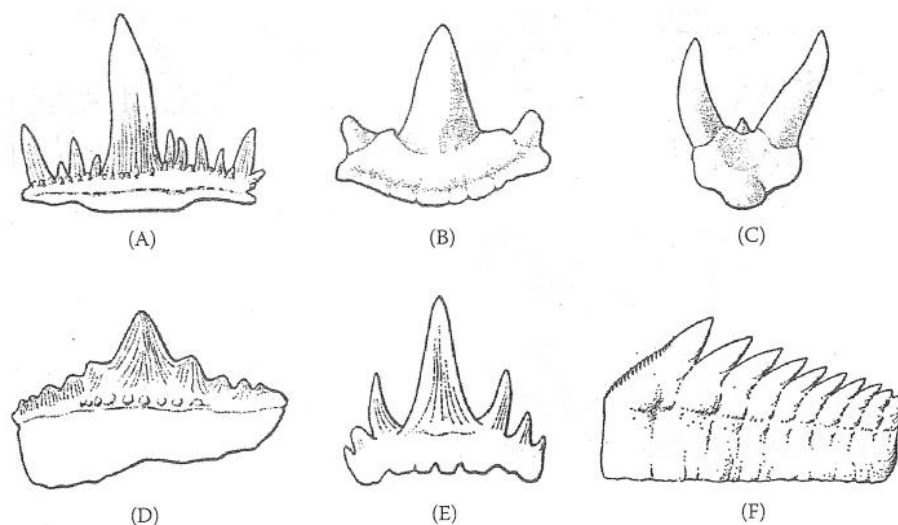
FIGURE 6.32
Ancestral shark tooth types: (A, B) acrodont teeth of *Cladodus* sp.; (C) diplodus teeth of *Xenacanthus* sp.; (D, E) hybodont type teeth; (F) tooth from extant *Hexanchus griseus*. (Parts A to E from Schaeffer, B., in *Sharks, Skates and Rays*, Gilbert, P.W. et al., Eds., The Johns Hopkins University Press, Baltimore, MD, 1967, pp. 3–35. With permission. Part F from Bigelow, H.B. and Schroeder, W.C., *Mem. Sears Found. Mar. Res.*, 1(1), 1–576, 1948. Courtesy of the Peabody Museum of Natural History, Yale University.)

exhibited some specialization. The Carboniferous shark *Carcharopsis prototypus* possessed increased density of enameloid crystallites in the single crystallite enameloid layer of its tooth serrations, as has also been found in fossil neoselachians (Andreev, 2010; Duffin and Cuny, 2008). The general lack of tooth serrations in Paleozoic species has been attributed to the rarity of such microstructural specialization and subsequent inability of the teeth to handle stresses associated with a sawing dentition (Duffin and Cuny, 2008).

Perhaps predicated on the evolution of microstructural diversification, the teeth of extant neoselachians display a considerable diversity of forms that are often ascribed functional roles (e.g., seizing/grasping, tearing, cutting, crushing, grinding) (Cappetta, 1986b, 1987). Teeth that apparently seize prey prior to swallowing are generally small, with multiple rows of lateral cusplets. These may be found on benthic-associated sharks and rays such as in the Orectolobiformes (e.g., *Ginglymostoma cirratum*) and male dasyatid rays (Figure 6.33). Some teeth appear suited for seizing and tearing, as they are long and pointed with narrow cusps. The dagger-like anterior teeth of the upper jaw in the sandtiger shark, *Carcharias taurus*, have a pronounced inward inclination and are thought to puncture and retain struggling prey after it has been grasped by the outwardly inclined anterior teeth of the lower jaw (Lucifora et al., 2001). The shortfin mako shark, *Isurus oxyrinchus*, has similar teeth anteriorly, with more triangular cutting teeth found toward the back of the jaw. The teeth of hexanchoids (*Hexanchus, Heptranchias, Notorhynchus, Chlamydoselachus*) can range from sawlike in *Hexanchus*

to three-pronged and grasping in *Chlamydoselachus* (Figure 6.32) (Cappetta, 1987; Carroll, 1988; Daniel, 1934; Pfeil, 1983). Many squaloid sharks, including *Etmopterus*, have a multicuspid grasping upper dentition and blade-like lower cutting teeth. Sharks with blade-like cutting teeth tend to have one fully erect functional row forming an almost continuous blade in which the bases of the teeth may interlock (e.g., *Dalatias, Etmopterus*) (Figure 6.33) or have edentulous spaces, such as are found in many lamnids (e.g., bigeye thresher, *Alopias superciliosus*; *Carcharodon carcharias*) (Shimada, 2002a; Shirai and Nakaya, 1990). In the tiger shark, *Galeocerdo cuvier*, the anterior and posterior margins of the teeth have coarse serrations and are markedly asymmetrical, with a distinct notch on the distal edge of the crown (Figure 6.33) (Bigelow and Schroeder, 1948; Cappetta, 1987; Williams, 2001). The more curved side of these teeth might serve to slice through tissue as they are dragged across a prey item, while the notch on the other side encounters and concentrates stress in more durable tissues such as collagen, cartilage, and bone (Figure 6.34). Witzell (1987) attributed the ability of *G. cuvier* to bite through whole large chelonid sea turtles to a suite of morphological and behavioral characters, including a single row of cusped, serrated teeth on a broad-based, heavily mineralized jaw that can be extensively protruded (Moss, 1965, 1972), and head shaking, which drags the teeth across the prey. Indigestible pieces of shell are regurgitated by stomach eversion, which has also been noted in other sharks and rays (Bell and Nichols, 1921; Brunnschweiler et al., 2005, 2011; Budker, 1971; Randall, 1992; Sims et al., 2000; Witzell, 1987).
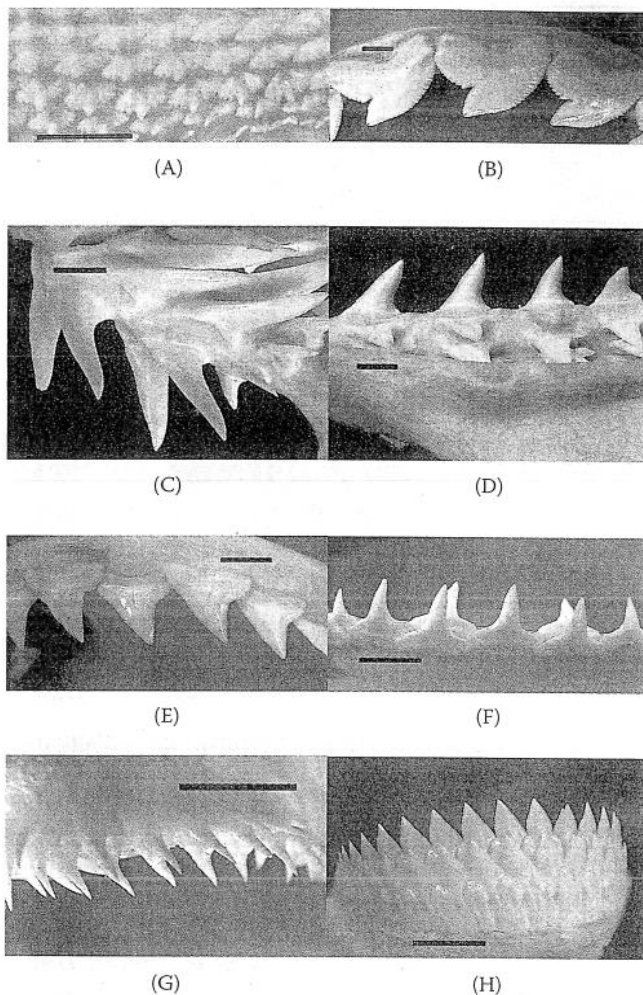
FIGURE 6.33
Modern tooth types: (A) lingual teeth of the nurse shark, *Ginglymostoma cirratum*; (B) upper lateral teeth of the tiger shark, *Galeocerdo cuvier*; (C) upper anterior teeth of shortfin mako shark, *Isurus oxyrinchus*; (D) lower lateral teeth of *I. oxyrinchus*; (E) upper anterior and lateral teeth of sandbar shark, *Carcharhinus plumbeus*; (F) lower anterior and lateral of *C. plumbeus*; (G) upper anterior and lateral teeth of the kitefin shark, *Dalatias licha*; (H) lower teeth of *D. licha*. Scale bar is 1 cm in all cases.

Durophagous dentitions have evolved numerous times among chondrichthyans. *Mustelus* has a crushing-type dentition, in which the teeth are low and have cutting edges with bluntly rounded apices (Bigelow and Schroeder, 1948; Cappetta, 1987). The crushing rear teeth of *Heterodontus* are closely opposed to each other such that the load on any one tooth is distributed to adjacent teeth in the same row (Nobiling, 1977). Ontogenetic differences in dentition occur in the Port Jackson shark, *Heterodontus portusjacksoni*, coinciding with a dietary shift. Juvenile sharks have sharp, cuspidate anterior teeth and the head is shorter and narrower. As they mature, the posterior molariform teeth begin to

dominate, and the head broadens and lengthens. These changes are accompanied by a dietary change from soft-bodied benthic invertebrates to a more durophagous adult diet (Powter et al., 2010). Jaw stiffness increases from anterior to posterior in the horn shark, *Heterodontus francisci*, with the stiffest regions of the upper and lower jaws underlying the molariform teeth (Summers et al., 2004). Imbricated, flattened teeth that form a dental plate suited for grinding hard benthic prey are widespread among myliobatid stingrays (Cappetta, 1986a,b, 1987) (see Figures 6.19 and 6.30). Maschner (2000) found that the teeth of the cownose ray, *Rhinoptera bonasus*, are also interlocked so that point loads are effectively distributed to the jaw, decreasing the stress concentration at any one point. The spotted eagle ray, *Aetobatus narinari*, has an interlocking dentition similar to that of *R. bonasus*, underlain by a fused jaw symphysis which is the stiffest part of the jaw. Although maximum stiffness occurs in different regions of the jaws of *H. francisci* and *A. narinari*, this parameter coincides with the location of molariform teeth in both species (Summers et al., 2004).

In contrast to these rigidly interlocking dentitions, numerous species possess teeth that are quite kinetic. Frazzetta (1988, 1994) has proposed that the relatively loose fibrous connection of shark teeth to the jaw cartilage allows the teeth to conform to irregularities in soft tissue and guide around solid obstructions such as bone. For example, the front teeth of the white shark, *Carcharodon carcharias*, are angled inward, perhaps making them more effective at gouging chunks of flesh, grasping prey items, or preventing prey escape from the mouth. During mouth closure, the crown angle of the anterior teeth initially increases by 8.7° and then decreases by 15.7° as the jaw is adducted through an arc of 35° or more. Although the mechanism is not clear, this is believed to facilitate a plucking action during feeding (Powlik, 1995). In many orectolobiform sharks, such as the whitespotted bamboo shark, *Chiloscyllium plagiosum*, the teeth have an inward inclination in their resting state but are capable of passively rotating about their connection to the jaw to form an imbricated crushing surface when hard prey is contacted (Ramsay and Wilga, 2007). Finally, individual teeth can have diverse functions even when they are firmly attached to the jaw, provided that the jaws themselves are capable of dynamic behaviors. The lesser electric ray, *Narcine bancroftii*, ballistically protrudes its jaws into the sediment in search of benthic prey, during which the halves of its jaws are adducted medially. Medial rotation of the jaw halves is accompanied by medial rotation of the teeth into positions that augment both normal and frictional forces as prey are sucked into the oral cavity. These forces hold prey in place as the buccal cavity is flushed of sediment prior to swallowing (Dean et al., 2008).
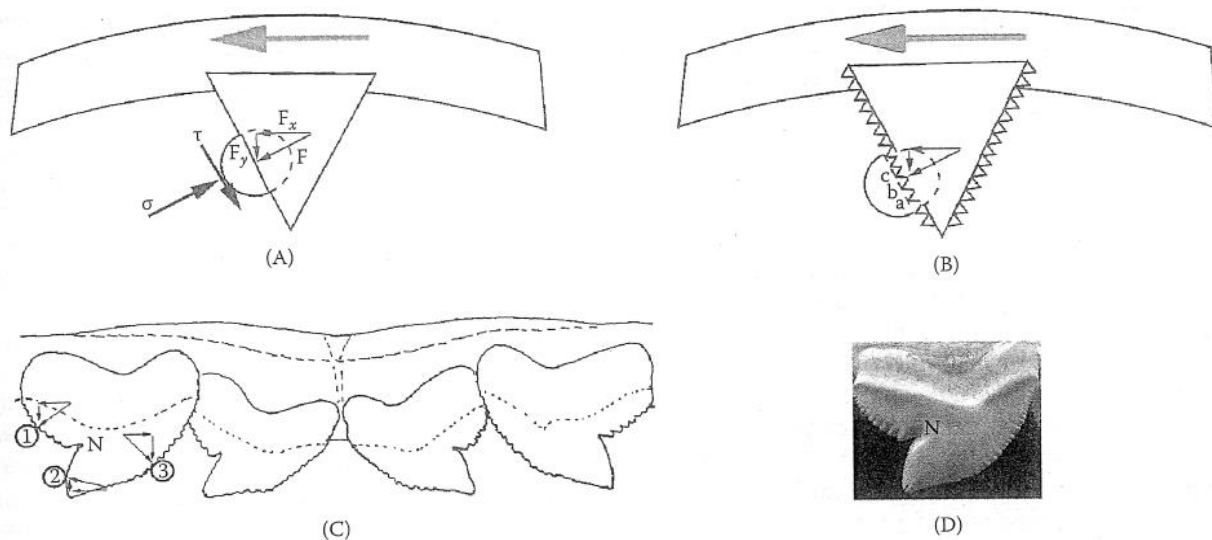
FIGURE 6.34
Proposed cutting mechanism for nonserrated, serrated, and notched shark teeth. (A) When tooth is drawn across an object as indicated by the large gray arrow, the object (denoted as a circular shape) impacts the leading edge of the beveled tooth (triangle). As the nonserrated tooth edge cuts into the object, a force normal to the object (F) can be resolved into a force in the x plane (F_x) and a force in the y plane (F_y). These forces result in a stress normal to the tooth (σ) and a shear stress (τ) that result in the object being deflected toward the tip of the tooth as the tooth edge cuts into the object. The sharp leading edge of the tooth results in stress concentration that helps cut into the object (σ = Force/Area; the sharp leading edge has a very small area in contact with the object at any time). (B) As a serrated tooth is similarly drawn across an object, the object is similarly deflected toward the tooth tip, but the very small area at the tip of each serration further increases the stress, resulting in even greater penetration into the object. For example, when serration (a) encounters a region of the object, it results in stress concentration, resulting in penetration of the tooth margin into the object; similarly, serrations (b) and (c) encounter additional uncut material as the tooth is driven toward (F_x) and across (F_y) the object; in this manner, serrations result in localized regions of high stress that facilitate cutting through the object. These serrations can be linearly arranged, as they are on most fish teeth, and need not be laterally staggered as they are on a carpenter's wood saw. The latter serrations may reduce the entrapment of cut material from among the serrations. (C) Tiger shark, *Galeocerdo cuvier*, teeth are arranged and shaped in the indicated manner about the palatoquadrate symphysis. Different faces of these teeth may serve different functions. On the notched surface of these teeth, objects encountered at positions (1) or (2) are driven toward the notch (N), which is extremely narrow and thin, consequently increasing the stress in this region. This action serves to cut the material in a manner similar to a notched paper cutter or scissors. If the tooth is moving in the other direction, the object (3) is driven toward the tooth tip and cut in the manner explained above. As the shark swings its jaws from side to side while biting down on a prey item, the different faces of the teeth, which are arranged in a mirror image on the opposite jaw, cut through the prey by both of these methods. Tougher material, such as ligaments, tendons, and bundles of collagen fibers, may be cut more easily on the notched side of the tooth. (D) Fourth upper lateral tooth of *G. cuvier* with the notch (N) indicated.

Despite this extensive attribution of function to form, there are almost no quantitative functional studies of tooth use in cartilaginous fishes, and the mechanics of piercing and cutting are poorly understood (Anderson, 2009; Atkins, 2006; Atkins and Xu, 2005; Cappetta, 1986b, 1987; Whitenack and Motta, 2010). Carcharhinid lower jaw teeth may be used to grasp prey during mandibular elevation, after which the serrated, triangular upper jaw teeth descend and saw through the prey, often facilitated by rapid head shaking (Frazzetta, 1988, 1994; Frazzetta and Prange, 1987; Moss, 1972, 1977b; Motta et al., 1997; Smale et al., 1995; Springer, 1961). Some squaloid sharks have blade-like teeth in both jaws with large, laterally directed cusps that cut through prey during lateral head shaking (Compagno, 1984; Wilga and Motta, 1998a), and upper jaw protrusion in both groups may expose the serrated or blade-like upper teeth, facilitating their unobstructed lateral movement through the prey (Motta and Wilga, 2001). These examples illustrate several key points regarding the fracture of tough, extensible tissues. Bladed edges are clearly better at cutting than blunted edges, but the presence of angled or notched blades dramatically increases cutting efficiency relative to a straight blade. In particular, notched blades can decrease the work to fracture of compliant tissues by up to 60% because notching traps the substrate at the cutting surface, thereby concentrating stress and facilitating material rupture (Abler, 1992; Anderson, 2009; Anderson and LaBarbera, 2008). These effects are apparent at multiple scales, ranging from the single large notch in the teeth of the tiger shark, *Galeocerdo cuvier*, to the serrations (small notches) on the teeth of numerous other species, and can be augmented by behaviors such as lateral head shaking. Drawing a

blade across a substrate reduces the force required to initiate downward penetration. This penetration force is minimized for blades with larger radii of curvature and at higher "slice-to-push" ratios (tangential blade movement greater than normal blade movement), as would occur when the teeth are drawn rapidly to the side as they sink into the prey during lateral head shaking (Atkins, 2006).

Whitenack et al. (2010, 2011) conducted a comprehensive analysis of the relationship between tooth morphology, prey type, and cutting mechanics in sharks. Teeth from ten extant species and aluminum casts of teeth from three extinct species were punctured and drawn through five prey items of varying thickness and toughness (three teleosts, one elasmobranch, one crustacean). Significant differences in puncture and draw forces were found among species and prey types, with some species incapable of initiating tissue damage through either puncture or draw on particular prey items. For example, teeth with distally inclined cusps were less effective at initiating puncture, although there was little correlation between puncture performance and prey type, whereas teeth from the knifetooth dogfish, *Scymnodon ringens*, were incapable of cutting via draw on any prey type. Teeth from extinct species (*Cladodus*, *Xenacanthus*, *Hybodus*) performed comparably to those of extant species in puncture but were less effective in draw, and broad triangular teeth were generally less efficient at cutting (require greater force to penetrate).

Nonetheless, no clear relationships between cutting performance and phylogeny, tooth shape, or the presence of serrations were found, suggesting that the functional morphotypes to which shark teeth have long been categorized (e.g., tearing, cutting, cutting–clutching) are not supported by their cutting performance. Furthermore, finite element analysis revealed that shark teeth are structurally strong, and the majority of the teeth have stress patterns consistent with a well-designed cantilever beam. Notches, such as those of the tiger shark, *Galeocerdo cuvier*, result in stress concentration and may serve as a weak point, but they are functionally important for cutting prey during lateral head shaking. It is proposed that frequent tooth replacement in sharks is driven by tooth wear, not tooth failure.

6.6 Summary, Conclusions, and Future Directions

The feeding mechanism of sharks and their relatives displays remarkable diversity, especially when considering the simplicity of this system. Elasmobranchs will hunt by speculation, ambush, stalk, or lure and will scavenge their prey. Elasmobranchs are versatile in how and where they capture their prey; however, the capture kinematics and motor action patterns are very similar among sharks but differ somewhat from those of batoids. Sharks capture their prey by ram, biting, and suction or some combination of the three, whereas batoids primarily use suction-dominated prey capture. The jaw suspension in elasmobranchs plays a significant role in the kinesis of the jaws and consequently the feeding mechanisms. Batoids have a unique suspensory apparatus, the most kinetic jaws, and a highly versatile and protrusible mouth.

The mineralized layer of skeletal elements in elasmobranch feeding mechanisms is load bearing, and the distribution of mineral within these skeletal elements plays a major role in their mechanical function. Although it is unknown whether the material properties of either the mineralized or unmineralized portions of the feeding mechanism vary with feeding ecology, it is clear that the tessellated cartilaginous skeleton is an elegant solution to the need to maintain mechanical integrity while permitting growth in a skeletal system that is incapable of remodeling. This skeletal design represents the highly economical use of structural material (i.e., limited mineral ideally located) and facilitates high-performance feeding where intuition would suggest that a system predominantly composed of pliant, unmineralized cartilage would have compromised performance. Nonetheless, cartilaginous fishes are capable of some of the highest bite forces of any animal, and some species are capable of processing prey items that are harder than their own skeletons. The causative factors of this high-performance feeding—muscle cross-sectional area and mechanical advantage—both demonstrate strong ecomorphological signatures, and recent evidence suggests the correlated evolution of these traits in taxa with above-average feeding performance for their body size. Furthermore, smaller species and juveniles of larger species exhibit positive allometry of bite force due to the benefits of attaining high-performance feeding early in their life history, whereas selection for size-specific performance apparently decreases in large species due to their high absolute bite forces.

Elasmobranch teeth are diverse in structure and arrangement, ranging from the flattened pads of mollusk-crushing batoids to the villiform-like teeth of plankton-feeding whale sharks. Throughout evolution there have been multiple forays into different tooth forms, with a general trend toward increased complexity of the enameloid microstructure in modern sharks. Shark teeth have been ascribed functional roles, but only recently have quantitative analyses revealed that teeth from extinct species perform comparably to those of extant species in puncture but are less effective in draw, and broad triangular teeth are generally less

efficient at cutting. There appears to be no clear relationships among cutting performance and phylogeny, tooth shape, or the presence of serrations. Regardless, shark teeth are structurally strong, and it is proposed that frequent tooth replacement in sharks is driven by tooth wear, not tooth failure.

Despite great advances in our understanding of the feeding biology of elasmobranchs, major gaps in our knowledge still remain. Even though there have been consistent and excellent studies on the anatomy of the feeding apparatus and diet, the ethology of predation is less studied, most likely because of the inherent difficulties of *in situ* studies of such large, mobile predators. Surprisingly, rays and skates would seem relatively easy to study but are less understood and investigated than sharks. In particular, studies on batoid feeding mechanics are lacking. We are only beginning to understand how prey capture behavior differs within and among species and the link between feeding behavior and the morphology of the feeding apparatus. Feeding mechanics, particularly those of jaw protrusion, have only been investigated in a handful of taxa representing a few families. The putative functions of jaw protrusion are still elusive, as discussed in the first edition of this chapter (Motta, 2004). Studies of tooth performance and the biomechanical properties of shark biomaterials have only just begun, and this remains an area ripe for quantitative analyses. Finally, perhaps the most challenging task lies in our understanding of the evolution of feeding types in the elasmobranchs, a task we can only accomplish with a thorough understanding and comparative analyses of extant forms.

References

Aalbers, S.A., Vernal, D., and Sepulveda, C.A. (2010). The functional role of the caudal fin in the feeding ecology of the common thresher shark *Alopias vulpinus*. *J. Fish Biol.* 76:1863–1868.

Abd El-Aziz, S.H. (1986). Food and feeding habits of *Raja* species (Batoidei) in the Mediterranean waters of Alexandria. *Bull. Inst. Oceanogr. Fish. (Arab. Repub. Egypt)* 12:265–276.

Abler, W.L. (1992). The serrated teeth of tyrannosaurid dinosaurs and biting structures in other animals. *Paleobiology* 18:161–183.

Aguirre, L.F., Herrel, A., Van Damme, R., and Matthysen, E. (2002). Ecomorphological analysis of trophic niche partitioning in a tropical savanna bat community. *Proc. R. Soc. Lond. B Biol. Sci.* 269:1271–1278.

Aguirre, L.F., Herrel, A., Van Damme, R., and Matthysen, E. (2003). The implications of food hardness for diet in bats. *Func. Ecol.* 17:201–212.

Ajayi, T.O. (1982). Food and feeding habits of *Raja* species (Batoidei) in Carmarthen Bay, Bristol Channel. *J. Mar. Biol. Assoc. U.K.* 62:215–223.

Ajemian, M.J. and Sanford, C.P. (2007). Food capture kinematics in the deep-water chain catshark *Scliorhinus retifer*. *J. Mar. Biol. Assoc. U.K.* 87:1277–1286.

Allis, E.P.J. (1923). The cranial anatomy of *Chlamydoselachus anguineus*. *Acta Zool.* 4:123–221.

Anderson, P.S.L. (2009). The effects of trapping and blade angle of notched dentitions on fracture of biological tissues. *J. Exp. Biol.* 212:3627–3632.

Anderson, P.S.L. and LaBarbera, M. (2008). Functional consequences of tooth design: effects of blade shape on energetics of cutting. *J. Exp. Biol.* 211:3619–3626.

Anderson, R.A., McBrayer, L.D., and Herrel, A. (2008). Bite force in vertebrates: opportunities and caveats for use of a nonpareil whole-animal performance measure. *Biol. J. Linn. Soc. Lond.* 93:709–720.

Andreev, P.S. (2010). Enameloid microstructure of the serrated cutting edges in certain fossil carcharhiniform and lamniform sharks. *Microsc. Res. Tech.* 73:704–713.

Applegate, S.P. (1965). Tooth terminology and variation in sharks with special reference to the sand shark, *Carcharias taurus* Rafinesque. *Contrib. Sci. Mus. Nat. Hist. Los Angeles County* 86:1–18.

Ashhurst, D.E. (2004). The cartilaginous skeleton of an elasmobranch fish does not heal. *Matrix Biol.* 23:15–22.

Atkins, A.G. and Xu, X. (2005). Slicing of soft flexible solids with industrial application. *Int. J. Mech. Sci.* 47:479–492.

Atkins, T. (2006). Optimum blade configurations for the cutting of soft solids. *Eng. Fracture Mech.* 73:2523–2531.

Au, D.W. (1991). Polyspecific nature of tuna schools: shark, dolphin, and seabird associates. *U.S. Fish. Bull.* 89:343–354.

Babel, J.S. (1967). Reproduction, life history, and ecology of the round stingray, *Urolophus halleri* Cooper. *U.S. Fish. Bull.* 137:76–104.

Barbini, S.A., Scenna, L.B., Figueroa, D.E., Cousseau, M.B., and Díaz de Astarloa, J.M. (2010). Feeding habits of the Magellan skate: effects of sex, maturity stage, and body size on diet. *Hydrobiologia* 641:275–286.

Belbenoit, P. (1986). Fine analysis of predatory and defensive motor events in *Torpedo marmorata* (Pisces). *J. Exp. Biol.* 121:197–226.

Belbenoit, P. and Bauer, R. (1972). Video recordings of prey capture behaviour and associated electric organ discharge of *Torpedo marmorata* (Chondrichthyes). *Mar. Biol.* 17:93–99.

Bell, J.C. and Nichols, J.T. (1921). Notes on the food of Carolina sharks. *Copeia* 1921:17–20.

Bethea, D.M., Buckel, J.A., and Carlson, J.K. (2004). Foraging ecology of the early life stages of four sympatric shark species. *Mar. Ecol. Prog. Ser.* 268:245–264.

Bigelow, H.B. and Schroeder, W.C. (1948). Fishes of the Western North Atlantic: lancelets, cyclostomes, sharks. *Mem. Sears Found. Mar. Res.* 1(1):1–576.

Bigelow, H.B. and Schroeder, W.C. (1953). Fishes of the Western North Atlantic: sawfishes, guitarfishes, skates, and rays. *Mem. Sears Found. Mar. Res.* 1(2):1–588.

Binder, W.J. and Van Valkenburgh, B.V. (2000). Development of bite strength and feeding behavior in juvenile spotted hyenas (*Crocuta crocuta*). *J. Zool.* 252:273–283.

Botella, H., Valenzuela-Ríos, J.I., and Martínez-Pérez, C. (2009). Tooth replacement rates in early chondrichthyans: a qualitative approach. *Lethaia* 42(3):365–376.

Bourke, J., Wroe, S., Moreno, K., McHenry, C., and Clausen, P. (2008). Effects of gape and tooth position on bite force and skull stress in the dingo (*Canis lupus dingo*) using a 3-dimensional finite element approach. *PLoS ONE* 3:e2200.

Branstetter, S. and Stiles, R. (1987). Age and growth of the bull shark, *Carcharhinus leucas*, from the northern Gulf of Mexico. *Environ. Biol. Fish.* 20(3):169–181.

Bray, R.N. and Hixon, M.A. (1978). Night-shocker: predatory behavior of the Pacific electric ray (*Torpedo californica*). *Science* 200:333–334.

Brunnschweiler, J.M., Andrews, P.L.R., Southall, E.J., Pickering, M., and Sims, D.W. (2005). Rapid voluntary stomach eversion in a free-living shark. *J. Mar. Biol. Assoc. U.K.* 85:1141–1144.

Brunnschweiler, J.M., Nielsen, F., and Motta, P. (2011). *In situ* observation of stomach eversion in a line-caught shortfin mako (*Isurus oxyrinchus*). *Fish Res.* 109:212–216.

Budker, P. (1971). *The Life of Sharks*. Columbia University Press, New York.

Bullis, H.R. (1961). Observations on the feeding behavior of white-tip sharks on schooling fishes. *Ecology* 42:194–195.

Cappetta, H. (1986a). Myliobatidae nouveaux (Neoselachii, Batomorphii) de l'Ypresien des Ouled Abdoun, Maroc. *Geol. Palaeontol.* 20:185–207.

Cappetta, H. (1986b). Types dentaires adaptatifs chez les selaciens actuels et post-paleozoiques. *Palaeovertebrata* 16:57–76.

Cappetta, H. (1987). Chondrichthyes II: Mesozoic and Cenozoic Elasmobranchii. In: Schultze, H.P. (Ed.), *Handbook of Paleoichthyology*, Vol. 3B. Gustav Fischer Verlag, Stuttgart, 193 pp.

Carroll, A.M., Wainwright, P.C., Huskey, S.H., Collar, D.C., and Turingan, R.G. (2004). Morphology predicts suction feeding performance in centrarchid fishes. *J. Exp. Biol.* 207:3873–3881.

Carroll, R.L. (1988). *Vertebrate Paleontology and Evolution*. W.H. Freeman, New York.

Carter, D.R. and Wong, M. (2003). Modelling cartilage mechanobiology. *Phil. Trans. R. Soc. Lond. B. Biol. Sci.* 358:1461–1471.

Casey, J.G. and Pratt, Jr., H.L. (1985). Distribution of the white shark, *Carcharodon carcharias*, in the western North Atlantic. *Mem. South. Calif. Acad. Sci.* 9:2–14.

Castro, J.I. (1996). *The Sharks of North American Waters*. Texas A&M University Press, College Station.

Chapman, D.D. and Gruber, S.H. (2002). A further observation of batoid prey handling by the great hammerhead shark, *Sphyrna mokarran*, upon a spotted eagle ray, *Aetobatus narinari*. *Bull. Mar. Sci.* 70:947–952.

Chen, P., Lin, A.Y.M., Lin, Y.S., Seki, Y., Stokes, A.G., Peyras, J., Olevsky, E.A., Meyers, M.A., and McKittrick, J. (2008). Structure and mechanical properties of selected biological materials. *J. Mech. Behav. Biomed. Mater.* 1:208–226.

Cherel, Y. and Duhamel, G. (2004). Antarctic jaws: cephalopod prey of sharks in Kerguelen waters. *Deep-Sea Res. I* 50:17–31.

Christiansen, P. and Wroe, S. (2007). Bite forces and evolutionary adaptations to feeding ecology in carnivores. *Ecology* 88:347–358.

Clark, E. and Kristof, E. (1990). Deep sea elasmobranchs observed from submersibles in Grand Cayman, Bermuda and Bahamas. In: Pratt, Jr., H.L., Gruber, S.H., and Taniuchi, T. (Eds.), *Elasmobranchs as Living Resources: Advances in the Biology, Ecology, Systematics, and the Status of the Fisheries*, NOAA Tech. Rep. NMFS 90. National Oceanic and Atmospheric Administration, Washington, D.C., pp. 269–284.

Clark, E. and Nelson, D.R. (1997). Young whale sharks, *Rhincodon typus*, feeding on a copepod bloom near La Paz, Mexico. *Environ. Biol. Fish.* 50:63–73.

Clement, J.G. (1992). Re-examination of the fine structure of endoskeletal mineralization in Chondrichthyans: implications for growth, ageing, and calcium homeostasis. *Aust. J. Mar. Freshwat. Res.* 43:157–181.

Cliff, G. and Dudley, S.F.J. (1991). Sharks caught in the protective gill nets off Natal, South Africa. 4. The bull shark *Carhcarhinus leucas* Valenciennes. *S. Afr. J. Mar. Sci.* 10:253–270.

Clifton, K.B. and Motta, P.J. (1998). Feeding morphology, diet, and ecomorphological relationships among five Caribbean labrids (Teleostei, Labridae). *Copeia* 1998:953–966.

Coles, R.J. (1915). Notes on the sharks and rays of Cape Lookout, NC. *Proc. Biol. Soc. Wash.* 28:89–94.

Collins, A.B., Heupel, M.R., Hueter, R.E., and Motta, P.J. (2007). Hard prey specialists or opportunistics generalists? An examination of the diet of the Atlantic cownose ray *Rhinoptera bonasus*. *Mar. Freshwat. Res.* 58:135–144.

Colman, J.G. (1997). A review of the biology and ecology of the whale shark. *J. Fish Biol.* 51:1219–1234.

Compagno, L.J.V. (1970). Systematics of the genus *Hemitriakis* (Selachii: Carcharhinidae) and related genera. *Proc. Calif. Acad. Sci. Ser. 4* 38:63–98.

Compagno, L.J.V. (1977). Phyletic relationships of living sharks and rays. *Am. Zool.* 17:303–322.

Compagno, L.J.V. (1984). *FAO Species Catalogue.* Vol. 4. *Sharks of the World: An Annotated and Illustrated Catalogue of Shark Species Known to Date.* Part 1. *Hexanchiformes to Lamniformes.* United Nations Food and Agriculture Organization, Rome, 250 pp.

Compagno, L.J.V. (1988). *Sharks of the Order Carcharhiniformes.* Princeton University Press, Princeton, NJ.

Compagno, L.J.V. (1990). Relationships of the megamouth shark, *Megachasma pelagios* (Lamniformes: Megachasmidae), with comments on its feeding habits. In: Pratt, Jr., H.L., Gruber, S.H., and Taniuchi, T. (Eds.), *Elasmobranchs as Living Resources: Advances in the Biology, Ecology, Systematics, and the Status of the Fisheries,* NOAA Tech. Rep. NMFS 90. National Oceanic and Atmospheric Administration, Washington, D.C., pp. 357–380.

Compagno, L.J.V. (1999). Endoskeleton in sharks, skates, and rays. In: Hamlett, W.C. (Ed.), *The Biology of Elasmobranch Fishes.* The Johns Hopkins University Press, Baltimore, MD, pp. 69–92.

Compagno, L.J.V. (2001). *FAO Species Catalogue for Fishery Purposes. Sharks of the World: An Annotated and Illustrated Catalogue of Shark Species Known to Date.* Vol. 2. *Bullhead, Mackerel and Carpet Sharks (Heterodontiformes, Lamniformes, and Orectolobiformes).* United Nations Food and Agriculture Organization, Rome, 269 pp.

Compagno, L.J.V., Dando, M., and Fowler, S. (2005). *Sharks of the World.* Princeton University Press, Princeton, NJ.

Cortés, E. (1999). Standardized diet compositions and trophic levels of sharks. *ICES J. Mar. Sci.* 56:707–717.

Courtland, H., Wright, G.M., Root, R.G., and DeMont, M.E. (2003). Comparative equilibrium mechanical properties of bovine and lamprey cartilaginous tissues. *J. Exp. Biol.* 206:1397–1408.

Curio, E. (1976). *The Ethology of Predation.* Springer–Verlag, Berlin.

Currey, J. (2008). Collagen and the mechanical properties of bone and calcified cartilage. In: Fratzl, P. (Ed.), *Collagen: Structure and Mechanics.* Springer, New York, pp. 397–420.

Currey, J.D. (1980). Mechanical properties of mollusc shell. In: Vincent, J.F.V. and Currey, J.D. (Eds.), *The Mechanical Properties of Biological Materials.* Press Syndicate of the University of Cambridge, Cambridge, U.K., pp. 75–98.

Currey, J.D. (1987). The evolution of the mechanical properties of amniote bone. *J. Biomech.* 20:1035–1044.

Currey, J.D. (1998). Mechanical properties of vertebrate hard tissues. *Proc. Inst. Mech. Eng. Part H* 212:399–411.

Currey, J.D. and Abeysekera, R.M. (2003). The microhardness and fracture surface of the petrodentine of *Lepidosiren* (Dipnoi), and of other mineralized tissues. *Arch. Oral Biol.* 48:439–470.

Currey, J.D. and Butler, G. (1975). The mechanical properties of bone tissue in children. *J. Bone Joint Surg.* 57:810–814.

Curtin, N.A., Lou, F., and Woledge, R.C. (2010). Sustained performance by red and white muscle fibers from the dogfish *Scyliorhinus canicula. J. Exp. Biol.* 213:1921–1929.

Curtis, T.H., Kelly, J.T., Menard, K.L., Laroche, R.K., Jones, R.E., and Klimley, A.P. (2006). Observations on the behavior of white sharks scavenging from a whale carcass at Point Reyes, California. *Calif. Fish Game* 92:113–124.

Daniel, J.F. (1915). The anatomy of *Heterodontus francisci.* II. The endoskeleton. *J. Morphol.* 26:447–493.

Daniel, J.F. (1934). *The Elasmobranch Fishes.* University of California Press, Berkeley.

De Schepper, N., Van Wassenburgh, S., and Adriaens, D. (2008). Morphology of the jaw system in trichiurids: trade-offs between mouth closing and biting performance. *Zool. J. Linn. Soc.* 152:717–736.

Dean, M.N. and Motta, P.J. (2004a). Anatomy and functional morphology of the feeding apparatus of the lesser electric ray, *Narcine basiliensis* (Elasmobranchii: Batoidea). *J. Morphol.* 262:462–483.

Dean, M.N. and Motta, P.J. (2004b). Feeding behavior and kinematics of the lesser electric ray, *Narcine brasiliensis* (Elasmobranchii: Batoidea). *Zoology* 107:171–189.

Dean, M.N. and Summers, A.P. (2006). Mineralized cartilage in the skeleton of chondrichthyan fishes. *Zoology* 109:164–168.

Dean, M.N., Wilga, C.D., and Summers, A.P. (2005). Eating without hands or tongue: specialization, elaboration and the evolution of prey processing mechanisms in cartilaginous fishes. *Biol. Lett.* 1:357–361.

Dean, M.N., Huber, D.R., and Nance, H.A. (2006). Functional morphology of jaw trabeculation in the lesser electric ray *Narcine brasiliensis,* with comments on the evolution of structural support in the Batoidea. *J. Morphol.* 267:1137–1146.

Dean, M.N., Azizi, E., and Summers, A.P. (2007a). Uniform strain in broad muscles: active and passive effects of the twisted tendon of the ratfish, *Hydrolagus colliei. J. Exp. Biol.* 210:3395–3406.

Dean, M.N., Bizzarro, J.J., and Summers, A.P. (2007b). The evolution of cranial design, diet, and feeding mechanisms in batoids fishes. *Integr. Comp. Biol.* 47:70–81.

Dean, M.N., Ramsay, J.B., and Schaefer, J.T. (2008). Tooth reorientation affects tooth function during prey processing and tooth ontogeny in the lesser electric ray, *Narcine brasiliensis. Zoology* 111:123–134.

Dean, M.N., Mull, C.G., Gorb, S.N., and Summers, A.P. (2009a). Ontogeny of the tesselated skeleton: insight from the skeletal growth of the round stingray *Urobatis halleri. J. Anat.* 215:227–239.

Dean, M.N., Youssefpour, H., Earthman, J.C., Gorb, S.N., and Summers, A.P. (2009b). Micro-mechanics and material properties of the tesselated skeleton of cartilaginous fishes. *Integr. Comp. Biol.* 49:e45.

Dean, M.N., Swanson, B.O., and Summers, A.P. (2009c). Biomaterials: properties, variation and evolution. *Integr. Comp. Biol.* 49:15–20.

Dean, M.N., Socha, J.J., Hall, B.K., and Summers, A.P. (2010). Canaliculi in the tesselated skeleton of cartilaginous fishes. *J. Appl. Ichthyol.* 26:263–267.

DeBeer, G.R. (1932). *Vertebrate Zoology.* Macmillan, New York.

Diamond, J.M. (1985). Filter-feeding on a grand scale. *Nature* 316:679–680.

Dicken, M.L. (2008). First observations of young of the year and juvenile white sharks (*Carcharodon carcharias*) scavenging from a whale carcass. *Mar. Freshwat. Res.* 59:596–602.

Didier, D.A. (1995). Phylogenetic systematics of extant chimaeroid fishes (Holocephali, Chimaeroidei). *Am. Mus. Novit.* 3119:1–86.

Dingerkus, G., Seret, B., and Guilbert, E. (1991). Multiple prismatic calcium phosphate layers in the jaws of present-day sharks (Chondrichthyes; Selachii). *Experientia* 47:38–40.

Domeier, M.L. and Nasby-Lucas, N. (2008). Migration patterns of white sharks *Carcharodon carcharias* tagged at Guadalupe Island, Mexico, and identification of an eastern Pacific shared offshore foraging area. *Mar. Ecol. Prog. Ser.* 370:221–237.

Dudley, S.F.J., Anderson-Reade, M.D., Thompson, G.S., and McMullen, P.B. (2000). Concurrent scavenging of a whale carcass by great white sharks, *Carcharodon carcharias*, and tiger sharks, *Galeocerdo cuvier*. *Fish. Bull.* 98:646–649.

Duffin, C.J. and Cuny, G. (2008). *Carcharopsis prototypus* and the adaptations of single crystallite enameloid in cutting dentitions. *Acta Geol. Polon.* 58:181–184.

Dumont, E.R. and Herrel, A. (2003). The effect of gape angle and bite point on bite force in bats. *J. Exp. Biol.* 206:2117–2123.

Dunn, M.R., Griggs, L., Forman, J., and Horn, P. (2010). Feeding habits and niche separation among the deep-sea chimaeroid fishes *Harriotta raleighana*, *Hydrolagus bemisi*, and *Hydrolagus novaezealandiae*. *Mar. Ecol. Prog. Ser.* 407:209–225.

Eames, B.F., Allen, N., Young, J., Kaplan, A., Helms, J.A., and Schneider, R.A. (2007). Skeletogenesis in the swell shark *Cephaloscyllium ventriosum*. *J. Anat.* 210:542–554.

Ebert, D.A. (1991). Observations on the predatory behaviour of the sevengill shark *Notorynchus cepedianus*. *S. Afr. J. Mar. Sci.* 11:455–465.

Ebert, D.A., Cowley, P.D., and Compagno, L.J.V. (1991). A preliminary investigation of the feeding ecology of skates (Batoidea: Rajidae) off the West coast of southern Africa. *S. Afr. J. Mar. Sci.* 10:71–81.

Edgeworth, F.H. (1935). *Cranial Muscles of Vertebrates.* Cambridge University Press, Cambridge, U.K.

Edmonds, M.A., Motta, P.J., and Hueter, R.E. (2001). Food capture kinematics of the suction feeding horn shark *Heterodontus francisci*. *Environ. Biol. Fish.* 62:415–427.

Edwards, R.R.C. (1980). Aspects of the population dynamics and ecology of the white spotted stingray, *Urolophus paucimaculatus* Dixon, in Port Phillip Bay, Victoria. *Aust. J. Mar. Freshwat. Res.* 31:459–467.

Eibl-Eibesfeldt, I. and Hass, H. (1959). Erfahrungen mit Haien. *Z. Tierpsychol.* 16:733–746.

Ellis, J.R. and Shackley, S.E. (1995). Ontogenetic changes and sexual dimorphism in the head, mouth and teeth of the lesser spotted dogfish. *J. Fish Biol.* 47:155–164.

Erickson, G.M., Cavanese III, J.C., and Keaveny, T.M. (2002). Evolution of the biomechanical material properties of the femur. *Anat. Rec.* 268:115–124.

Erickson, G.M., Lappin, A.K., and Vliet, K.A. (2003). The ontogeny of bite-performance in American alligator (*Alligator mississippiensis*). *J. Zool.* 260:317–327.

Estrada, J.A., Rice, A.N., Natanson, L.J., and Skomal, G.B. (2006). Use of isotopic analysis of vertebrae in reconstructing ontogenetic feeding ecology in white sharks. *Ecology* 87:829–834.

Fahle, S.R. and Thomason, J.C. (2008). Measurement of jaw viscoelasticity in newborn and adult lesser spotted dogfish *Scyliorhinus canicula* (L., 1758). *J. Fish Biol.* 72:1553–1557.

Feduccia, A. and Slaughter, B.H. (1974). Sexual dimorphism in skates (Rajidae) and its possible role in differential niche utilization. *Evolution* 28:164–168.

Fergusson, I.K., Compagno, L.J.V., and Marks, M.A. (2000). Predation by white sharks *Carcharodon carcharias* (Chondrichthyes: Lamnidae) upon chelonians, with new records from the Mediterranean Sea and a first record of the ocean sunfish *Mola mola* (Osteichthyes: Molidae) as stomach contents. *Environ. Biol. Fish.* 58:447–453.

Ferrara, T.L., Clausen, P., Huber, D.R., McHenry, C.R., Peddemors, V., and Wroe, S. (2011). Mechanics of biting in great white and sandtiger sharks. *J. Biomech.* 44(3):430–435.

Ferry-Graham, L.A. (1997a). Effects of prey size and elusivity on prey capture kinematics in leopard sharks, *Triakis semifasciata*. *Am. Zool.* 37:82A.

Ferry-Graham, L.A. (1997b). Feeding kinematics of juvenile swellsharks, *Cephaloscyllium ventriosum*. *J. Exp. Biol.* 200:1255–1269.

Ferry-Graham, L.A. (1998a). Feeding kinematics of hatchling swellsharks, *Cephaloscyllium ventriosum* (Scyliorhinidae): the importance of predator size. *Mar. Biol.* 131:703–718.

Ferry-Graham, L.A. (1998b). Effects of prey size and mobility on prey-capture kinematics in leopard sharks, *Triakis semifasciata*. *J. Exp. Biol.* 201:2433–2444.

Fisher, R.A., Call, G.C., and Grubbs, R.D. (2011). Cownose ray (*Rhinoptera bonasus*) predation relative to bivalve ontogeny. *J. Shellfish Res.* 30(1):187–196.

Fouts, W.R. (1995). The Feeding Behavior and Associated Ambush Site Characteristics of the Pacific Angel Shark, *Squatina californica*, at Santa Catalina Island, California, doctoral thesis, California State University.

Fouts, W.R. and Nelson, D.R. (1999). Prey capture by the Pacific angel shark, *Squatina californica*: visually mediated strikes and ambush-site characteristics. *Copeia* 1999:304–312.

Francis, M.P. and Duffy, C. (2002). Distribution, seasonal abundance and bycatch of basking sharks (*Cetorhinus maximus*) in New Zealand, with observations on their winter habitat. *Mar. Biol.* 140:831–842.

Frazzetta, T.H. (1988). The mechanics of cutting and the form of shark teeth (Chondrichthyes, Elasmobranchii). *Zoomorphology* 108:93–107.

Frazzetta, T.H. (1994). Feeding mechanisms in sharks and other elasmobranchs. *Adv. Comp. Environ. Physiol.* 18:31–57.

Frazzetta, T.H. and Prange, C.D. (1987). Movements of cephalic components during feeding in some requiem sharks (Carcharhiniformes: Carcharhinidae). *Copeia* 1987:979–993.

Friedman, M. (2009). Ecomorphological selectivity among marine teleost fishes during the end-Cretaceous extinction. *Proc. Natl. Acad. Sci. USA* 106:5218–5223.

Funicelli, N.A. (1975). Taxonomy, Feeding, Limiting Factors and Sex Ratios of *Dasyatis sabina, Dasyatis americana, Dasyatis sayi,* and *Narcine brasiliensis,* doctoral dissertation, University of Southern Mississippi, Hattiesburg.

Gadow, H. (1888). On the modifications of the first and second visceral arches, with special reference to the homologies of the auditory ossicles. *Phil. Trans. R. Soc. Lond. B. Biol. Sci.* 179:451–485.

Gans, C. and Gaunt, A.S. (1991). Muscle architecture in relation to function. *J. Biomech.* 24:53–65.

Gerry, S.P., Ramsay, J.B., Dean, M.N., and Wilga, C.D. (2008). Evolution of asynchronous motor activity in paired muscles: effects of ecology, morphology, and phylogeny. *Integr. Comp. Biol.* 48:272–282.

Gilbert, P.W. (1962). The behavior of sharks. *Sci. Am.* 207:60–68.

Gillis, J.A. and Donoghue, C.J. (2007). The homology and phylogeny of chondrichthyan tooth enameloid. *J. Morphol.* 268:33–49.

Gohar, H.A.F. and Mazhar, F.M. (1964). The internal anatomy of Selachii from the north western Red Sea. *Publ. Mar. Biol. Stn. Ghardaqa, Red Sea* 13:145–240.

Goitein, R.F., Torres, S., and Signorini, C.E. (1998). Morphological aspects related to feeding of two marine skates *Narcine brasiliensis* and *Rhinobatos horkelli* Muller and Henle. *Acta Sci.* 20:165–169.

Gonzalez-Isais, M. (2003). Anatomical comparison of the cephalic musculature of some members of the superfamily Myliobatoidea (Chondrichthyes): implications for evolutionary understanding. *Anat. Rec.* 271A:259–272.

Goo, B.Y., Dean, M.N., Huber, D.R., and Summers, A.P. (2010). Jaw morphology and structure in lamniform sharks. *Integr. Comp. Biol.* 50:e234.

Goodey, T. (1910). A contribution to the skeletal anatomy of the frilled shark, *Chlamydoselachus anguineus* (Gar.). *Proc. Zool. Soc. Lond.* 2:540–571.

Goto, T. (2001). Comparative anatomy, phylogeny, and cladistic classification of the order Orectolobiformes (Chondrichthyes, Elasmobranchii). *Mem. Grad. Sch. Fish. Sci. Hokkaido Univ.* 48:1–100.

Gray, A.E., Mulligan, T.J., and Hannah, R.W. (1997). Food habits, occurrence, and population structure of the bat ray, *Myliobatis californica,* in Humboldt Bay, California. *Environ. Biol. Fish.* 49:227–238.

Gregory, M.R., Balance, P.F., Gibson, G.W., and Ayling, A.M. (1979). On how some rays (Elasmobranchia) excavate feeding depressions by jetting water. *J. Sed. Petrol.* 49:1125–1130.

Grogan, E.D. and Lund, R. (2000). *Debeerius ellefseni* (fam. nov., gen. nov., spec. nov.), an autodiastylic chondrichthyan from the Mississippian Bear Gulch Limestone of Montana (USA), the relationships of the Chondrichthyes, and comments on gnathostome evolution. *J. Morphol.* 243:219–245.

Grogan, E.D. and Lund, R. (2004). The origin and relationships of early Chondrichthyes. In: Carrier, J.C., Musick, J.A., and Heithaus, M.R. (Eds.), *Biology of Sharks and Their Relatives.* CRC Press, Boca Raton, FL, pp. 3–31.

Grogan, E.D., Lund, R., and Didier, D. (1999). Description of the chimaerid jaw and its phylogenetic origins. *J. Morphol.* 239:45–59.

Gudger, E.W. (1907). A note on the hammerhead shark (*Sphyrna zygaena*) and its food. *Science* 25:1005.

Gudger, E.W. (1941a). The food and feeding habits of the whale shark *Rhineodon typus. J. Elisha Mitchell Sci. Soc.* 57:57–72.

Gudger, E.W. (1941b). The feeding organs of the whale shark, *Rhineodon typus. J. Morphol.* 68:81–99.

Gunn, J.S., Stevens, J.D., Davis, T.L.O., and Norman, B.M. (1999). Observations on the short-term movements and behaviour of whale sharks (*Rhincodon typus*) at Ningaloo Reef, Western Australia. *Mar. Biol.* 135:553–559.

Habegger, M.L., Motta, P.J., Huber, D.R., and Dean, M.N. (In review). Feeding biomechanics in bull sharks (*Carcharhinus leucas*) during ontogeny. *Zoology.*

Habelitz, S., Marshall, S.J., Marshall, Jr., G.W., and Balooch, M. (2001). Mechanical properties of human dental enamel on the nanometre scale. *Arch. Oral Biol.* 46:173–83.

Heemstra, P.C. and Smith, M.M. (1980). Hexatrygonidae, a new family of stingrays (Myliobatiformes: Batoidae) from South Africa, with comments on the classification of batoid fishes. *Ichthyol. Bull. J.L.B. Smith Inst. Ichthyol.* 43:1–17.

Heithaus, M.R. (2001). The biology of tiger sharks, *Galeocerdo cuvier,* in Shark Bay, Western Australia: sex ratio, size distribution, diet, and seasonal changes in catch rates. *Environ. Biol. Fish.* 61:25–36.

Heithaus, M.R., Marshall, G.J., Buhleier, B., and Dill, L.M. (2001). Employing CritterCam to study habitat use and behavior of large sharks. *Mar. Ecol. Prog. Ser.* 209:307–310.

Heithaus, M.R., Dill, L.M., Marshall, G.J., and Buhleier, B. (2002a). Habitat use and foraging behavior of tiger sharks (*Galeocerdo cuvier*) in a seagrass ecosystem. *Mar. Biol.* 140:237–248.

Heithaus, M.R., Frid, A., and Dill, L.M. (2002b). Shark-inflicted injury frequencies, escape ability, and habitat use of green and loggerhead turtles. *Mar. Biol.* 140:229–236.

Henderson, A.C., Flannery, K., and Dunne, J. (2001). Observations on the biology and ecology of the blue shark in the North-East Atlantic. *J. Fish Biol.* 58:1347–1358.

Herman, J., Hovestadt-Euler, M., Hovestadt, D.C., and Stehmann, M. (1995). Contributions to the study of the comparative morphology of teeth and other relevant ichthyodorulites in living supra-specific taxa of Chondrichthyan fishes. *Biologie* 65:237–307.

Hernandez, L.P. and Morgan, R.J. (2009). Size and distribution of muscle fiber types within chondrichthyan muscles. *Integr. Comp. Biol.* 49:E242.

Hernandez, L.P. and Motta, P.J. (1997). Trophic consequences of differential performance: ontogeny of oral jaw-crushing performance in the sheepshead, *Archosargus probatocephalus* (Teleostei, Sparidae). *J. Zool.* 243:737–756.

Herrel, A. and Gibb, A.C. (2006). Ontogeny of performance in vertebrates. *Physiol. Biochem. Zool.* 79:1–6.

Herrel, A. and O'Reilly, J.C. (2006). Ontogenetic scaling of bite force in lizards and turtles. *Physiol. Biochem. Zool.* 79:31–42.

Herrel, A., Spithoven, L., Van Damme, R., and De Vree, F. (1999). Sexual dimorphism of head size in *Gallotia galloti*: testing the niche divergence hypothesis by functional analyses. *Func. Ecol.* 13:289–297.

Herrel, A., Grauw, E., and Lemos-Espinal, J.A. (2001a). Head shape and bite performance in xenosaurid lizards. *J. Exp. Zool.* 290:101–107.

Herrel, A., Van Damme, R., Vanhooydonck, B., and De Vree, F. (2001b). The implications of bite force for diet in two species of lacertid lizards. *Can. J. Zool.* 79:662–670.

Herrel, A., O'Reilly, J.C., and Richmond, A.M. (2002). Evolution of bite performance in turtles. *J. Evol. Biol.* 15:1083–1094.

Herrel, A., Vanhooydonck, B., and Van Damme, R. (2004). Omnivory in lacertid lizards: adaptive evolution or constraint. *J. Evol. Biol.* 17:974–984.

Herrel, A., Podos, J., Huber, S.K., and Hendry, A.P. (2005). Evolution of bite force in Darwin's finches: a key role for head width. *J. Evol. Biol.* 18:669–675.

Hess, P.W. (1961). Food habits of two dasyatid rays in Delaware Bay. *Copeia* 1961:239–241.

Heupel, M.R. and Bennett, M.B. (1998). Observations on the diet and feeding habits of the epaulette shark, *Hemiscyllium ocellatum*, on Heron Island Reef, Great Barrier Reef. *Aust. Mar. Freshwat. Res.* 49:753–756.

Heyman, W.D., Graham, R.T., Kjerfve, B., and Johannes, R.E. (2001). Whale sharks *Rhincodon typus* aggregate to feed on fish spawn in Belize. *Mar. Ecol. Prog. Ser.* 215:275–282.

Hines, A.H., Whitlatch, R.B., Thrush, S.F., Hewitt, J.E., Cummings, V.J., Dayton, P.K., and Legendre, P. (1997). Nonlinear foraging response of a large marine predator to benthic prey: eagle ray pits and bivalves in a New Zealand sandflat. *J. Exp. Mar. Biol. Ecol.* 216:191–210.

Hobson, E.S. (1963). Feeding behavior in three species of sharks. *Pac. Sci.* 17:171–194.

Hoffmayer, E.R., Franks, J.S., Driggers III, W.B., Oswald, K.J., and Quattro, J.M. (2007). Observations of a feeding aggregation of whale sharks, *Rhincodon typus*, in the north central Gulf of Mexico. *Gulf Caribb. Res.* 19:1–5.

Hoh, J.F.Y. (2002). 'Superfast' or masticatory myosin and the evolution of jaw-closing muscles of vertebrates. *J. Exp. Biol.* 205:2203–2210.

Holden, M.J. and Tucker, R.N. (1974). The food of *Raja clavata* Linnaeus 1758, *Raja montagui* Fowler 1910, *Raja naevus* Muller and Henle 1841 and *Raja brachyura* Lafont 1873 in British waters. *J. Cons. Int. Explor. Mer.* 35:189–193.

Holland, K.N., Wetherbee, B.M., Lowe, C.G., and Meyer, C.G. (1999). Movements of tiger sharks (*Galeocerdo cuvier*) in coastal Hawaiian waters. *Mar. Biol.* 134:665–673.

Hotton III, N. (1952). Jaws and teeth of American xenacanth sharks. *J. Paleontol.* 26:489–500.

Howard, J.D., Mayou, T.V., and Heard, R.W. (1977). Biogenic sedimentary structures formed by rays. *J. Sed. Petrol.* 47:339–346.

Hubbell, G. (1996). Using tooth structure to determine the evolutionary history of the white shark. In: Klimley, A.P. and Ainley, D.G. (Eds.), *Great White Sharks: The Biology of Carcharodon carcharias*. Academic Press, New York, pp. 9–18.

Huber, D.R. (2006). Cranial Biomechanics and Feeding Performance in Sharks, doctoral dissertation, University of South Florida, Tampa.

Huber, D.R. and Motta, P.J. (2004). Comparative analysis of methods for determining bite force in the spiny dogfish *Squalus acanthias*. *J. Exp. Zool.* 301A:26–37.

Huber, D.R., Eason, T.G., Hueter, R.E., and Motta, P.J. (2005). Analysis of the bite force and mechanical design of the feeding mechanism of the durophagous horn shark *Heterodontus francisci*. *J. Exp. Biol.* 208:3553–3571.

Huber, D.R., Weggelaar, C.L., and Motta, P.J. (2006). Scaling of bite force in the blacktip shark *Carcharhinus limbatus*. *Zoology* 109:109–119.

Huber, D.R., Dean, M.N., and Summers, A.P. (2008). Hard prey, soft jaws, and the ontogeny of feeding biomechanics in the spotted ratfish *Hydrolagus colliei*. *J. Roy. Soc. Interface* 5:941–952.

Huber, D.R., Claes, J.M., Mallefet, J., and Herrel, A. (2009). Is extreme bite performance associated with extreme morphologies in sharks? *Physiol. Biochem. Zool.* 82:20–28.

Hudson, N.J., Bennett, M.B., and Franklin, C.E. (2004). Effect of aestivation on long bone mechanical properties in the green-striped burrowing frog, *Cyclorana alboguttata*. *J. Exp. Biol.* 207:475–482.

Hueter, R.E., Tyminski, J.P., and de la Parra, R. (2008). The geographic movements of whale sharks tagged with pop-up archival tags off Quintana Roo, Mexico. In: *Proceedings of the Second International Whale Shark Conference*, Holbox, Quintana Roo, Mexico, July 15–20.

Husak, J.F., Lappin, A.K., Fox, S.F., and Lemos-Espinal, J.A. (2006). Bite-force performance predicts dominance in male venerable collared lizards (*Crotaphytus antiquus*). *Copeia* 2006:301–306.

Huxley, T.H. (1876). Contributions to morphology. Ichthyopsida No 1. On *Ceratodus forsteri*, with observations on the classification of fishes. *Proc. Zool. Soc. Lond.* 1876:24–59.

Jagnandan, K. and Huber, D. (2010). Structural and material properties of the jaws of the lemon shark *Negaprion brevirostris* and horn shark *Heterodontus francisci*. *Fla. Sci.* 73:38.

James, W.W. (1953). The succession of teeth in elasmobranchs. *Proc. Zool. Soc. Lond.* 123:419–475.

Jones, E.C. (1971). *Isitius brasiliensis*, a squaloid shark, the probable cause of crater wounds on fishes and cetaceans. *U.S. Fish. Bull.* 69:791–798.

Kajiura, S.M. and Tricas, T.C. (1996). Seasonal dynamics of dental sexual dimorphism in the Atlantic stingray, *Dasyatis sabina*. *J. Exp. Biol.* 199:2297–2306.

Kemp, N.S. and Westrin, S.K. (1979). Ultrastructure of calcified cartilage in the endoskeletal tesserae of sharks. *J. Morphol.* 160:75–102.

Kemp, T.J., Bachus, K.N., Nairn, J.A., and Carrier, D.R. (2005). Functional trade-offs in the limb bones of dogs selected for running versus fighting. *J. Exp. Biol.* 208:3475–3482.

Kittiphattanabawon, P., Benjakul, S., Visessanguan, W., and Shahidi, F. (2010). Isolation and characterization of collagen from the cartilages of brownbanded bamboo shark (*Chiloscyllium punctatum*) and blacktip shark (*Carcharhinus limbatus*). *LWT Food Sci. Technol.* 43:792–800.

Klimley, P.A. (1994). The predatory behavior of the white shark. *Am. Sci.* 82:122–133.

Klimley, P.A., Pyle, P., and Anderson, S.D. (1996). The behavior of white sharks and their pinniped prey during predatory attacks. In: Klimley, A.P. and Ainley, D.G. (Eds.), *Great White Sharks: The Biology of Carcharodon carcharias.* Academic Press, New York, pp. 175–191.

Klimley, P.A., Leboeuf, B.J., Cantara, K.M., Richert, J.E., Davis, S.F., Van Sommeran, S., and Kelly, J.T. (2001). The hunting strategy of white sharks (*Carcharodon carcharias*) near a seal colony. *Mar. Biol.* 138:617–636.

Kolmann, M.A. and Huber, D.R. (2009). Scaling of feeding biomechanics in the horn shark *Heterodontus francisci*: ontogenetic constraints on durophagy. *Zoology* 112:351–361.

Kyne, P.M. and Simpfendorfer, C. (2010). Deepwater chondrichthyans. In: Carrier, J.C. et al. (Eds.), *Sharks and Their Relatives II: Biodiversity, Adaptive Physiology, and Conservation.* CRC Press, Boca Raton, FL, pp. 37–113.

Laasanen, M.S., Saarakkala, S., and Toyras, J. (2003). Ultrasound indentation of bovine knee articular cartilage *in situ. J. Biomech.* 36:1259–1267.

Lappin, A.K. and Husak, J.F. (2005). Weapon performance, not size, determines mating success and potential reproductive output in the collared lizard (*Crotaphytus collaris*). *Am. Nat.* 166:426–436.

Lauder, G.V. (1980). The suction feeding mechanism in sunfishes (*Lepomis*): an experimental analysis. *J. Exp. Biol.* 88:49–72.

Lauder, G.V. (1985). Aquatic feeding in lower vertebrates. In: Hildebrand, M., Bramble, D.M., Liem, K.F., and Wake, D.B. (Eds.), *Functional Vertebrate Morphology.* Belknap Press, Cambridge, MA, pp. 210–229.

LeBoeuf, B.J., McCosker, J.E., and Hewitt, J. (1987). Crater wounds on northern elephant seals: the cookiecutter shark strikes again. *U.S. Fish. Bull.* 85:387–392.

Liem, K.F. (1978). Modulatory multiplicity in the functional repertoire of the feeding mechanisms in cichlid fishes. *J. Morphol.* 158:323–360.

Liem, K.F. (1993). Ecomorphology of the teleostean skull. In: Hanken, J. and Hall, B.K. (Eds.), *The Skull: Functional and Evolutionary Mechanisms*, Vol. 3. University of Chicago Press, Chicago, pp. 422–452.

Liem, K.F. and Summers, A.P. (1999). Muscular system: gross anatomy and functional morphology of muscles. In: Hamlett, W.C. (Ed.), *Sharks, Skates, and Rays: The Biology of Elasmobranch Fishes.* The Johns Hopkins Press, Baltimore, MD, pp. 93–114.

Liem, K.F., Bemis, W.E., Walker, Jr., W.F., and Grande, L. (2001). *Functional Anatomy of the Vertebrates: An Evolutionary Perspective.* Harcourt, New York.

Lightoller, G.H.S. (1939). Probable homologues: a study of the comparative anatomy of the mandibular and hyoid arches and their musculature. Part I. Comparative morphology. *Trans. Zool. Soc. Lond.* 24:349–444.

Long, D.J. and Jones, R.E. (1996). White shark predation and scavenging on cetaceans in the eastern North Pacific Ocean. In: Klimley, A.P. and Ainley, D.G. (Eds.), *Great White Sharks: The Biology of Carcharodon carcharias.* Academic Press, New York, pp. 293–307.

Long, J.A. (1995). *The Rise of Fishes.* The Johns Hopkins University Press, Baltimore, MD.

Lou, F., Curtin, N.A., and Woledge, R.C. (2002). Isometric and isovelocity contractile performance of red muscle fibers from the dogfish *Scyliorhinus canicula. J. Exp. Biol.* 205:1585–1595.

Lowe, C.G. (1991). The *in situ* Feeding Behavior and Associated Electric Organ Discharge of the Pacific Electric Ray, *Torpedo californica*, master's thesis, The California State University, Long Beach.

Lowe, C.G., Bray, R.N., and Nelson, D.R. (1994). Feeding and associated electrical behavior of the Pacific electric ray *Torpedo californica* in the field. *Mar. Biol.* 120:161–169.

Lowe, C.G., Wetherbee, B.M., Crow, G.L., and Tester, A.L. (1996). Ontogenetic dietary shifts and feeding behavior of the tiger shark, *Galeocerdo cuvier*, in Hawaiian waters. *Environ. Biol. Fish.* 47:203–211.

Lowe, C.G., Wetherbee, B.M., Holland, K.N., and Meyer, C.G. (2003). Movement patterns of tiger and Galapagos sharks around French Frigate Shoals, Hawaii. In *Abstracts of the American Society of Ichthyologists and Herpetologists Joint Meeting*, Manaus, Brazil, June 26–July 1.

Lowry, D. and Motta, P.J. (2007). Ontogeny of feeding behavior and cranial morphology in the whitespotted bamboo shark *Chiloscyllium plagiosum. Mar. Biol.* 151:2013–2023.

Lowry, D. and Motta, P.J. (2008). Relative importance of growth and behavior to elasmobranch suction-feeding performance over early ontogeny. *J. Roy. Soc. Interface* 5:641–652.

Lowry, D., Motta, P.J., and Hueter, R.E. (2007). The ontogeny of feeding behavior and cranial morphology in the leopard shark *Triakis semifasciata* (Girard 1854): a longitudinal perspective. *J. Exp. Mar. Biol. Ecol.* 341:153–167.

Lucifora, L.O., Valero, J.L., Bremec, C.S., and Lasta, M.L. (2000). Feeding habits and prey selection by the skate *Dipterus chilensis* (Elasmobranchii: Rijidae) from the South-Western Atlantic. *J. Mar. Biol. Assoc. U.K.* 80:953–954.

Lucifora, L.O., Menni, R.C., and Escalante, A.H. (2001). Analysis of dental insertion angles in the sand tiger shark, *Carcharias taurus* (Chondrichthyes: Lamniformes). *Cybium* 25:23–31.

Luer, C.A., Blum, P.C., and Gilbert, P.W. (1990). Rate of tooth replacement in the nurse shark, *Ginglymostoma cirratum. Copeia* 1990:182–191.

Lund, R. and Grogan, E.D. (1997). Relationships of the Chimaeriformes and the basal radiation of the Chondrichthyes. *Rev. Fish Biol. Fisher.* 7:65–123.

Luther, A. (1909). Untersuchungen über die vom n. trigeminus innervierte Muskulatur der Selachier (Haie und Rochen) unter Berücksichtigung ihrer Beziehungen zu benachbarten Organen. *Acta Soc. Sci. Fenn.* 36:1–176.

Maas, H., Baan, G.C., and Huijing, P.A. (2004). Muscle force is determined by muscle position relative position: isolated effects. *J. Biomech.* 37:99–110.

MacPherson, E. (1980). Food and feeding of *Chimaera monstrosa*, Linnaeus, 1758, in the western Mediterranean. *ICES J. Mar. Sci.* 39:26–29.

Mahoney, E., Holt, A., Swain, M., and Kikpatrick, N. (2000). The hardness and modulus of elasticity of primary molar teeth: an ultra-micro-indentation study. *J. Dent.* 28:589–594.

Maisey, J.G. (1980). An evaluation of jaw suspension in sharks. *Am. Mus. Novit.* 2706:1–17.

Maisey, J.G. (2008). The postorbital palatoquadrate articulation in elasmobranchs. *J. Morphol.* 269:1022–1040.

Maisey, J.G. and de Carvalho, M.R. (1997). A new look at old sharks. *Nature* 385:779–780.

Mallat, J. (1996). Ventilation and the origin of jawed vertebrates: a new mouth. *Zool. J. Linn. Soc.* 117:329–404.

Mara, K.R. (2010). Evolution of the Hammerhead Cephalofoil: Shape Change, Space Utilization, and Feeding Biomechanics in Hammerhead Sharks (Sphyrnidae), doctoral dissertation, University of South Florida, Tampa.

Mara, K.R., Motta, P.J., and Huber, D.R. (2010). Bite force and performance in the durophagous bonnethead shark *Sphyrna tiburo*. *J. Exp. Zool.* 313A:95–105.

Marinelli, W. and Strenger, A. (1959). *Vergleichende Anatomie und Morphologie der Wirbeltiere. III. Lieferung (Squalus acanthias)*. Franz Deuticke, Vienna.

Marion, G.E. (1905). Mandibular and pharyngeal muscles of acanthias and raia. *Tufts Coll. Stud.* 2:1–34.

Markaida, U. and Sosa-Nishizaki, O. (2010). Food and feeding habits of the blue shark *Prionace glauca* caught off Ensenada, Baja California, Mexico, with a review on its feeding. *J. Mar. Biol. Assoc. U.K.* 90:977–994.

Märkel, V.K. and Laubier, L. (1969). Zum Zahnerzatz bei Elasmobranchiern. *Zool. Beiträge* 15:41–44.

Martin, R.A. and Naylor, G.J.P. (1997). Independent origins of filter-feeding in megamouth and basking sharks (order Lamniformes) inferred from phylogenetic analysis of cytochrome *b* gene sequences. In: Yano, K., Morrissey, J.F., Yabumoto, Y., and Nakaya, K. (Eds.), *Biology of Megamouth Shark*. Tokai University Press, Tokyo, pp. 39–50.

Martin, R.A., Hammerschlag, N., Collier, R.S., and Fallows, C. (2005). Predatory behavior of white sharks (*Carcharodon carcharias*) at Seal Island, South Africa. *J. Mar. Biol. Assoc. U.K.* 85:1121–1135.

Maschner, Jr., R.P. (2000). Studies of the Tooth Strength of the Atlantic Cow-Nose Ray, *Rhinoptera bonasus*, master's thesis, California State Polytechnic University, Pomona.

Matott, M.P., Motta, P.J., and Hueter, R.E. (2005). Modulation in feeding kinematics and motor pattern of the nurse shark *Ginglymostoma cirratum*. *Environ. Biol. Fish.* 74:163–174.

Matthews, L.H. and Parker, H.W. (1950). Notes on the anatomy and biology of the basking shark *Cetorhinus maximus* (Gunner). *Proc. Zool. Soc. Lond.* 120:535–576.

Mauchline, J. and Gordon, J.D.M. (1983). Diets of the sharks and chimaeroids of the Rockall Trough, northeastern Atlantic Ocean. *Mar. Biol.* 75:269–278.

McCosker, J.E. (1985). White shark attack behavior: observations of and speculations about predator and prey strategies. *Mem. South. Calif. Acad. Sci.* 9:123–135.

McCourt, R.M. and Kerstitch, A.N. (1980). Mating behavior and sexual dimorphism in dentition in the stingray *Urolophus concentricus* from the Gulf of California. *Copeia* 1980:900–901.

McEachran, J.D. (1977). Reply to "sexual dimorphism in skates (Rajidae)." *Evolution* 31:218–220.

McEachran, J.D., Dunn, K.A., and Miyake, T. (1996). Interrelationships of the batoid fishes (Chondrichthyes: Batoidea). In: Johnson, G.D. (Ed.), *Interrelationships of Fishes*. Academic Press, New York, pp. 63–84.

McLaughlin, R.H. and O'Gower, A.K. (1971). Life history and underwater studies of a heterodont shark. *Ecol. Monogr.* 41:271–289.

Meyers, J.J., Herrel, A., and Birch, J. (2002). Scaling of morphology, bite force and feeding kinematics in an iguanian and scleroglossan lizard. In: Aerts, P., D'Aout, K., Herrel, A., and Van Damme, R. (Eds.), *Topics in Functional and Ecological Vertebrate Morphology*. Shaker Publishing, The Netherlands, pp. 47–62.

Meyers, M.A., Chen, P., Lin, A.Y., and Seki, Y. (2008). Biological materials: structure and mechanical properties. *Prog. Mater. Sci.* 53:1–206.

Michaelson, D.M., Sternberg, D., and Fishelson, L. (1979). Observations on feeding, growth and electric discharge of newborn *Torpedo ocellata* (Chondrichthyes, Batoidei). *J. Fish Biol.* 15:159–163.

Miyake, T. and McEachran, J.D. (1991). The morphology and evolution of the ventral gill arch skeleton in batoid fishes (Chondrichthyes: Batoidea). *Zool. J. Linn. Soc.* 102:75–100.

Miyake, T., McEachran, J.D., and Hall, B.K. (1992). Edgeworth's legacy of cranial muscle development with an analysis of muscles in the ventral gill arch region of batoid fishes (Chondrichthyes: Batoidea). *J. Morphol.* 212:213–256.

Morrissey, J.F. (1991). Home range of juvenile lemon sharks. In: Gruber, S.H. (Ed.), *Discovering Sharks*. American Littoral Society, Highlands, NJ, pp. 85–86.

Moss, M.L. (1977a). Skeletal tissues in sharks. *Am. Zool.* 17:335–342.

Moss, S.A. (1965). The Feeding Mechanisms of Three Sharks: *Galeocerdo cuvieri* (Peron & LeSueur), *Negaprion brevirostris* (Poey), and *Ginglymostoma cirratum* (Bonnaterre), doctoral dissertation, Cornell University, Ithaca, NY.

Moss, S.A. (1967). Tooth replacement in the lemon shark, *Negaprion brevirostris*. In: Gilbert, P.W., Mathewson, R.F., and Rall, D.P. (Eds.), *Sharks, Skates and Rays*. The Johns Hopkins University Press, Baltimore, MD, pp. 319–329.

Moss, S.A. (1972). The feeding mechanism of sharks of the family Carcharhinidae. *J. Zool. Lond.* 167:423–436.

Moss, S.A. (1977b). Feeding mechanisms in sharks. *Am. Zool.* 17:355–364.

Motta, P.J. (2004). Prey capture behavior and feeding mechanics of elasmobranchs. In: Carrier, J.C., Musick, J.A., and Heithaus, M.R. (Eds.), *Biology of Sharks and Their Relatives*. CRC Press, Boca Raton, FL, pp. 165–202.

Motta, P.J. and Wilga, C.D. (1995). Anatomy of the feeding apparatus of the lemon shark, *Negaprion brevirostris*. *J. Morphol.* 226:309–329.

Motta, P.J. and Wilga, C.D. (1999). Anatomy of the feeding apparatus of the nurse shark, *Ginglymostoma cirratum*. *J. Morphol.* 241:1–29.

Motta, P.J. and Wilga, C.D. (2001). Advances in the study of feeding behaviors, mechanisms, and mechanics of sharks. *Environ. Biol. Fish.* 60:131–156.

Motta, P.J., Hueter, R.E., and Tricas, T.C. (1991). An electromyographic analysis of the biting mechanism of the lemon shark, *Negaprion brevirostris*: functional and evolutionary implications. *J. Morphol.* 201:55–69.

Motta, P.J., Hueter, R.E., Tricas, T.C., and Summers, A.P. (1997). Feeding mechanism and functional morphology of the jaws of the lemon shark, *Negaprion brevirostris* (Chondrichthyes, Carcharhinidae). *J. Exp. Biol.* 200:2765–2780.

Motta, P.J., Hueter, R.E., Tricas, T.C., and Summers, A.P. (2002). Kinematic analysis of suction feeding in the nurse shark, *Ginglymostoma cirratum* (Orectolobiformes, Ginglymostomatidae). *Copeia* 2002:24–38.

Motta, P.J., Hueter, R.E., Tricas, T.C., Summers, A.P., Huber, D.R., Lowry, D., Mara, K.R., Matott, M.P., Whitenack, L.B., and Wintzer, A.P. (2008). Functional morphology of the feeding apparatus, feeding constraints, and suction performance in the nurse shark *Ginglymostoma cirratum*. *J. Morphol.* 269:1041–1055.

Motta, P.J., Maslanka, M., Hueter, R.E., Davis, R.L., de la Parra, R., Mulvany, S.L., Habegger, M.L., Strother, J.A., Mara, K.R., Gardiner, J.M., Tyminski, J.P., and Zeigler, L.D. (2010). Feeding anatomy, filter-feeding rate, and diet of whale sharks *Rhincodon typus* during surface ram filter feeding off the Yucatan Peninsula, Mexico. *Zoology* 113:199–212.

Moy-Thomas, J.A. and Miles, R.S. (1971). *Paleozoic Fishes*. Chapman & Hall, London.

Muller, M., Osse, J.W.M., and Verhagen, J.H.G. (1982). A quantitative hydrodynamic model of suction feeding in fish. *J. Theor. Biol.* 95:49–79.

Muto, E.Y., Soares, L.S.H., and Goitein, R. (2001). Food resource utilization of the skates *Rioraja agassizii* (Muller and Henle, 1841) and *Psammobatis extenta* (Garman, 1913) on the continental shelf off Ubatuba, south-eastern Brazil. *Rev. Brasil Biol.* 61:217–238.

Myrberg, Jr., A.A. (1991). Distinctive markings of sharks: ethological considerations of visual function. *J. Exp. Zool.* 5:156–166.

Nakaya, K. (1975). Taxonomy, comparative anatomy and phylogeny of Japanese catsharks, Scyliorhinidae. *Mem. Fac. Fish. Hokkaido Univ.* 23:1–94.

Nakaya, K., Matsumoto, R., and Suda, K. (2008). Feeding strategy of the megamouth shark *Megachasma pelagios* (Lamniformes: Megachasmidae). *J. Fish Biol.* 73:17–34.

Nauwelaerts, S., Wilga, C., Sanford, C., and Lauder, G. (2007). Hydrodynamics of pray capture in sharks: effects of substrate. *J. Roy. Soc. Interface* 4:341–345.

Nauwelaerts, S., Wilga, C.D., Lauder, G.V., and Sanford, C.P. (2008). Fluid dynamics of feeding behavior in whitespotted bamboo sharks. *J. Exp. Biol.* 211:3095–3102.

Neiva, J., Coelho, R., and Erzini, K. (2006). Feeding habits of the velvet belly lanternshark *Etmopterus spinax* (Chondrichthyes: Etmopteridae) off the Algarve, southern Portugal. *J. Mar. Biol. Assoc. U.K.* 86:835–841.

Nelson, D.R. (1969). The silent savages. *Oceans* 1:8–22.

Nelson, J.D. and Eckert, S.A. (2007). Foraging ecology of whale sharks (*Rhincodon typus*) within Bahia de Los Angeles, Baja California Norte, Mexico. *Fish. Res.* 84:47–64.

Nelson, J.S. (1994). *Fishes of the World*. John Wiley & Sons, New York.

Nobiling, G. (1977). Die Biomechanik des Kiefferapparates beim Stierkopfhai (*Heterodontus portusjacksoni* = *Heterodontus philippi*). *Adv. Anat. Embryol. Cell Biol.* 52:1–52.

Nordell, S.E. (1994). Observations of the mating behavior and dentition of the round stingray, *Urolophus halleri*. *Environ. Biol. Fish.* 39:219–229.

Norton, S.F. and Brainerd, E.L. (1993). Convergence in the feeding mechanics of ecomorphologically similar species in the Centrarchidae and Cichlidae. *J. Exp. Biol.* 176:11–29.

Notarbartolo di Sciara, G. and Hillyer, E.V. (1989). Mobulid rays off Eastern Venezuela. *Copeia* 1989:607–614.

Orth, R.J. (1975). Destruction of eelgrass, *Zostera marina*, by the cownose ray, *Rhinoptera bonasus*, in the Chesapeake Bay. *Chesapeake Sci.* 16:205–208.

Orvig, T. (1951). Histologic studies of placoderm and fossil elasmobranchs. I. The endoskeleton, with remarks on the hard tissues of lower vertebrates in general. *Arkiv. Zool.* 2:321–454.

Papastamatiou, Y.P., Wetherbee, B.M., O'Sullivan, J., Goodmanlowe, G.D., and Lowe, C.G. (2010). Foraging ecology of cookiecutter sharks (*Isistius brasiliensis*) on pelagic fishes in Hawaii, inferred from prey bite wounds. *Environ. Biol. Fish.* 88(4):361–368.

Parker, H.W. and Boeseman, M. (1954). The basking shark (*Cetorhinus maximus*) in winter. *Proc. Zool. Soc. Lond.* 124:185–194.

Peterson, C.H., Fodrie, F.J., Summerson, H.C., and Powers, S.P. (2001). Site-specific and density-dependent extinction of prey by schooling rays: generation of a population sink in top-quality habitat for bay scallops. *Oecologia* 129:349–356.

Peyer, B. (1968). *Comparative Odontology*. University of Chicago Press, Chicago.

Pfeil, F.H. (1983). Zahmorphologische Untersuchungen an rezenten und fossilen Haien der Ordnungen Chlamydoselachiformes und Echinorhiniformes. *Palaeoichthyologica* 1:1–135.

Porter, M.E., Beltran, J.L., Koob, T.J., and Summers, A.P. (2006). Material properties and biochemical composition of mineralized vertebral cartilage in seven elasmobranch species (Chondrichthyes). *J. Exp. Biol.* 209:2920–2928.

Powell, P.L., Roy, R.R., Kanim, P., Bello, M.A., and Edgerton, V.R. (1984). Predictability of skeletal muscle tension from architectural determinations in guinea pigs. *J. Appl. Physiol.* 57:1715–1721.

Powlik, J.J. (1995). On the geometry and mechanics of tooth position in the white shark, *Carcharodon carcharias*. *J. Morphol.* 226:277–288.

Powter, D.M., Gladstone, W., and Platell, M. (2010). The influence of sex and maturity on the diet, mouth morphology and dentition of the Port Jackson shark, *Heterodontus portusjacksoni*. *Mar. Freshwat. Res.* 61:74–85.

Pratt, Jr., H.L., Casey, J.G., and Conklin, R.B. (1982). Observations on large white shark, *Carcharodon, carcharias*, off Long Island, New York. *U.S. Fish. Bull.* 80:153–156.

Preuschoft, H., Reif, W.E., and Muller, W.H. (1974). Funktionsanpassungen in form und struktur an haifischzahnen. *Z. Anat. Entwickl.-Gesch.* 143:315–344.

Pyle, P., Klimley, A.P., Anderson, S.D., and Henderson, R.P. (1996). Environmental factors affecting the occurrence and behavior of white sharks at the Farrallon Islands, California. In: Klimley, A.P. and Ainley, D.G. (Eds.), *Great White Sharks: The Biology of Carcharodon carcharias*. Academic Press, New York, pp. 281–291.

Qin, H., Hsu, M.K.H., Morris, B.J., and Hoh, J.F.Y. (2002). A distinct subclass of mammalian striated myosins: structure and molecular evolution of "superfast" or masticatory myosin heavy chain. *J. Mol. Evol.* 55:544–552.

Rama, S. and Chandrakasan, G. (1984). Distribution of different molecular species of collagen in the vertebral cartilage of shark (*Carcharhinus acutus*). *Connect. Tissue Res.* 12:111–118.

Ramsay, J.B. and Wilga, C.D. (2007). Morphology and mechanics of the teeth and jaws of white-spotted bamboo sharks (*Chiloscyllium plagiosum*). *J. Morphol.* 268:664–682.

Randall, J.E. (1992). Review of the biology of the tiger shark (*Galeocerdo cuvier*). *Aust. J. Mar. Freshwat. Res.* 43:21–31.

Rath, N.C., Balog, J.M., Huff, W.E., Huff, G.R., Kulkarni, G.B., and Tierce, J.F. (1999). Comparative differences in the composition and biomechanical properties of tibiae of seven- and seventy-two-week-old male and female broiler breeder chickens. *Poult. Sci.* 78:1232–1239.

Reif, W.E. (1976). Morphogenesis, pattern formation, and function of the dentition of *Heterodontus* (Selachii). *Zoomorphology* 83:1–46.

Reif, W.E. (1977). Tooth enameloid as a taxonomic criterion. Part 1. A new euselachian shark from the Rhaetic–Liassic boundary. *Neues Jahrbuch Geol. Paläontol. Monatsh.* 1977(9):565–576.

Reif, W.E. (1978). Shark dentitions: morphogenetic processes and evolution. *Geol. Paleontol. Abh.* 157:107–115.

Reif, W.E. (1980). Development of dentition and dermal skeleton in embryonic *Scyliorhinus canicula*. *J. Morphol.* 166:275–288.

Reif, W.E. (1984). Pattern regulation in shark dentitions. In: Malacinski, G.M. and Bryant, S.V. (Eds.), *Pattern Formation: A Primer in Developmental Biology*. Macmillan, New York, pp. 603–621.

Reif, W.E., McGill, D., and Motta, P. (1978). Tooth replacement rates of the sharks *Triakis semifasciata* and *Ginglymostoma cirratum*. *Zoll. Jahrb. Anat. Bd.* 99:151–156.

Rho, J.Y., Mishra, S.R., Chung, K., Bai, J., and Pharr, G.M. (2001). Relationship between ultrastructure and the nanoindentation properties of intramuscular herring bones. *Ann. Biomed. Eng.* 29:1082–1088.

Robinson, M.P. and Motta, P.J. (2002). Patterns of growth and the effects of scale on the feeding kinematics of the nurse shark (*Ginglymostoma cirratum*). *J. Zool.* 256:449–462.

Rosenberg, L.R. (1998). A Comparison of the Mineralized Endoskeletal Tissues of Several Recent and Fossil Chondrichthyans from the Bear Gulch Limestone of Montana, master's thesis, Adelphi University, Long Island, NY.

Rudloe, A. (1989). Captive maintenance of the lesser electric ray, with observations of feeding behavior. *Prog. Fish-Cult.* 51:37–41.

Russo, R.A. (1975). Observations on the food habits of leopard sharks (*Triakis semifasciata*) and brown smooth-hounds (*Mustelus henlei*). *Calif. Fish Game* 61:95–103.

Sanderson, S.L. and Wassersug, R. (1993). Convergent and alternative designs for vertebrate suspension feeding. In: Hanken, J. and Hall, B.K. (Eds.), *The Skull*, Vol. 3. University of Chicago Press, Chicago, pp. 37–112.

Sanford, C.P. and Wainwright, P.C. (2002). Use of sonomicrometry demonstrates the link between prey capture kinematics and suction pressure in largemouth bass. *J. Exp. Biol.* 205:3445–3457.

Sasko, D.E. (2000). The Prey Capture Behavior of the Atlantic Cownose Ray, *Rhinoptera bonasus*, master's thesis, University of South Florida, Tampa.

Sasko, D.E., Dean, M.N., Motta, P.J., and Hueter, R.E. (2006). Prey capture behavior and kinematics of the Atlantic cownose ray, *Rhinoptera bonasus*. *Zoology* 109:171–181.

Schaeffer, B. (1967). Comments on elasmobranch evolution. In: Gilbert, P.W., Matthewson, R.F., and Rall, D.P. (Eds.), *Sharks, Skates and Rays*. The Johns Hopkins University Press, Baltimore, MD, pp. 3–35.

Schaeffer, B. and Williams, M. (1977). Relationship of fossil and living elasmobranchs. *Am. Zool.* 17:293–302.

Schmidt-Nielson, K. (1984). *Scaling: Why Is Animal Size So Important?* Cambridge University Press, Cambridge, U.K.

Schwartz, F.J. (1967). Embryology and feeding behavior of the Atlantic cownose ray *Rhinoptera bonasus*, presented at the Seventh Meeting of the Association of Island Marine Laboratories of the Caribbean, August 24–26, 1966, Barbados, West Indies.

Schwartz, F.J. (1989). Feeding behavior of the cownose ray, *Rhinoptera bonasus* (family Myliobatidae). *Assoc. Southeast Biol. Bull.* 36:66.

Sherman, K.M., Reidenauer, J.A., Thistle, D., and Meeter, D. (1983). Role of a natural disturbance in an assemblage of marine free-living nematodes. *Mar. Ecol. Prog. Ser.* 11:23–30.

Shimada, K. (2002a). Dental homologies in lamniform sharks (Chondrichthyes: Elasmobranchii). *J. Morphol.* 251:38–72.

Shimada, K. (2002b). Teeth of embryos in lamniform sharks (Chondrichthyes: Elasmobranchii). *Environ. Biol. Fish.* 63:309–319.

Shirai, S. and Nakaya, K. (1990). Interrelationships of the Etmopterinae (Chondrichthyes, Squaliformes). In: Pratt, Jr., H.L., Gruber, S.H., and Taniuchi, T. (Eds.), *Elasmobranchs as Living Resources: Advances in the Biology, Ecology, Systematics, and the Status of the Fisheries*, NOAA Tech. Rep. NMFS 90. National Oceanic and Atmospheric Administration, Washington, D.C., pp. 347–356.

Shirai, S. and Nakaya, K. (1992). Functional morphology of feeding apparatus of the cookie-cutter shark, *Isistius brasiliensis* (Elasmobranchii, Dalatiinae). *Zool. Sci.* 9:811–821.

Shirai, S. and Okamura, O. (1992). Anatomy of *Trigonognathus kabeyai*, with comments on feeding mechanism and phylogenetic relationships (Elasmobranchii, Squalidae). *Jpn. J. Icthyol.* 39:139–150.

Sims, D.W. (1999). Threshold foraging behaviour of basking sharks on zooplankton: life on an energetic knife-edge? *Proc. R. Soc. Lond. B Biol. Sci.* 266:1437–1443.

Sims, D.W. (2000). Filter-feeding and cruising swimming speeds of basking sharks compared with optimal models: they filter-feed slower than predicted for their size. *J. Exp. Mar. Biol. Ecol.* 249:65–76.

Sims, D.W. (2008). Sieving a living: a review of the biology, ecology and conservation status of the plankton-feeding basking shark *Cetorhinus maximus. Adv. Mar. Biol.* 54:171–220.

Sims, D.W. (2010). Tracking and analysis techniques for understanding free-ranging shark movements and behavior. In: Carrier, J.C., Musick, J.A., and Heithaus, M.R. (Eds.), *Sharks and Their Relatives II: Biodiversity, Adaptive Physiology, and Conservation.* CRC Press, Boca Raton, FL, pp. 351–392.

Sims, D.W. and Merrett, D.A. (1997). Determination of zooplankton characteristics in the presence of surface feeding basking sharks *Cetorhinus maximus. Mar. Ecol. Prog. Ser.* 158:297–302.

Sims, D.W. and Quayle, V.A. (1998). Selective foraging behaviour of basking sharks on zooplankton in a small-scale front. *Nature* 393:460–464.

Sims, D.W., Fox, A.M., and Merrett, D.A. (1997). Basking shark occurrence off South-West England in relation to zooplankton abundance. *J. Fish Biol.* 51:436–440.

Sims, D.W., Andrews, P.L.R., and Young, J.Z. (2000). Stomach rinsing in rays. *Nature* 404:566.

Skjaeraasen, J.E. and Bergstad, O.A. (2000). Distribution and feeding ecology of *Raja radiata* in the northeastern North Sea and Skagerrak (Norwegian Deep). *ICES J. Mar. Sci.* 57:1249–1260.

Smale, M.J. and Cliff, G. (1998). Cephalopods in the diets of four shark species (*Galeocerdo cuvier, Sphyrna lewini, S. zygaena* and *S. mokarran*) from KwaZulu-Natal, South Africa. *S. Afr. J. Mar. Sci.* 20:241–253.

Smale, M.J. and Cowley, P.D. (1992). The feeding ecology of skates (Batoidea: Rajidae) off the Cape South coast, South Africa. *S. Afr. J. Mar. Sci.* 12:823–834.

Smale, M.J., Sauer, W.H.H., and Hanlon, R.T. (1995). Attempted ambush predation on spawning squids *Loligo vulgaris reynaudii* by benthic pyjama sharks, *Poroderma africanum*, off South Africa. *J. Mar. Biol. Assoc. U.K.* 75:739–742.

Smale, M.J., Sauer, W.H.H., and Roberts, M.J. (2001). Behavioural interactions of predators and spawning chokka squid off South Africa: towards quantification. *Mar. Biol.* 139:1095–1105.

Smith, B.G. (1942). The heterodontid sharks: their natural history, and the external development of *Heterodontus japonicus* based on notes and drawings by Bashford Dean. In: Gudger, E.W. (Ed.), *The Bashford Dean Memorial Volume: Archaic Fishes.* American Museum of Natural History, New York, pp. 647–784.

Smith, J.W. (1980). The Life History of the Cownose Ray, *Rhinoptera bonasus* (Mitchell 1815), in Lower Chesapeake Bay, with Notes on the Management of the Species, master's thesis, College of William and Mary, Williamsburg, VA.

Smith, J.W. and Merriner, J.V. (1985). Food habits and feeding behavior of the cownose ray, *Rhinoptera bonasus*, in lower Chesapeake Bay. *Estuaries* 8:305–310.

Southall, E.J. and Sims, D.W. (2003). Shark skin: a function in feeding. *Proc. R. Soc. Lond. B Biol. Sci.* 270(Suppl.):47–49.

Springer, S. (1961). Dynamics of the feeding mechanism of large galeoid sharks. *Am. Zool.* 1:183–185.

Springer, S. (1967). Social organization of shark populations. In: Gilbert, P.W., Mattewson, R.F., and Rall, D.P. (Eds.), *Sharks, Skates and Rays.* The Johns Hopkins Press, Baltimore, MD, pp. 149–174.

Stevens, J.D. (1976). The Ecology of the Blue Shark (*Prionace glauca* L.) in British Waters, doctoral dissertation, University of London.

Stevens, J.D. (2010). Epipelagic oceanic elasmobranchs. In: Carrier, J.C., Musick, J.A., and Heithaus, M.R. (Eds.), *Sharks and Their Relatives II: Biodiversity, Adaptive Physiology, and Conservation.* CRC Press, Boca Raton, FL, pp. 3–35.

Stokes, M.D. and Holland, N.D. (1992). Southern stingray (*Dasyatis americana*) feeding on lancelets (*Branchiostoma floridae*). *J. Fish Biol.* 41:1043–1044.

Strasburg, D.W. (1958). Distribution, abundance, and habits of pelagic sharks in the central Pacific Ocean. *U.S. Fish. Bull.* 58:335–361.

Strasburg, D.W. (1963). The diet and dentition of *Isistius brasiliensis*, with remarks on tooth replacement in other sharks. *Copeia* 1963:33–40.

Strong, Jr., W.R. (1989). Behavioral Ecology of Horn Sharks, *Heterodontus francisci*, at Santa Catalina Island, California, with Emphasis on Patterns of Space Utilization, master's thesis, The California State University, Long Beach.

Strong, Jr., W.R. (1990). Hammerhead shark predation on stingrays: an observation of prey handling by *Sphyrna mokarran. Copeia* 1990:836–840.

Summers, A.P. (2000). Stiffening the stingray skeleton: an investigation of durophagy in myliobatid stingrays (Chondrichthyes, Batoidea, Myliobatidae). *J. Morphol.* 243:113–126.

Summers, A.P. and Long, Jr., J.H. (2006). Skin and bones, sinew and gristle: the mechanical behavior of fish skeletal tissues. In: Shadwick, R.E. and Lauder, G.V. (Eds.), *Fish Biomechanics.* Elsevier, San Diego, pp. 141–178.

Summers, A.P., Koob, T.J., and Brainerd, E.L. (1998). Stingray jaws strut their stuff. *Nature* 395:450–451.

Summers, A.P., Koob-Emunds, M.M., Kajiura, S.M., and Koob, T.J. (2003). A novel fibrocartilaginous tendon from an elasmobranch fish (*Rhinoptera bonasus*). *Cell Tissue Res.* 312:221–227.

Summers, A.P., Ketcham, R., and Rowe, T. (2004). Structure and function of the horn shark (*Heterodontus francisci*) cranium through ontogeny: the development of a hard prey specialist. *J. Morphol.* 260:1–12.

Svanback, R., Wainwright, P.C., and Ferry-Graham, L.A. (2002). Linking cranial kinematics, buccal pressure, and suction feeding performance in largemouth bass. *Physiol. Biochem. Zool.* 75:532–543.

Talent, L.G. (1976). Food habits of the leopard shark, *Triakis semifasciata*, in Elkhorn Slough, Monterey Bay, California. *Calif. Fish Game* 62:286–298.

Tanaka, S.K. (1973). Suction feeding by the nurse shark. *Copeia* 1973:606–608.

Tanne, K., Tanaka, E., and Sakuda, M. (1991). The elastic modulus of the temporomandibular joint disc from adult dogs. *J. Dent. Res.* 70:1545–1548.

Taylor, J.G. (2007). Ram filter-feeding and nocturnal feeding of whale sharks (*Rhincodon typus*) at Ningaloo Reef, Western Australia. *Fish. Res.* 84:65–70.

Taylor, J.G. and Pearce, A.F. (1999). Ningaloo reef currents: implications for coral spawn dispersal, zooplankton and whale shark abundance. *J. Roy. Soc. West. Aust.* 82:57–65.

Taylor, L.R. (1972). A Revision of the Sharks of the Family Heterodontidae (Heterodontiformes, Selachii), doctoral dissertation, University of California, San Diego.

Taylor, L.R., Compagno, L.J.V., and Struhsaker, P.J. (1983). Megamouth, a new species, genus, and family of lamnoid shark (*Megachasma pelagios*, family Megachasmidae) from the Hawaiian Islands. *Proc. Calif. Acad. Sci.* 43:87–110.

Thrush, S.F., Pridmore, R.D., Hewitt, J.E., and Cummings, V.J. (1991). Impact of ray feeding disturbances on sandflat macrobenthos: do communities dominated by polychaetes or shellfish respond differently? *Mar. Ecol. Prog. Ser.* 69:245–252.

Tricas, T.C. (1979). Relationships of the blue shark, *Prionace glauca*, and its prey species near Santa Catalina Island, California. *U.S. Fish. Bull.* 77:175–182.

Tricas, T.C. (1985). Feeding ethology of the white shark, *Carcharodon carcharias. Mem. South. Calif. Acad. Sci.* 9:81–91.

Tricas, T.C. and McCosker, J.E. (1984). Predatory behavior of the white shark (*Carcharodon carcharias*) with notes on its biology. *Proc. Calif. Acad. Sci.* 43:221–238.

Turingan, R.G., Wainwright, P.C., and Hensley, D.A. (1995). Interpopulation variation in prey use and feeding biomechanics in Caribbean triggerfishes. *Oecologia* 102:296–304.

Valadez-Gonzalez, C., Anguilar-Palomino, B., and Hernandez-Vazquez, S. (2001). Feeding habits of the round stingray *Urobatis halleri* (Cooper, 1863) (Chonrichthyes: Urolophidae) from the continental shelf of Jalisco and Colima, Mexico. *Cien. Mar.* 27:91–104.

van der Meij, M.A.A., Griekspoor, M., and Bout, R.G. (2004). The effect of seed hardness on husking time in finches. *Anim. Biol.* 54:195–205.

Van Wassenbergh, S., Aerts, P., Adriaens, D., and Herrel, A. (2005). A dynamic model of mouth closing movements in clariid fishes: the role of enlarged adductors. *J. Theor. Biol.* 234:49–65.

Van Wassenbergh, S., Aerts, P., and Herrel, A. (2006). Hydrodynamic modeling of aquatic suction performance and intra-oral pressures: limitation for comparative studies. *J. Roy. Soc. Interface* 3:507–514.

VanBlaricom, G.R. (1976). *Preliminary Observations on Interactions between Two Bottom-Feeding Rays and a Community of Potential Prey in a Sublittoral Sand Habitat in Southern California.* National Oceanic and Atmospheric Administration, Astoria, OR, pp. 153–162.

Verwaijen, D., Van Damme, R., and Herrel, A. (2002). Relationships between head size, bite force, prey handling efficiency and diet in two sympatric lacertid lizards. *Funct. Ecol.* 16:842–850.

Vorenberg, M.M. (1962). Cannibalistic tendencies of lemon and bull sharks. *Copeia* 1962:455–456.

Wainwright, P.C. (1988). Morphology and ecology: functional basis of feeding constraints in Caribbean labrid fishes. *Ecology* 69:635–645.

Wainwright, P.C. and Day, S.W. (2007). The forces exerted by aquatic suction feeders on their prey. *J. Roy. Soc. Interface* 4:553–560.

Wainwright, P.C. and Shaw SS. (1999). Morphological basis of kinematic diversity in feeding sunfishes. *J. Exp. Biol.* 202:3101–3110.

Wainwright, P.C., Westneat, M.W., and Bellwood, D.R. (2000). Linking feeding behavior and jaw mechanics in fishes. In: Domenici, P. and Blake, R.W. (Ed.), *Biomechanics in Animal Behavior.* BIOS Scientific, Oxford, pp. 207–221.

Wainwright, P.C., Ferry-Graham, L.A., Waltzek, T.B., Carroll, A.M., Hulsey, C.D., and Grubich, J.R. (2001a). Evaluating the use of ram and suction during prey capture by cichlid fishes. *J. Exp. Biol.* 204:3039–3051.

Wainwright, P.C., Ferry-Graham, L.A., Waltzek, T.B., Hulsey, C.D., Carroll, A.M., and Svanback, R. (2001b). Evaluating suction feeding performance in fishes. *Am. Zool.* 41:1617–1617.

Wainwright, P.C., Bellwood, D.R., Westneat, M.W., Grubich, J.R., and Hoey, A.S. (2004). A functional morphospace for the skull of labrid fishes: patterns of diversity in a complex biomechanical system. *Biol. J. Linn. Soc. Lond.* 82:1–25.

Wainwright, S.A., Biggs, W.D., Currey, J.D., and Gosline, J.M. (1976). *Mechanical Design in Organisms.* Princeton University Press, Princeton, NJ.

Waller, G.N.H. and Baranes, A. (1991). Chondrocranium morphology of northern Red Sea triakid sharks and relationships to feeding habits. *J. Fish Biol.* 38:715–730.

Waters, N.E. (1980). Some mechanical and physical properties of teeth. In: Vincent, J.F.V. and Currey, J.D. (Eds.), *The Mechanical Properties of Biological Materials.* Cambridge University Press, Cambridge, U.K., pp. 99–135.

Westneat, M.W. (1994). Transmission of force and velocity in the feeding mechanisms of labrid fishes (Teleostei, Perciformes). *Zoomorphology* 114:103–118.

Westneat, M.W. (2004). Evolution of levers and linkages in the feeding mechanisms of fishes. *Integr. Comp. Biol.* 44:378–389.

Wesneat, M.W. (2006). Skull biomechanics and suction feeding in fishes. In: Shadwick, R.E. and Lauder, G.V. (Eds.), *Fish Biomechanics.* Elsevier, Amsterdam, pp. 29–68.

Wetherbee, B.M., Crow, G.L., and Lowe, C.G. (1997). Distribution, reproduction, and diet of the gray reef shark *Carcharhinus amblyrhynchos* in Hawaii. *Mar. Ecol. Prog. Ser.* 151:181–189.

White, W.T. and Sommerville, E. (2010). Elasmobranchs of tropical marine ecosystems. In: Carrier, J.C., Musick, J.A., and Heithaus, M.R. (Eds.), *Sharks and Their Relatives II: Biodiversity, Adaptive Physiology, and Conservation.* CRC Press, Boca Raton, FL, pp. 159–239.

Whitenack, L.B. and Motta, P.J. (2010). Performance of shark teeth during puncture and draw: implications for the mechanics of cutting. *Biol. J. Linn. Soc. Lond.* 100:271–286.

Whitenack, L.B., Simkins, Jr., D.C., Motta, P.J., Hirai, M., and Kumar, A. (2010). Young's modulus and hardness of shark tooth materials. *Arch. Oral Biol.* 55:203–209.

Whitenack, L.B., Simkins, Jr., D.C., and Motta, P.J. (2011). Biology meets engineering: the structural mechanics of fossil and extant shark teeth. *J. Morphol.* 272:169–179.

Widder, E.A. (1998). A predatory use of counterillumination by the squaloid shark, *Isistius brasiliensis. Environ. Biol. Fish.* 53:267–273.

Wilga, C.D. (1997). Evolution of Feeding Mechanisms in Elasmobranchs: A Functional Morphological Approach, doctoral dissertation, University of South Florida, Tampa.

Wilga, C.D. (2002). A functional analysis of jaw suspension in elasmobranchs. *Biol. J. Linn. Soc.* 75:483–502.

Wilga, C.D. (2005). Morphology and evolution of the jaw suspension in lamniform sharks. *J. Morphol.* 265:102–119.

Wilga, C.D. (2008). Evolutionary divergence in the feeding mechanism of fishes. *Acta Geol. Polon.* 58:113–120.

Wilga, C.D. (2010). Hyoid and pharyngeal arch function during ventilation and feeding in elasmobranchs: conservation and modification in function. *J. Appl. Ichthyol.* 26:162–166.

Wilga, C.D. and Motta, P.J. (1998a). Conservation and variation in the feeding mechanism of the spiny dogfish *Squalus acanthias. J. Exp. Biol.* 201:1345–1358.

Wilga, C.D. and Motta, P.J. (1998b). Feeding mechanism of the Atlantic guitarfish *Rhinobatus lentiginosus*: modulation of kinematic and motor activity? *J. Exp. Biol.* 201:3167–3183.

Wilga, C.D. and Motta, P.J. (2000). Durophagy in sharks: feeding mechanics of the hammerhead *Sphyrna tiburo. J. Exp. Biol.* 203:2781–2796.

Wilga, C.D. and Sanford, C.P. (2008). Suction generation in white-spotted bamboo sharks *Chiloscyllium plagiosum. J. Exp. Biol.* 211:3128–3138.

Wilga, C.D., Wainwright, P.C., and Motta, P.J. (2000). Evolution of jaw depression mechanics in aquatic vertebrates: insights from Chondrichthyes. *Biol. J. Linn. Soc.* 71:165–185.

Wilga, C.D., Hueter, R.E., Wainwright, P.C., and Motta, P.J. (2001). Evolution of upper jaw protrusion mechanisms in elasmobranchs. *Am. Zool.* 41:1248–1257.

Wilga, C.D., Motta, P.J., and Sanford, C.P. (2007). Evolution and ecology of feeding in elasmobranchs. *Integr. Comp. Biol.* 47:55–69.

Williams, M. (2001). Tooth retention in cladodont sharks: with a comparison between primitive grasping and swallowing, and modern cutting and gouging feeding mechanisms. *J. Vertebr. Paleontol.* 21:214–226.

Wilson, D.P. (1953). Notes from the Plymouth Aquarium II. *J. Mar. Biol. Assoc. U.K.* 32:199–208.

Winterbottom, R. (1974). A descriptive synonymy of the striated muscles of the Teleostei. *Proc. Acad. Nat. Sci. Phil.* 125:225–317.

Wirsing, A.J., Heithaus, M.R., and Dill, L.M. (2007). Can measures of prey availability improve our ability to predict the abundance of large marine predators? *Oecologia* 153:563–568.

Witzell, W.N. (1987). Selective predation on large cheloniid sea turtles by tiger sharks (*Galeocerdo cuvier*). *Jpn. J. Herpetol.* 12:22–29.

Wroe, S., Huber, D.R., Lowry, M., McHenry, C., Moreno, K., Clausen, P., Ferrara, T., Cunningham, E., Dean, M.N., and Summers, A.P. (2008). Three-dimensional computer analysis of white shark jaw mechanics: how hard can a great white bite? *J. Zool.* 276:336–342.

Wu, E.H. (1994). Kinematic analysis of jaw protrusion in orectolobiform sharks: a new mechanism for jaw protrusion in elasmobranchs. *J. Morphol.* 222:175–190.

Wyckmans, M., Van Wassenburgh, S., Adriaens, D., Van Damme, R., and Herrel, A. (2007). Size-related changes in cranial morphology affect diet in the catfish *Clariallabes longicauda. Biol. J. Linn. Soc. Lond.* 92:323–334.

Zangerl, R. (1981). *Chondrichthyes I: Paleozoic Elasmobranchii.* Gustav Fischer Verlag, New York.

Zangerl, R. and Williams, M.W. (1975). New evidence on the nature of the jaw suspension in Paleozoic anacanthous sharks. *Paleobiology* 18:333–341.